Probabilistic lifetime prediction with application to high-performance p-aramid fiber

Knoester, H.

2017

“schedon panta rhei”

“almost everything flows”

if it ain’t flowing
it’s probably broken

VRIJE UNIVERSITEIT

Probabilistic lifetime prediction with application to high-performance p-aramid fiber

ACADEMISCH PROEFSCHRIFT

ter verkrijging van de graad Doctor aan
de Vrije Universiteit Amsterdam,
op gezag van de rector magnificus
prof.dr. V. Subramaniam,
in het openbaar te verdedigen
ten overstaan van de promotiecommissie
van de Faculteit der Exacte Wetenschappen
op donderdag 14 september 2017 om 13.45 uur
in de aula van de universiteit,
De Boelelaan 1105

door

Henk Knoester

geboren te Voorburg

promotoren: prof.dr. R.W.J. Meester
prof.dr. J. Hulshof

Contents

Chapter 1

Introduction

Abstract

This chapter discusses the necessity of theoretical modeling of failure, supplementary to experimental work, to improve our understanding of failure of p-aramid fibers. We propose a probabilistic damage model, which describes time-to-failure distribution of single fibers as function of arbitrary load program. To some extent, it is an envelop model of two physical models for fiber failure which dominate the literature for many decades. This damage model has been the point of departure for studying the failure behavior of p-aramid fibers. Although the model acceptably covers p-aramid fiber failure for constant load and constant load rate programs, its validity is eventually rejected for step-load programs.

1.1 Overview

This thesis is on load-induced failure of p-aramid fibers. These fibers, developed in the sixties of the previous century, are nowadays used in various industrial applications. The fibers combine high strength and modulus with chemical resistance, low specific weight, good fatigue and thermal stability. This makes p-aramid fibers a preferred high-end material in automotive and oil and gas industries, telecommunications industry and military and aerospace applications.

For the design of fiber-reinforced materials and products, applied in very demanding applications, it is of paramount importance that engineers can rely on sound experimental evidence on the long-term mechanical properties of the fibers. For obvious reasons, the most relevant experiments are not feasible because these would last for many years or even decades. Instead, failure *models* for the prediction of time-to-failure of p-aramid yarns offer an alternative. These models are powered with data obtained from relatively short experiments where fibers are subjected to easy, well-defined load programs. In this thesis we want to add to the engineering knowledge on p-aramid fibers' long-term mechanical properties. The objective of this thesis is to construct a model, preferably with its roots embedded in literature, which is in accordance with data obtained from short-term experiments. Data comprise existing data, mostly on the time-to-failure

of p-aramid fibers subjected to constant load. But we also collected new experimental data on residual strength (after preload) and on failure induced by single step constant load programs.

Section 1.2 illustrates the high load sensitivity of p-aramid fibers. Then, we briefly discuss different ways of failure modeling in Section 1.3. Many models primarily aim at improved understanding of the failure phenomenon inside fibers by studying the morphological or molecular changes during creep as a consequence of loading. Other models address 'the damage' in fibers due to loading in a more heuristic and generic way. These models are tuned with experimental data and their primary use is to predict material failure behavior, also beyond the boundaries of the experiments they are based upon. Section 1.5 sets out the framework of a generic damage model. Its relevancy is illustrated by the fact that it turns out to be largely compatible with two physical failure models which dominate the literature on this subject (described in Section 1.4). Finally, in Section 1.6 an overview is given of the chapters in this thesis. Chapter 2 and Chapter 4 were published separately as papers in Journal of Materials Science. In Chapter 4 evidence is found that the damage model, introduced in Section 1.5, is not fully capable to describe residual strength of p-aramid fibers. In Chapter 5 we show that the model, versatile as it may look, is fundamentally inconsistent with the observed failure of p-aramid fibers subjected to step load programs.

1.2 About failure of p-aramid fibers

P-aramid fibers (such as Twaron) are well-known for their high strength. Still, if fibers are subjected to loads well below their strength, they will fail after a finite time. During loading, damage accumulates inside the fiber which is manifested as creep: irreversible elongation of the fiber. Eventually, after reaching a critical creep level, the fiber fails (breaks). This failure is denoted by 'creep rupture'.

Creep rupture can be fast or slow, depending on the load level the fiber is subjected to. As an illustration, Table 1.1 shows approximate failure times of twisted Twaron 2300 fiber exposed to a load level equivalent to 90%, 70% and 50% of its strength. These failure times are representative for p-aramid fibers in general, with only slight modification per fiber type and twist level. Clearly for applications with a required (industrial / economic) lifetime of say 30 – 100 yr and including a safety factor, fibers should be loaded below 50% of their strength.

load	time-to-failure
90% of strength	minutes
70% of strength	1 month
50% of strength	1000 years

Table 1.1: *Approximate time-to-failure of twisted Twaron 2300 fiber as function of load.*

Experimental data on the lifetime of p-aramid fibers, as function of applied load, are scarce. For obvious reasons, measurement data are only available for relatively high loads which correspond to relatively short times-to-failure, say up to one year or so. How can we infer from these data the lifetime of p-aramid fibers subjected to low loads, representative for industrial applications? How is lifetime affected if the load is not entirely constant, but includes one ore more load steps, or incidental peak loads? During loading, irreversible damage builds up inside the yarns, e.g. by slippage of polymer chains. How well are mechanical properties retained during the lifetime of the fibers?

These questions explain the desire for a better understanding of creep failure. Doing experiments alone is not enough because long-term experiments (say > 2 years) are out of reach and the number of 'interesting experiments' is simply too large. Experimental work *in combination with modeling of failure* is inevitable to make progress in understanding the creep failure phenomenon. The next section briefly discusses different ways of modeling failure.

Apart from creep failure there are other failure mechanisms, such as fatigue, chemical attack and UV degradation. These are beyond the scope of this thesis.

The notion 'p-aramid fiber' used in this thesis relates to the fibers as end product of the spinning process. These fibers (also denoted by 'yarns') consist of a large number of filaments (typically 1000 or 2000). One may investigate the mechanical properties of filaments and infer yarn properties from these. The focus of this thesis is on the fibers themselves and treating these as indivisible objects. A more elaborate discussion on this matter is found in the Introduction of Chapter 4.

1.3 Modeling failure from different perspectives

There are different ways to study failure behavior of materials. From entirely empirical to very theoretical, and from rigorous analysis based on fundamental principles to more heuristic approaches. Find below a short overview of different perspectives in polymer fiber failure modeling.

1. Empirical modeling
If there is no prior knowledge of failure of the material under consideration, empirical investigation is a sensible choice. The main drawback of only doing experiments, without attempting any theoretical modeling, is that knowledge remains limited to the area of experimental settings.

For this reason, experimental programs are often accompanied with a superficial theoretical framework, allowing to explore how the material is likely to behave outside the experimental domain. Frequently, failure is tested in a series of experiments, and experimental results are simply extrapolated to obtain estimated failure behavior at conditions beyond the experimental settings. For example, if fiber failure times of a fiber subjected to a series of increasingly lower constant loads are obtained experimentally, these data can be extrapolated, e.g. by simple regression, to obtain the estimated fiber failure time at such a low load that experimental measurement of this time-to-failure would take far too much time.

In case the fiber or material is subjected to a cyclic program, one can investigate the influence of cycle frequency, amplitude or load shape (sine, block shape etc.) on the failure time. Because of multiple parameters defining the cycle, the amount of interesting experiments increases dramatically. Again there is a need to classify material behavior is some sort of engineering rule, which describes material failure for this type of load program in a general way. In fatigue research of metal-like materials, $S - N$ curves are commonly used which visualize the number of cycles-to-failure N as function of load amplitude S (say for fixed mean load).

Polymeric materials are built from macromolecules and generally show viscoelastic behavior. Recognition of patterns in this behavior offers an opportunity to exploit experimental data beyond experimental conditions. For polymers with linear viscoelastic behavior, the time-temperature superposition principle holds and there is congruency of creep curves at different temperatures. Alwis [1] uses this principle to calculate long time-to-failure (at low load) by doing experiments at elevated temperatures and constructing a creep master curve. However, it is uncertain how well mechanical behavior of p-aramid fibers fit into the theory of linear viscoelasticity. Generally, there are multiple deformation processes running simultaneously during loading and polymer properties are likely to change in time. Changing material properties, for example due to degradation or re-orientation of polymer chains, is associated with nonlinear viscoelastic behavior.

2. Mechanical modeling
Mechanical modeling primarily aims at better understanding what happens *inside* the fiber during loading. If it is understood how localized internal failure scales up to global fiber failure, such

modeling eventually leads to the fiber's failure time. Synthetic fibers are commonly built from a large number of parallel filaments. During loading, due to local failure of these filaments, the load on the fiber is redistributed over its constituents. Phoenix [2, 3] has extensively studied load distribution inside fibers and fiber reinforced composites. Another type of mechanical modeling is by focusing on small cracks and defects, perpendicular to the fiber axis. Due to a load on the fiber, stress intensification at the tip of these cracks will bring about growth of the crack and eventually fiber failure.

3. Modeling of failure on molecular scale

Many times, fiber failure is explained from processes on a molecular level. In synthetic fibers, long polymer chains are almost perfectly aligned along the fiber axis. Fiber strength is dependent on polymer chain length. Loading of the fiber can cause (local) destruction of the molecular structure. Polymer chains can break (chain scission) which directly reduces fiber strength. Polymer chains may slide along each other (chain slippage) due to breakage of inter-molecular bonds (in case of p-aramid fibers: H-bonding and Van der Waals bonding). By linking fiber failure to molecular failure, the rate of fiber failure can directly be described in terms of well-established kinetic theory. This also sets the temperature dependency of fiber failure.

Baltussen and Northolt [4] focused on the crystalline structure of highly oriented p-aramid fiber and show how the structure deforms as a result of external loading. They modeled the mechanical response of p-aramid fibers in terms of local orientation, and could predict reversible and irreversible elongation and stiffening.

4. Damage modeling

Although damage modeling finds its origin in the growth of real material defects during loading, this type of modeling has gradually shifted towards a more heuristic direction. Damage modeling is particularly popular if a material is subjected to complex but cyclic load programs. Damage models then boil down to arithmetic rules how to 'add up' damage inflicted on the material during the various steps in the load program. Failure is foreseen if the accumulated damage exceeds a critical damage level. A well-known example of damage modeling is Palmgren-Miner's Rule in fatigue analysis. For an extensive introduction into the field of damage modeling, the reader is referred to the Introduction of Chapter 5.

In practice, research on material failure is not easily classified in terms of the above types of modeling. Many research projects combine two or more of these, heavily interlinked lines of research.

In the next section we introduce two physical models for material failure which found widespread acceptance in literature for various materials. In Section 1.5 a probabilistic damage model is presented which is capable to mimic the response of these physical models to a large extent. This damage model is used as starting point for the work in this thesis, see Section 1.6.

1.4 Trends in failure modeling at constant load

The easiest way to test failure behavior of a material is by subjecting it to a constant load and wait until it breaks. The load sensitivity is measured by recording the time up to failure (or: time-to-failure) for a series of loads. Load sensitivity is visualized by plotting the time-to-failure as function of load, the so-called load curve. For many materials, including synthetic fibers, time-to-failure is very sensitive to the applied load. The resulting steep load curves are therefore almost always plotted using the logarithm of time-to-failure. Let T be time-to-failure and σ the applied load. Both in empirical studies and much of the theoretical modeling, there are two dominating types of relationships between time-to-failure and applied load: exponential ($T \sim e^{-a\sigma}$) and power-law ($T \sim \sigma^{-b}$), with a and b model parameters.

In this section, we will briefly discuss two widely used models in failure theory which are associated to exponential and power-law behavior. In 1.4.1, failure of polymers is described kinetically in terms of chain scission: the load activated breaking of polymer molecules. In 1.4.2 we describe crack growth due to stress intensification at the crack tip, eventually leading to failure of materials.

Both models will be treated deterministically, i.e. time-to-failure is a scalar. In practice, if samples of the same material are repeatedly subjected to the same load, a distribution of times-to-failure will be observed rather than a single scalar value. We will later see that the models are easily extended to encompass the stochastic nature of time-to-failure.

1.4.1 A kinetic description of failure

Tobolsky and Eyring [5] developed a kinetic model for fracture of polymeric materials on a molecular level. In their model, molecular bond breaking ('chain scission') is described as a thermally activated process where the energy barrier for breaking is lowered by externally applied tension. Henderson et al. [6] simplified the rate process formulations of Tobolsky and Eyring for large tension σ. Then, the following equation describes the rate at which molecular bonds M are broken ignoring the reverse mending process:

$$M' = \frac{dM}{dt} = -\frac{M}{\tau} \exp\left\{-\frac{(U - \gamma\sigma)}{kT}\right\}, \tag{1.1}$$

with M the number of non-broken bonds, U the activation energy, γ the activation volume, σ the applied tension, k the Boltzmann constant, T absolute temperature and τ a characteristic molecular time scale. To avoid confusion with time-to-failure T we abbreviate the product of Boltzmann constant and temperature by writing $\tilde{k} = kT$. Equation (1.1) is easily integrated up to the moment of failure:

$$\ln R = \ln\left(\frac{M_0}{M_1}\right) = \frac{1}{\tau}\int_0^T \exp\left\{-\frac{(U - \gamma\sigma)}{\tilde{k}}\right\} dt, \tag{1.2}$$

with M_0 the initial number of non-broken bonds, M_1 the final number of non-broken bonds at the moment of breaking and T the time-to-failure. Clearly, variable $\ln R$ is simply a measure for

the molecular damage required for breaking. In case of a constant load $\sigma(t) = \sigma$ and assuming the required damage for breaking $\ln R$ is independent of the applied load σ, then:

$$T \sim \exp\left\{\frac{(U - \gamma\sigma)}{\tilde{k}}\right\}. \tag{1.3}$$

Within the framework of the Tobolsky-Eyring model, this result has found widespread acceptance through the work of Zhurkov [7]. Note the exponential relationship between time-to-failure and load. Nowadays, it is generally accepted that creep rupture of p-aramid fibers is disconnected from polymer chain scission. Instead, chain slippage is much more likely to explain irreversible creep. Still, slippage may also be well described as a thermally activated process for it requires breakage of (relatively weak) inter-chain hydrogen bonds.

1.4.2 Stress Corrosion Cracking (SCC)

Glass fibers are sensitive to growth of surface cracks due to the combined action of both stress and the chemical environment. This Stress Corrosion Cracking (SCC) process eventually leads to a critical crack size and corresponding failure of the fiber. Crack growth is usually described by a power-law relationship which is confirmed experimentally for many materials. For a crack with crack size a, the growth rate is given by Paris' law:

$$v = \frac{da}{dt} = AK_I^n \quad a(t=0) = a_0 \quad \text{and} \quad K_I = Y\sigma\sqrt{a}, \tag{1.4}$$

with A and Y material constants, K_I the stress intensity factor (subscript I refers to the first mode of crack growth which is often assumed to be the prevailing mode for the whole process) and n the stress corrosion factor. Both crack size a and load σ may be considered as function of time t. Note that the stress intensity factor increases in time because of crack growth. Equation (1.4) is well-known in fatigue analysis. Here, da/dt is replaced by da/dN, the crack growth rate per load cycle due to fatigue.

Under the condition that the initial crack size a_0 is negligible compared to the critical crack size at the moment of breaking and under the condition that $n >> 1$, Pauchard [8] integrates equation (1.4):

$$\int_0^T \sigma^n dt = \frac{2a_0^{(n-2)/2}}{AY^n(n-2)}, \tag{1.5}$$

with T the time-to-failure. The material breaks if the stress intensity factor reaches a critical value K_{Ic}, the breaking criterion thus becomes $K_{Ic} = Y\sigma\sqrt{a}$. This criterion allows definition of the initial strength S of the material via $K_{Ic} = YS\sqrt{a_0}$. Elimination of the initial crack size a_0 in equation (1.5) leads to the following relationship for time-to-failure:

$$\int_0^T \sigma^n dt = \frac{2K_{Ic}^{2-n}S^{n-2}}{AY^2(n-2)} = C. \tag{1.6}$$

For constant load experiments, the relation simplifies to:

$$T = C\sigma^{-n}. \tag{1.7}$$

1.5 A versatile damage model

Coleman [9] developed a failure model for single fibers, which plays a central role in this thesis. It is a probabilistic model since time-to-failure T is treated as random variable. He proposed a cumulative distribution function for time-to-failure of the following form:

$$P\left(T<t\right)=F_T(t)=1-\exp\left\{-\ell\left(\int_0^t\kappa(\sigma(x))dx\right)^k\right\}, \tag{1.8}$$

with ℓ the length of the fiber sample and $\sigma(t)$ the load the fiber is subjected to at time t. The so-called breakdown rule function $\kappa(\cdot)$ generally takes on one of two popular forms:

$$\kappa(x) = \gamma x^\rho \qquad \text{(power-law breakdown), or} \tag{1.9a}$$

$$\kappa(x) = \alpha\exp\left(\beta x\right) \quad \text{(exponential breakdown).} \tag{1.9b}$$

This model can be derived in several ways. Coleman used the well-known weakest link principle and a mathematically improved version can be found in Section 2.2 (Chapter 2). In Section 5.3 (Chapter 5) we show that the model readily follows from a couple of mild assumptions. The model can be classified as damage model, with random variable:

$$\Omega=\int_0^T\kappa(\sigma(x))dx, \tag{1.10}$$

representing the amount of damage inflicted on the fiber at the moment of breaking. For arbitrary load program $\sigma(\cdot)$, the 'damage-at-breaking' Ω is Weibull distributed and independent of load. Ω turns out to be very helpful in formally deriving probability distributions for residual mechanical properties. It allows for a natural definition of residual strength in the framework of Coleman's model. See Chapter 4 for more details.

For constant load, i.e. $\sigma(t)=\sigma$, it readily follows that time-to-failure is Weibull distributed ($T\sim W(k,t_0)$):

$$F_T(t)=1-\exp\left\{-\left(\frac{t}{t_0}\right)^k\right\} \text{ with } t_0=\frac{\ell^{-1/k}}{\kappa(\sigma)}. \tag{1.11}$$

For the mean time-to-failure we find $\overline{T}=t_0\Gamma(1+1/k)=\ell^{-1/k}\Gamma(1+1/k)/\kappa(\sigma)$ or $T\sim e^{-\beta\sigma}$ for the exponential breakdown rule function and $T\sim\sigma^{-\rho}$ for the power-law breakdown rule function. At least with respect to the response on a constant load program, the Coleman model is an envelop model for both families of physical fiber failure models discussed in the previous section. If we assume that T is Weibull distributed, the analogy extends to arbitrary load programs as is argued below.

The Tobolsky-Eyring model discussed in 1.4.1 can be interpreted probabilistically by considering T as random variable. Equation (1.2) fits in (1.10) if $\kappa(\sigma)$ is chosen proportional to

$\exp\left\{-\frac{(U-\gamma\sigma)}{\tilde{k}}\right\}$ and $\ln R$ is considered as a damage-at-breaking variable. It is concluded that the Tobolsky-Eyring model (1.1) in combination with Weibull distributed time-to-failure (at constant load) and load independent failure criterion is fully embedded in the Coleman model (choosing the exponential breakdown rule function), also for complex load programs.

To appreciate that Coleman's model also partly encompasses the Stress Corrosion Cracking (SCC) model in 1.4.2, first treat T and S as random variables in equation (1.6). Equation (1.6) now fits in (1.10) if $\kappa(\sigma)$ is chosen proportional to σ^n and C is considered as a damage-at-breaking random variable. Two serious remarks need to be made here. First of all, the SCC model apparently uses a fixed virgin strength S (or strength distribution in our case). S is fixed because it only depends on material constants and not on the load rate. Within the Coleman model it makes sense to define strength on the basis of the load program with which the strength is measured. After all, Coleman's model allows for arbitrary load program. In Section 2.2 we define material strength S as maximum load during a constant load rate program. Consequently, strength S is a function of load rate and therefore does not match with strength in the SCC model.

There is a second, even more serious remark to be made. Integration of equations (1.4) was performed under the condition that initial crack size is much smaller than final crack size and/or $n >> 1$. If this criterion is not fulfilled, integration formally results in

$$\int_0^T \sigma^n dt = \frac{1}{AY^n}\int_{a_0}^{a_T} a^{-n/2} da = C \cdot \left(1 - \left(\frac{\sigma(T)}{S}\right)^{n-2}\right) = C \cdot f(\sigma(T)), \qquad (1.12)$$

where a_T is the crack size at the moment of breaking obtained from the breaking criterion $a_T = \left(\frac{K_{Ic}}{Y\sigma(T)}\right)^2$ and $\sigma(T)$ the actual load at the moment of breaking. The new damage-at-breaking variable $C \cdot f(\sigma(T))$ depends on load and therefore, the SCC model is not embedded in the Coleman model anymore. In Section 5.4 we developed a new model (model A) with a load dependent damage-at-breaking variable and we analyzed the response of this model on a step load program. Summarizing, the SCC model in combination with a Weibull distributed time-to-failure (at constant load) is embedded in the Coleman model only under the simplifying conditions used in 1.4.2. Analysis of the full SCC model inevitably leads to 'non-Coleman' material behavior.

1.6 Objectives and overview of thesis

The objective of our research is to obtain a simple model for failure behavior, i.e. time-to-failure, of Twaron p-aramid yarns. Such a model could be helpful in using short time-to-failure experiments' data (obtained by subjecting fiber samples to relatively large constant loads) to estimate long-term time-to-failure in case the fibers would have been subjected to relatively low constant loads. Another objective is to predict the response of Twaron yarns in case of non-constant load programs, such as a step load programs.

It is well-known that p-aramid yarns have a fully crystalline structure. They do not exhibit a glass transition temperature as commonly observed for amorphous (glassy) and semi-crystalline polymer materials. For the latter materials it is generally accepted that failure satisfies an exponential model as long as the constant load is large enough to bring about ductile failure, and failure satisfies a power-law model for lower loads (brittle failure). That means the the load curve of these materials is not straight and shows a knee, demonstrating that there are multiple failure mechanisms at work. For Twaron fibers, there is no indication of such a knee. Besides, it is not known if failure is ductile or brittle. Empirical evidence for either of these mechanisms could in principle be found from cyclic experiments (accelerated failure (brittle), delayed failure (ductile)) [10]. For Twaron fibers, available cyclic experiments are inconclusive to decide between ductile and brittle failure. From earlier studies it is doubtful if p-aramid yarn can be classified as linear viscoelastic material. It is therefore uncertain if the time-temperature superposition principle can be used, for instance to predict long-term time-to-failure at room temperature based on much shorter failure experiments at elevated temperature. For another of our fiber products, copolymer Technora, we know for certain that the time-temperature superposition principle does not hold.

We do know that Twaron fibers subjected to constant load until failure demonstrate a large sensitivity to load, i.e. if load is a little bit lower, the time-to-failure is much longer. Plotted in a load curve, it is hardly possible to decide which model fits the data best, power-law or exponential. Currently, we use the exponential model for extrapolations because this will give us the most conservative estimates for long-term time-to-failure. We also know that Twaron fibers have significant variability in time-to-failure, e.g. repeated measurements at the same constant load result in a wide range of observed times-to-failure. There is much more scatter in the data than can reasonably be attributed to measurement noise. It was earlier found and again confirmed in this thesis that Twaron fiber variability is well captured by the Weibull distribution. Strength data of Twaron fibers are known to be dependent on load rate. The smaller the load rate, the lower the strength. Variability in strength is much smaller than variability in time-to-failure. Both observations are in line with the Coleman model.

For Twaron fibers, there are presently no engineering rules available. Furthermore, measurements of Twaron fiber subjected to constant load (time-to-failure) or constant load rate (strength) are not in conflict with the Coleman model. The variability in time-to-failure is well described

by the Weibull distribution, which is also in accordance with the Coleman model. As pointed out earlier, the Coleman model is a versatile model. With some restrictions, it may be considered as envelop model for kinetic models based on Tobolsky-Eyring theory and stress corrosion cracking models, both families of physical models are widely used in literature. For all these reasons it makes sense to further investigate the validity of the Coleman model to describe Twaron fiber failure behavior. This model at least has potential to realize our objectives. Therefore, the Coleman model was the starting point in our investigations.

We will now outline the steps in our research and we will do so per chapter separately.

1.6.1 Chapter 2: predicting long-term time-to-failure

This chapter is on accurately predicting long times-to-failure, say 30 years or beyond, for Twaron fibers which are subjected to low loads, representative for industrial load applications. Naturally, it is not feasible to measure these times-to-failure experimentally. Alternatively, short-term experiments are done on Twaron yarns subjected to relatively high loads. Regression can then be used to estimate time-to-failure at low load.

In this chapter it is simply adopted that the Coleman model is indeed a valid model for Twaron fibers. The availability of this model offers an alternative to regression analysis. The model parameters can be estimated based on short-term time-to-failure measurements by means of Maximum Likelihood Estimation (MLE). Once the model and its parameters are known, one can calculate any model response for arbitrary load program. The model can therefore also be used to estimate long-term time-to-failure for relatively low loads.

Except from a comparison between MLE and regression, the design of the 'experimental program' used for the measurement of short-term time-to-failure data is investigated as well. The more data available and the wider the span of loads used in the experimental program, the better will be the estimates for long time-to-failure. It is also shown that the variability in time-to-failure has strong influence on the accuracy of the estimation procedure.

Chapter 2 does not contain real short-term measurement data on Twaron yarn. Instead, data of the experimental program were randomly selected from an appropriate Weibull distribution and MLE and regression estimators were calculated based on these data. By repeating this procedure a large number of times (Monte Carlo simulation), distributions of estimators were obtained rather than single estimators.

1.6.2 Chapter 3: recovering erroneous literature on the truncated Weibull distribution

This is a short chapter on the moments of truncated Weibull distributions. If failure of p-aramid fibers is correctly described by the Coleman model, the residual time-to-failure of these fibers is distributed according to a translated, truncated Weibull distribution. In order to compute mean, variance and other properties of residual time-to-failure, we calculated expressions for the

moments of left-truncated Weibull distributions. We checked our expressions by comparison with expressions in open literature. This caused a lot of confusion because, as was found out later, quite some papers using truncated Weibull distributions carried one or more errors in their moment expressions. Errors were simply copied from one paper to another.

In Chapter 3, an overview is given of the errors we encountered. Naturally, the correct moment expressions for all kinds of truncated Weibull distributions are listed as well.

1.6.3 Chapter 4: residual strength of Twaron fibers

It needs no explication that residual strength of p-aramid fibers, after having served part of their economic lifetime, is of paramount importance. Series of Twaron 2300 fibers were proof tested: they were subjected to a constant preload for some time and, in case of survival, the residual strength was measured. From a theoretical point of view, it was once more assumed that the Coleman model is a valid model for time-to-failure and strength of Twaron fibers. Via introduction of a damage-at-break variable, we derived a translated, left-truncated Weibull distribution as probability density function (pdf) for residual time-to-failure. Intimately related to the pdf for residual time-to-failure, we also derived a slightly more complex probability density function for residual strength. Using the Kolmogorov-Smirnov test, we tested whether we could or could not reject the hypothesis that our residual strength measurements were originating from that probability density function.

The residual strength measurements are very close to the virgin strength of Twaron fiber. By employing a large number of repetitive residual strength measurements we demonstrated that the residual strength distribution, constructed from the Coleman model, statistically significantly underpredicts the residual strength of Twaron fiber.

1.6.4 Chapter 5: non-Coleman behavior of Twaron fibers

Twaron fibers were subjected sequentially to two different loads with a rapid load switch at some specified moment in time. The experiment is continued until failure of the fiber. Naturally, the fiber may also fail prior to the load switch. Such load program is called a single step constant load program or SSP. For each experiment, we calculated the Life Fraction L defined by

$$L = \frac{t_1}{\overline{T}_1} + \frac{t_2}{\overline{T}_2}, \tag{1.13}$$

with t_i the residence time at the i-th load and $\overline{T}_i$ the time-to-failure corresponding to the i-th load. By repeating the experiment many times for the same single step constant load program, a distribution of observations for L is obtained.

For the Coleman model, and a much wider class of models containing the Coleman model as subclass, we proved that the mean of the Life Fraction is unity, i.e. $E[L] = 1$, for arbitrary choice of the SSP. This is in flagrant contradiction with our experimental findings. For some

SSPs we found the complete distribution of L-values to be larger than unity. This clearly proves that the Coleman model is not a valid model for Twaron fiber failure behavior.

In an endeavour to find a more appropriate model for Twaron fiber, we constructed two new classes of probabilistic failure models. Both models have strong roots in open literature. The first model was inspired by the stress corrosion cracking model accommodated with a load dependent failure criterion (see discussion following equation (1.12)). The second model is based on damage growth at constant load via a power function of time with a load dependent power, i.e. $\omega(t) \sim t^{f(\sigma)}$ where ω represents damage at time t. This model was proposed by Marco and Starkey [11] to explain deviation from Palmgren-Miner's Rule in fatigue analysis.

The new models have very distinctive properties with respect to the Life Fraction observed for single step load programs. This offers great opportunity to recognize the underlying failure mechanism. The basic principles of the two models have widespread occurrence in literature, however they are presented almost always in a deterministic form. Our two models, where the same principles are elaborated probabilistically, show distinctive features if applied to single step constant load programs. This means that single step constant load programs are a key tool to ascertain the true nature of failure. Single step constant load programs are also recommended because they require a low number of model parameters.

Unfortunately, Twaron fiber measurements on single step constant load programs do not match with either of the new models. For some specific choices of the loads we even observed partial improvement of the mechanical properties during loading. Such behavior can never be explained by damage models for which damage always grows during loading. Finding an appropriate model for the failure of Twaron fiber therefore requires breaking new ground.

Chapter 2

Modeling failure of high performance fibers: on the prediction of long-term time-to-failure

Abstract

This chapter is based on a paper by Knoester, Hulshof and Meester [12].
Our objective is to predict the time-to-failure distribution of fibers at loads for which mean time-to-failure is comparable or longer than the fibers' economic lifetime. We describe load induced time-to-failure of high performance fiber in terms of a classical probabilistic failure model developed by Coleman. Mimicking a series of time-to-failure measurements, using Monte Carlo simulations, we will show how to capture model parameters and their variability using the least squares method (LSM) and maximum likelihood estimation (MLE). It is relatively easy to obtain an accurate prediction for the maximum allowable fiber load such that time-to-failure exceeds a predefined minimum time-to-failure with high probability. However, obtaining a reliable lower prediction limit for time-to-failure at a given, low fiber load is very difficult and requires an unfeasible extensive program of time-to-failure measurements.

2.1 Introduction

Even if synthetic fibers are loaded far below their tensile strength they fail within finite time. This failure does not require external sources such as chemical or frictional interaction with the environment, but is the result of accumulation of internal damage. The total time a fiber can withstand a constant load is called *the time-to-failure*, and depends on many things like applied load, temperature and material properties.

For long-term applications of high performance fibers in load bearing constructions, the time-to-failure at a certain constant load and temperature is of utmost importance. In practical

applications (e.g. ropes, reinforced pipes) high performance fibers are commonly subjected to stresses below 50% of their strength. Usually, ropes and pipes are replaced after several decades and lifetime is more important than strength. In the laboratory, constant-load experiments on fibers subjected to low loads representative for practical applications, are not feasible because such experiments would last for many years or even decades. To get around this problem, the time-temperature superposition principle (TTSP) may be exploited to predict long-term time-to-failure based on short-term experiments at elevated temperature. For p-aramid fibers this technique was used by Alwis [1] and later a faster version, the stepped isothermal method (SIM), was developed [13]. TTSP supposes linear viscoelastic behavior, which is claimed to be valid for p-aramid fibers subjected to at least 40% of their breaking load [14]. Recently, Giannopoulos [15] applied a superposition principle between time and stress (SSM) to predict long-term time-to-failure. All these superposition methods boil down to the construction of a so-called creep master curve. In effect, the amount of creep is assumed to be directly related to the residual time until failure.

In this chapter a more conventional method is used, detached from creep behavior, simply assuming a functional relationship between time-to-failure and load. Preferably such relationship is embedded in a failure model, and model parameters are estimated from constant load experiments at high load corresponding to short time-to-failure. Long-term time-to-failure at low load is found by extrapolation of the functional relationship. However, justification of such extrapolation is a major problem in lifetime estimation of synthetic fibers.

Repetitive measurements of a fiber's time-to-failure at the same constant load demonstrate large variability. Ignoring differences in fiber handling during the experiments, variability of time-to-failure while exposed to the same constant load is considered to be a natural property of the fiber. Coleman [9] developed a model for time-to-failure of fibers combining a deterministic description of accumulation of damage as function of load history, the *breakdown rule function*, with a probabilistic model for fiber failure given a certain level of damage. Focusing on fibers with the property that damage accumulation only depends on the current load (and not, for instance, on the current damage level), Coleman's model predicts that time-to-failure of such fibers is Weibull distributed with constant shape factor (Weibull modulus) and a scale factor which decreases with increasing applied load. The *strength* can also be Weibull distributed for this class of fibers, however, contrary to time-to-failure, this distribution will depend on the breakdown rule function.

Suppose a fiber was subjected to a set of time-to-failure experiments using relatively high loads with correspondingly short time-to-failure. Under the presumption that the Coleman model is valid for the fiber, application of maximum likelihood estimation (MLE) reworks the experimental data into estimators for the model parameters. These can be used to predict time-to-failure at low loads, being too long to measure experimentally. Alternatively, the least squares method can be used to obtain a linear relationship between measured time-to-failure and applied load, the so-called 'load curve'. Naturally, extrapolation of this load curve is another

way to predict long time-to-failure.

By means of Monte Carlo simulations the estimation procedure for model parameters (MLE) and construction of load curves (LSM) is mimicked. First an 'experimental program' is designed consisting of repeated time-to-failure measurements at a set of support loads. Instead of laboratory measurements, time-to-failure data are randomly drawn from an appropriate Weibull distribution, therefore we use quotation marks around 'experimental program'. Each Monte Carlo simulation consists of this random time-to-failure drawing process followed by MLE and LSM analysis and estimation of the time-to-failure distribution at low load. The short time-to-failure tail of the time-to-failure distribution is important from an engineer's point of view.

In this chapter we show that obtaining reliable estimates for the lower prediction limit of this distribution (e.g. its 5% quantile) for Twaron fibers at a given, low 'object' load is undoable. The variability of the estimates is simply enormous. The problem should be addressed differently by reversing the point of view. Reliable estimates can very well be obtained for the maximum allowable fiber load keeping time-to-failure longer than some predefined 'object' time-to-failure. These conclusions generally hold for estimates obtained from both LSM and MLE. Surprisingly, the extent of the underlying 'experimental program' of time-to-failure measurements has little influence, at least for high performance fibers with a natural time-to-failure variability comparable to Twaron fibers.

The analysis in this study is not only relevant to fibers but also to fiber reinforced products or any product for which lifetime is an important quality. Naturally, a (preferred) shape of the probability distribution function for time-to-failure will generally not be available and tools are thus limited to LSM. In many empirical studies, a load curve is a natural way to visualize lifetime as function of applied load [16–20]. In all these studies, whenever lifetime is a sensitive function of load, the results of our analysis will be of interest.

The chapter is organized as follows. In Section 2.2 we give an introduction and analysis of Coleman's model. In Section 2.3 we describe the various estimation procedures, which we illustrate numerically in Section 2.4. We formulate our conclusions in Section 2.5.

2.2 Introduction and theoretical analysis of the Coleman model

We denote by $\sigma(t)$ the load the fiber is subjected to at time t. Typically we will put $\sigma(t) = \sigma$ (constant load program) or $\sigma(t) = \dot{\sigma}t$ for some $\dot{\sigma} > 0$ (constant load rate program). The load to which the fiber is subjected over a time interval $[0, t]$ is transformed into a *damage intensity* ω_t as follows:

$$\omega_t = \int_0^t \kappa(\sigma(x))dx, \tag{2.1}$$

where the so-called breakdown rule function κ can take two different forms, namely

$$\kappa(x) = \gamma x^\rho \qquad \text{(power-law breakdown), or} \tag{2.2a}$$

$$\kappa(x) = \alpha \exp(\beta x) \quad \text{(exponential breakdown).} \tag{2.2b}$$

In words, the transformed load program $\sigma(t)$ is integrated to yield the damage intensity. In this thesis, the notations ω_t and $\omega(t)$ for the damage intensity or damage function are interchangeably used. We denote the (random) moment of breaking, or *time-to-failure* of a fiber by T. Given a fiber of length ℓ and $t > 0$, Coleman assumes that given a load program and a choice for $\kappa(\cdot)$, the probability that the fiber breaks before time t is given by

$$F_T(t) = 1 - \exp\left\{-\ell(\omega_t)^k\right\}. \tag{2.3}$$

This choice boils down to assuming that the points at which the fiber would break before time t constitute a Poisson process on the interval $[0, \ell]$ with intensity given by $(\omega_t)^k$ and that the fiber does not break before time t exactly when there are no occurrences of the Poisson process in $[0, \ell]$.

There is a so-called weakest-link interpretation of this model choice. Indeed, if we subdivide the rope into n pieces of length ℓ/n, and assume that the probability that a break occurs before time t in a given interval is $(\omega_t)^k\ell/n$, and assume independence between different intervals, then the number of breaking intervals is binomially distributed with parameters n and $(\omega_t)^k\ell/n$. In the limit for $n \to \infty$, this approaches the Poisson distribution with parameter $(\omega_t)^k\ell$. The probability that the fiber does not break before time t is the probability that this Poisson random variable takes the value zero, hence (2.3). (We remark that this is not the way Coleman claims to derive this expression, nor is this his nomenclature. His derivation is different and difficult to make sense of mathematically, but close analysis of his argument reveals that in fact his model boils down exactly to the above mentioned model assumptions.)

Fiber failure is commonly modeled as kinetic process leading to exponential behavior [7, 21–23]. The exponential breakdown rule was also proposed by Coleman [24] as part of a simplified absolute reaction rate theory for the creep failure of oriented polymeric fibers. According to Phoenix [3], the power-law breakdown rule function is actually the superior

approximation despite, in Phoenix' own words, extensive literature supporting the exponential breakdown rule function. Anyway, failure of brittle materials due to stress enhanced crack growth is associated with power-law behavior and is widely and successfully applied to failure of glass fiber and glass fiber reinforced products [8, 25, 26].

In case of a constant load program, (2.3) reduces to the distribution function of a Weibull distribution:

$$F_T(t) = 1 - \exp\left\{-\ell(\kappa(\sigma))^k t^k\right\} = 1 - \exp\left\{-\left(\frac{t}{t_0}\right)^k\right\}, \tag{2.4}$$

with $t_0 = \frac{\ell^{-1/k}}{\kappa(\sigma)}$; hence T is Weibull distributed. We write $T \sim W(k, t_0)$.

In case of a constant load rate program $\sigma(t) = \dot{\sigma}t$, the load at the moment of breaking is defined as *strength* S, that is: $S := \dot{\sigma}T$. In case of the power-law breakdown rule function, it is found that S is also Weibull distributed: $S \sim W(k(\rho+1), s_0)$ with $s_0 = \left(\ell^{-1/k}(\rho+1)\gamma^{-1}\dot{\sigma}\right)^{1/(\rho+1)}$. For the exponential breakdown rule function, the analysis becomes markedly different. Coleman [9] has analyzed this special case in some detail and arrives at an approximate Gumbel distribution function for fiber strength. This approximation is only valid in case the product $\beta\dot{\sigma}t$ is not too small.

Suppose time-to-failure is repetitively measured for a certain fiber at a number of support loads (is 'experimental program'). The objective is to predict time-to-failure at a lower 'object' load (this time-to-failure much too long for direct measurement) based on measurement data of the 'experimental program'. If the fiber is assumed to satisfy the Coleman model ((2.1), (2.2) and (2.3)), we can employ two routes for time-to-failure prediction:

1. Application of the least squares method (LSM) to obtain a linear regression relationship between $\log T$ and $\log \sigma$ (power-law) or σ (exponential). Time-to-failure at object load follows from extrapolation of the regression line.

2. Prediction of model parameters $\gamma,\ \rho,\ k$ (power-law) or $\alpha,\ \beta,\ k$ (exponential) via maximum likelihood estimation (MLE) and subsequent calculation of time-to-failure at object load.

With respect to the LSM-route it is noted that for Weibull distributed T, $\log T$ must be Gumbel distributed (see Appendix A). Then the mean of $\log T$ depends linearly on load (exponential) or logarithm of load (power-law). This observation justifies the application of the least squares method to obtain this linear relationship. In principle, time-to-failure prediction is also possible based on strength measurements (at a number of different support load rates) via the MLE-route. This will not be further elaborated in this chapter.

Time-to-failure at the object load is Weibull distributed. Therefore our prediction methods focus on distribution quantiles such as t_{LPL} (the Lower Prediction Limit for time-to-failure at the object load) with $P(T < t_{\text{LPL}}|\sigma = \sigma_{\text{object}}) = \epsilon$. Similarly we predict the Maximum Allowable Load σ_{MAL} at object time-to-failure t_{object} such that $P(T < t_{\text{object}}|\sigma = \sigma_{\text{MAL}}) = \epsilon$.

In Section 2.3 we derive formulas for prediction of t_{LPL} and σ_{MAL} both for the LSM-route and the MLE-route. In practice, predictions are contaminated with prediction errors (bias and/or large prediction variability) caused by:

- the prediction method (LSM/MLE),
- the (limited) extent of the 'experimental program' and
- the intrinsic variability of time-to-failure.

In Section 2.4 prediction errors will be quantified theoretically by Monte Carlo simulations. It will be shown that the intrinsic variability of time-to-failure is decisive for the quality of the predictors.

2.3 Predicting long-term time-to-failure - theory

For practical purposes, the expected time-to-failure of high performance fibers at low load is of profound industrial importance. Up to which tension may individual fibers in some construction (e.g. rope, fiber-reinforced pipe) be loaded to guarantee a lifetime of at least 30 years? For proper engineering it is relevant to know the mean time-to-failure as well as its distribution. We identify two main routes for prediction of time-to-failure at low load for the constant load program.

LSM route

For fibers satisfying the Coleman model, T is Weibull distributed $T \sim W(k, t_0)$ with only t_0 a function of load ($t_0 \sim \kappa^{-1}(\sigma)$). In Appendix A.4 it is shown that the mean logarithm of time-to-failure $\overline{\log T} \sim -\log \kappa(\sigma)$. Therefore, assuming exponential or power-law behavior, a linear relationship exists between $y = \overline{\log T}$ and a load function v:

$$y = A + B\, v(\sigma) \qquad \text{with} \qquad v(x) = x \quad \text{or} \quad v(x) = \log x. \tag{2.5}$$

Without losing generality it is henceforth assumed that $\log T$ is the common or Briggsian logarithm $\log_{10} T$. The *least squares method* (LSM) is used to estimate intercept A and slope B of this 'load curve'. Having obtained regression estimates $\hat{A}$ and $\hat{B}$, an estimator $\hat{y}(\sigma)$ for $\overline{\log T}$ at arbitrary load σ is simply found from:

$$\hat{y}(\sigma) = \hat{A} + \hat{B}\, v(\sigma). \tag{2.6}$$

For proper application of standard linear regression theory there are three further requirements [27]:

1. Observations of the response variable $\log T$ should be independent and normally distributed. (The normal distribution requirement is necessary to obtain confidence intervals based on the Student t-distribution.)

2. For all observations $(\log T, v)$ the explanatory variable v should be deterministic; not subject to random variation itself.

3. The variance of $\log T$ should be independent of v (to avert weighted least squares techniques).

For fibers satisfying the Coleman model, requirements 2 and 3 are satisfied. With respect to requirement 3 note that if $T \sim W(k, t_0)$ then $\log T \sim G(\log t_0, \log(e)/k)$ (see Appendix A.4). Clearly, the variance of $\log T$ does not depend on the load. The first requirement is not satisfied because $\log T$ is Gumbel, not normally distributed. However, error analysis associated with linear regression analysis is well-known for its robustness as it comes to violation of this requirement.

Regression estimates for the slope and intercept $\hat{A}$ and $\hat{B}$ in equation (2.6) will be based on a series of time-to-failure measurements. Suppose that times-to-failure t_{ij} ($i = 1, 2, \ldots, n_j;\ j = 1, 2, \ldots, m$) are measured repetitively n_j times for m different support loads σ_j. Measurements

should be performed on arbitrary fiber samples to assure independency of the measurements results. We will not really do experiments. Instead, measurements are mimicked by random drawing from time-to-failure distributions (see Section 2.4), therefore our 'measurements' are always independent. The support loads are sufficiently high to obtain short times-to-failure, thus allowing the 'experimental program' to run in a limited period of time. Ultimately, regression analysis is performed on dataset $(\log t_{ij}, v(\sigma_j))$.

We will focus on the distribution of $\log T$ at prescribed object load $\sigma = \sigma_{\text{obj}}$. The object load σ_{obj} is chosen such as to correspond to a time-to-failure in the order of the economic lifetime of the fibers. Although the distribution of $\log T$ is not normal (violation of first requirement), it is simply assumed that $\log T$ is approximately normally distributed with mean $\hat{y}(\sigma_{\text{obj}})$ (see equation (2.6)) and sample standard deviation s, where

$$s^2 = \frac{\sum_{j=1}^{m} \sum_{i=1}^{n_j} \left(\log t_{ij} - \left(\hat{A} + \hat{B} v_j \right) \right)^2}{n-2}, \tag{2.7}$$

with $v_j = v(\sigma_j)$ and $n = \sum_{j=1}^{m} n_j$. Since $\log T$ is assumed to be normal, T itself is lognormally distributed and its estimated mean and variance can be calculated from $\hat{y}(\sigma_{\text{obj}})$ and s^2 (see Appendix A.3). Hence an estimate of the full time-to-failure distribution at object load σ_{obj} is available. For lifetime estimation, the short lifetime tail of the time-to-failure distribution is of utmost importance. We define the lower prediction limit t_{LPL} such that there is a small probability ϵ that an arbitrary observation of T remains below t_{LPL}: $P(T < t_{\text{LPL}} | \sigma = \sigma_{\text{obj}}) = \epsilon$. Multiple ways of t_{LPL} estimation are possible. In the following we propose two estimators for t_{LPL}. Since time-to-failure is lognormally distributed, our first estimate for t_{LPL} is readily obtained using the cumulative distribution function of the lognormal distribution (see equation (A.3) in Appendix A):

$$\begin{aligned} \hat{t}_{\text{LPL, LSMa}} &:= \exp\left\{ \hat{y}(\sigma_{\text{obj}}) \ln 10 - \sqrt{2} \cdot \text{erf}^{-1}(1-2\epsilon) \cdot s \ln 10 \right\}, \text{ or:} \\ \log\left(\hat{t}_{\text{LPL, LSMa}} \right) &:= \hat{y}(\sigma_{\text{obj}}) - \sqrt{2} \cdot \text{erf}^{-1}(1-2\epsilon) \cdot s. \end{aligned} \tag{2.8}$$

Only in case $\hat{y}(\sigma_{\text{obj}})$ and s are close to the true mean and standard deviation of the $\log T$ distribution, the above estimate will prove accurate. Estimator (2.8) does not reckon with uncertainty in the mean $\hat{y}(\sigma_{\text{obj}})$ which depends on the quality of regression via $\hat{A}$ and $\hat{B}$. An estimate for the standard deviation of the estimator $\hat{y}(\sigma_{\text{obj}})$ distribution is derived from standard regression analysis:

$$\hat{s}_{\hat{y}}(\sigma_{\text{obj}}) = s \sqrt{\frac{1}{n} + \frac{\left(v(\sigma_{\text{obj}}) - \bar{v}\right)^2}{n\left(\overline{v^2} - \bar{v}^2\right)}}, \tag{2.9}$$

where $\bar{v} = \frac{1}{n} \sum_{j=1}^{m} n_j v_j$ and $\overline{v^2} = \frac{1}{n} \sum_{j=1}^{m} n_j v_j^2$. So there are two, uncorrelated sources of variability for $\log T$, notably its intrinsic variability (a material property) and additional variability induced

by extrapolation of the regression line. The reliability of their estimators, s and $\hat{s}_{\hat{y}}(\sigma_{\text{obj}})$ respectively, depends on the extent and design of the experimental program. The overall standard deviation of $\log T$ is commonly estimated [27, 28] as:

$$\hat{s}_{\log T}(\sigma_{\text{obj}}) = \sqrt{\hat{s}^2_{\hat{y}}(\sigma_{\text{obj}}) + s^2} = s\sqrt{1 + \frac{1}{n} + \frac{\left(v(\sigma_{\text{obj}}) - \overline{v}\right)^2}{n\left(\overline{v^2} - \overline{v}^2\right)}}. \tag{2.10}$$

The corresponding $100(1-2\epsilon)\%$ prediction interval for $\log T$ from regression theory is then given by

$$\left(\hat{y}(\sigma_{\text{obj}}) - t_{\epsilon,n-2} \cdot \hat{s}_{\log T}(\sigma_{\text{obj}}), \quad \hat{y}(\sigma_{\text{obj}}) + t_{\epsilon,n-2} \cdot \hat{s}_{\log T}(\sigma_{\text{obj}})\right), \tag{2.11}$$

with constant $t_{\epsilon,n-2}$ defined such that $P(\tau < -t_{\epsilon,n-2}) = P(\tau > t_{\epsilon,n-2}) = \epsilon$ with τ a Student t distributed variable with $(n-2)$ degrees of freedom. The lower boundary of the prediction interval can easily be reworked into a lower prediction limit for T:

$$\log\left(\hat{t}_{\text{LPL, LSMb}}\right) := \hat{y}(\sigma_{\text{obj}}) - t_{\epsilon,n-2} \cdot \hat{s}_{\log T}(\sigma_{\text{obj}}). \tag{2.12}$$

Estimator (2.12) is more conservative than estimator (2.8), i.e. gives the shortest lower prediction limit for time-to-failure. Note that for large n, $\hat{s}_{\log T}(\sigma_{\text{obj}}) \downarrow s$ and $t_{\epsilon,n-2} \downarrow \sqrt{2} \cdot \text{erf}^{-1}(1-2\epsilon)$ so both estimates become equivalent. (Student t distribution approaches the Standard Normal distribution for $n \to \infty$). There are hybrid definitions of t_{LPL} possible, in between estimators (2.12) and (2.8). For example $\log\left(\hat{t}_{\text{LPL, LSMc}}\right) := \hat{y}(\sigma_{\text{obj}}) - t_{\epsilon,n-2} \cdot s$, which seems to be a proper choice if $s >> \hat{s}_{\hat{y}}(\sigma_{\text{obj}})$. For $\epsilon = 0.05$ the distance of this hybrid to estimator (2.8) is insignificant because $t_{\epsilon,n-2}$ is at most 5% larger than $\sqrt{2} \cdot \text{erf}^{-1}(1-2\epsilon)$ for $n > 22$. Anyway, one should be careful while focusing on the tails of the time-to-failure distribution. Errors in estimators may be significant if the true distribution of $\log T$ deviates from the normal distribution. The more so while concentrating on ever smaller tails, containing the most extreme (short) times-to-failure. Since the shape of the tail of the time-to-failure distribution is not known in detail, we recommend not to choose ϵ too low.

In Section 2.4 we will show that the lower prediction limit of time-to-failure is anyway difficult to predict, even for extended experimental programs. A promising alternative is to perform inverse regression [27]. Given an object time-to-failure t_{obj}, we can derive estimates for the maximum allowable load σ_{MAL} such that: $P(T < t_{\text{obj}} | \sigma = \sigma_{\text{MAL}}) = \epsilon$. Estimates for σ_{MAL} are found by equating estimates for t_{LPL} (equations (2.8) and (2.12)) to t_{obj} while replacing σ_{obj} by σ_{MAL} and solving for the latter:

$$\begin{aligned} v(\hat{\sigma}_{\text{MAL, LSMa}}) &:= \left(\log t_{\text{obj}} + \sqrt{2} \cdot \text{erf}^{-1}(1-2\epsilon) \cdot s - \hat{A}\right)/\hat{B}, \\ v(\hat{\sigma}_{\text{MAL, LSMb}}) &:= \left(\log t_{\text{obj}} + t_{\epsilon,n-2}\, \hat{s}_{\log T}(\hat{\sigma}_{\text{MAL, LSMb}}) - \hat{A}\right)/\hat{B}. \end{aligned} \tag{2.13}$$

The equation for $\hat{\sigma}_{\text{MAL, LSMb}}$ is implicit but can readily be solved using elementary calculus.

MLE route

Another route to obtain a prediction for time-to-failure is by accepting the validity of Coleman's model and subsequently estimating the parameters (γ, ρ, k) or (α, β, k). This set of parameters fully determines the Weibull distribution of time-to-failure for any object load σ_{obj}. Parameter estimation can be performed with maximum likelihood estimation (MLE) as explained in Appendix B. Let $(\hat{\gamma}, \hat{\rho}, \hat{k})$ or $(\hat{\alpha}, \hat{\beta}, \hat{k})$ be the corresponding ML estimators. Again focusing on the short time-to-failure tail of the distribution, $100\epsilon\%$ of the observed times-to-failure (ϵ is the significance level) at load $\sigma = \sigma_{\text{obj}}$ is expected to be shorter than the ϵ-quantile given by:

$$\hat{t}_{\text{LPL,MLE}} = \hat{t}_0 \left(-\ln(1-\epsilon)\right)^{1/\hat{k}}, \tag{2.14}$$

where: $\hat{t}_0 = \ell^{-1/\hat{k}} \cdot e^{-\hat{\rho}\ln\sigma_{\text{obj}} - \ln\hat{\gamma}}$ (power-law) or $\hat{t}_0 = \ell^{-1/\hat{k}} \cdot e^{-\hat{\beta}\sigma_{\text{obj}} - \ln\hat{\alpha}}$ (exponential). Ignoring variability of the model parameters themselves, this estimate for t_{LPL} only takes into account intrinsic variability of time-to-failure. Rewriting formula (2.14) with $t_{\text{LPL}} = t_{\text{obj}}$, $\sigma_{\text{obj}} = \sigma_{\text{MAL}}$ and solving for σ_{MAL} yields:

$$\begin{aligned}
\hat{\sigma}_{\text{MAL, MLE}} &:= \left\{ \frac{\left(-\ln(1-\epsilon)\right)^{1/\hat{k}}}{\ell^{1/\hat{k}}\,\hat{\gamma}\,t_{\text{obj}}} \right\}^{1/\hat{\rho}} \qquad \text{(power-law)}, \\
\hat{\sigma}_{\text{MAL, MLE}} &:= \frac{1}{\hat{\beta}} \ln\left\{ \frac{\left(-\ln(1-\epsilon)\right)^{1/\hat{k}}}{\ell^{1/\hat{k}}\,\hat{\alpha}\,t_{\text{obj}}} \right\} \qquad \text{(exponential)}.
\end{aligned} \tag{2.15}$$

2.4 Predicting long-term time-to-failure - Monte Carlo simulations

We have outlined two main routes for predicting time-to-failure at low load. We explore these prediction routes by numerical simulation. The measurements underlying the predictions are simulated by randomly drawing time-to-failure from a Weibull distribution after choosing appropriate distribution parameters. Prior to this, an 'experimental program' is defined, specifying a set of support loads for which the times-to-failure are to be drawn. Each computation covers $10,000$ Monte Carlo simulations and runs through the following steps:

1. specify fiber properties: power-law or exponential breakdown rule function inclusive model parameters (these so-called 'target parameters' will serve as a reference for the estimators).

2. specify 'experimental program': select support loads and the number of to be observed times-to-failure per support load ('observations').

3. specify 'object load' or 'object time-to-failure'.

4. per Monte Carlo simulation, using MLE and LSM, compute time-to-failure distribution at object load and/or compute load distribution at object time-to-failure

Ad. 1
A fiber satisfying the Coleman model (henceforth called 'Coleman fiber') is fully described by three parameters: γ, ρ and k (power-law) or α, β and k (exponential). Selection of these (target) parameters is constrained as follows:

- Both the time-to-failure variability (determined by Weibull modulus k) and 'ρ' or 'β', describing how strongly time-to-failure depends on applied load for the power-law and exponential breakdown rule function respectively, are free to choose. They will be chosen in accordance with observed properties of high performance Twaron fibers.

- The third parameter, 'γ' or 'α' (describing the absolute level of time-to-failure at given load), is selected such as to enforce that the strength of a fiber (at load rate $\dot{\sigma} = 0.5\, GPa/s$) is fixed.

Ad. 2
The 'experimental program' is systemized by selecting support loads $\boldsymbol{\sigma} = (\sigma_1, \sigma_2, \sigma_3, \sigma_4, \sigma_5)$ in such a way that the mean time-to-failure at load σ_i is $10^{(i-1)}$ hr: thus the mean time-to-failure vector $\overline{\mathbf{T}} = (1, 10, 10^2, 10^3, 10^4)$ hr corresponds to $\boldsymbol{\sigma}$. Vector $\mathbf{n} = (n_1, n_2, n_3, n_4, n_5)$ contains the number of observations for support loads σ_1 to σ_5.

2.4.1 Estimation of model parameters

The first step in the process of predicting time-to-failure is the estimation of the Coleman model parameters (MLE) or the regression parameters (LSM). Figure 2.1 (top) clearly shows that the estimator for the Weibull modulus k overestimates its target value and the LSM sample standard deviation s (equation (2.7)) underestimates the target standard deviation of the Gumbel distribution for $\log T$. Apparently, for an unbiased estimate of the variability in the logarithm of time-to-failure, a relatively large number of observations in the 'experimental program' is required. All other parameter estimates (e.g. ρ or slope B) are unbiased, even in case of a small number of observations in the 'experimental program'. This does not automatically mean that accurate predictions are obtained for these parameters: the variability in the estimator distribution can be quite large, the more so if the number of observations is small (see Figure 2.1 (bottom)).

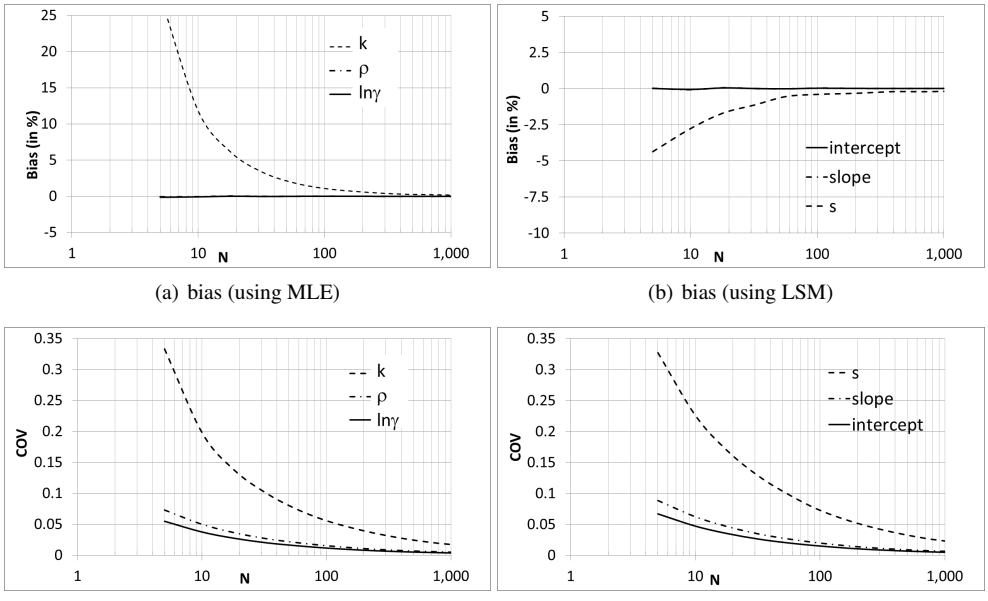

(a) bias (using MLE)

(b) bias (using LSM)

(c) COV (using MLE)

(d) COV (using LSM)

Figure 2.1: *Estimated model parameters using Maximum Likelihood Estimation (MLE) or Least Squares Method (LSM) for a power-law Coleman fiber ($S = 3$ GPa, $k = 2$, $\rho = 40$).*
Bias in % and coefficient of variation (COV) of Monte Carlo estimates.
Using $\mathbf{n} = (N,0,N,0,0)$ *with* $5 \leq N \leq 1{,}000$.

2.4.2 Prediction of time-to-failure distribution

For each Monte Carlo simulation, using MLE or LSM, a time-to-failure distribution can be computed at object load σ_{obj}. How well do all these distributions compare to the target time-to-failure distribution determined by the target parameters? Instead of inspecting $10,000$ different distributions, we construct one single, new distribution by randomly drawing one time-to-failure from each of these distributions. So for each Monte Carlo simulation and a prescribed object load σ_{obj}, one time-to-failure is drawn from the predicted Weibull distribution (MLE) and one time-to-failure is obtained from a randomly drawn $\log T$ from its predicted normal distribution (LSM).

In Figure 2.2 the $10,000$ times-to-failure are plotted as a bar chart, without plotting the bars themselves, but by dots with one dot per bar representing the normalized, mean number of observations in that bar (bar width is 4 years). These distributions, constructed via the MLE and LSM routes, are compared with the target Weibull distribution in Figure 2.2. Apparently, if the number of observations per support load N is large enough and using the MLE route, the predicted time-to-failure distribution closely resembles the pdf of the target Weibull distribution.

2.4.3 Prediction of the 'short times'-tail of the time-to-failure distribution

From a practical point of view, accurate prediction of σ_{MAL} at specified object time-to-failure or t_{LPL} at specified object load are important. In Figure 2.3, the sets $\{\hat{\sigma}_{\text{MAL}}\}$ and $\{\hat{t}_{\text{LPL}}\}$ (prediction sets collected over all Monte Carlo simulations) are plotted for significance level $\epsilon = 0.05$ and various 'experimental programs'. The vertical lines represent the targets. The object time-to-failure for calculation of $\hat{\sigma}_{\text{MAL}}$ was chosen $t_{\text{obj}} = 30$ yr. For $\hat{t}_{\text{LPL}}$ calculation, the specified object load $\sigma_{\text{obj}} = 1.655$ GPa enforces a target value of $t_{\text{LPL}} = 30$ yr for proper comparison. In Figure 2.3 (and succeeding figures), the estimator sets $\{\hat{\sigma}_{\text{MAL}}\}$ and $\{\hat{t}_{\text{LPL}}\}$ are represented as 'relative frequency curves'. The area below the curve, bounded by the verticals $x = x_1$ and $x = x_2$, equals the relative number of calculated estimators in the interval (x_1, x_2).

The predicted $\hat{t}_{\text{LPL}}$ can be far off its target value of $t_{\text{LPL}} = 30$ yr. Extending the 'experimental program' by adding extra observations (Figure 2.3 (top, right)) or increasing the span of the support loads (Figure 2.3 (bottom, right)) does push the estimates towards their target, but the probability of obtaining a much too optimistic or pessimistic value for t_{LPL} remains high. Neutralizing optimistic values by multiplication with a safety factor $0 < S_f < 1$ is no option: too many observations for $S_f\,\hat{t}_{\text{LPL}}$ would become unacceptably small. It is noted that extending the 'experimental program' with time-to-failure observations at 10^4 hr (instead of 10^3 hr) has hardly any effect: the spread in the estimates $\hat{t}_{\text{LPL}}$ is entirely due the natural variability of the Coleman fiber.

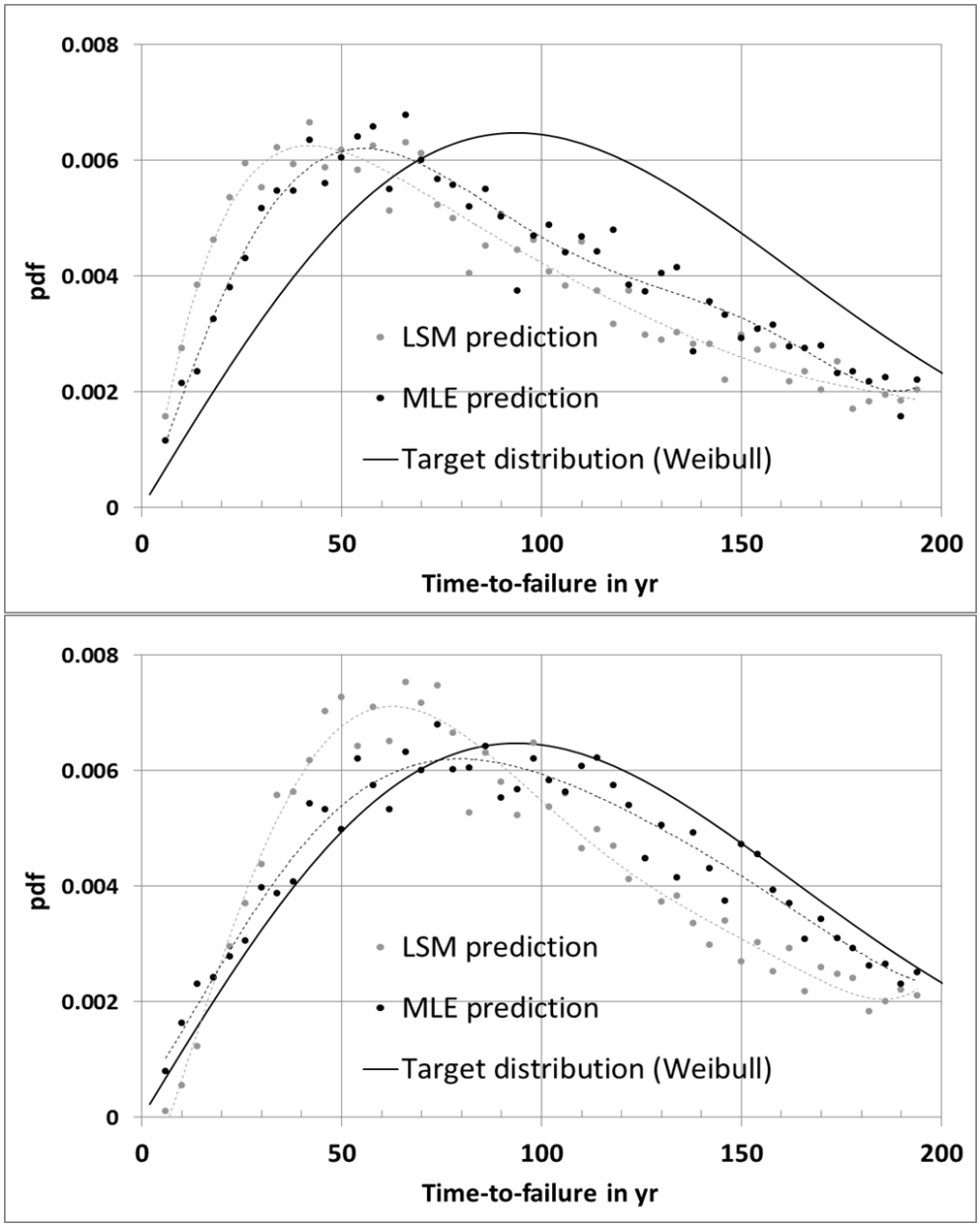

Figure 2.2: *Estimated time-to-failure probability distribution function (pdf) with target Weibull distribution (solid line) at object load 1.655 GPa for a power-law Coleman fiber ($S = 3$ GPa, $k = 2$, $\rho = 40$). Using $\mathbf{n} = (N,0,N,0,0)$ with $N = 10$ (top) and $N = 40$ (bottom). For clarification on the estimated distribution functions see text in 2.4.2.*

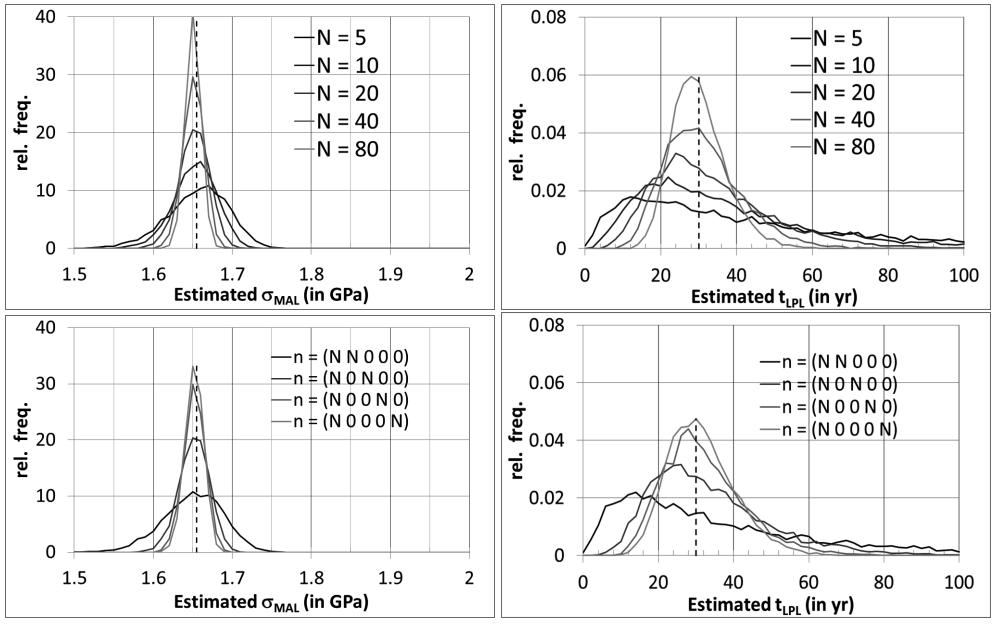

Figure 2.3: *MLE estimated σ_{MAL} (left @ $t_{\text{obj}} = 30$ yr) and t_{LPL} (right @ $\sigma_{\text{obj}} = 1.655$ GPa) for a power-law Coleman fiber ($S = 3$ GPa, $k = 2$, $\rho = 40$) and $\epsilon = 0.05$. Using $\mathbf{n} = (N,0,N,0,0)$ with variable N (top) and $N = 20$ with variable support load span (bottom).*
Dashed vertical lines are target values for σ_{MAL} and t_{LPL}.

Contrary to the time-to-failure lower prediction limit, estimates for the upper prediction limit for loads at given object time-to-failure are very close to their target value (Figure 2.3 (left)). A relatively high safety factor $S_f \sim 0.8$ is sufficient to force predictions below but still close to their target value. Anyway, an extensive 'experimental program' (with observations beyond 10^3 hr and/or huge numbers of observations per support load) certainly is no requirement for accurate predictions.

2.4.4 Effect of fiber properties on time-to-failure prediction

Naturally, for prediction of long-term time-to-failure it is of utmost importance to discover its load sensitiveness, i.e. the slope of the load curve. The steeper the curve, the higher the maximum allowable load will be for given object time-to-failure (see Figure 2.4 (right)). However, the predictability of σ_{MAL}, symbolized by the width of its Monte Carlo prediction set, is hardly affected by the load curve's slope. The natural time-to-failure variability (viz. Weibull modulus k) seems at least as important for prediction of σ_{MAL}. High variability (low k) reduces σ_{MAL} significantly and, even worse, cuts back its predictability thus necessitating more conservative safety factors (see Figure 2.4 (left)). Predictability can effectively be regained by extending the 'experimental program', e.g. by increasing the number of observations per support load as was shown earlier.

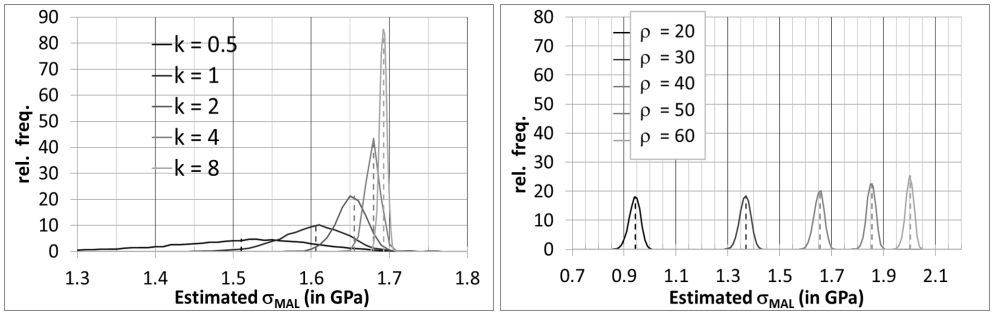

Figure 2.4: *MLE estimated σ_{MAL} for variable k while $\rho = 40$ (left) and variable ρ while $k = 2$ (right) for a power-law Coleman fiber ($S = 3$ GPa) and $\epsilon = 0.05$.*
Using $\mathbf{n} =$ (20,0,20,0,0) and $t_{\text{obj}} = 30$ yr.
Dashed vertical lines are targets.

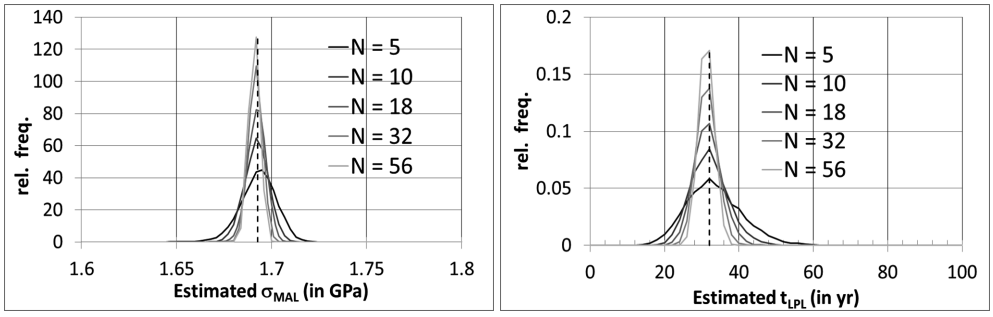

Figure 2.5: *MLE estimated σ_{MAL} (left @ $t_{\text{obj}} = 30$ yr) and t_{LPL} (right @ $\sigma_{\text{obj}} = 1.69$ GPa) for $k = 8$ and $\rho = 40$ for a power-law Coleman fiber ($S = 3$ GPa) and $\epsilon = 0.05$.*
Using $\mathbf{n} = (N,0,N,0,0)$ with variable N.
Dashed vertical lines are targets: $\sigma_{\text{MAL,target}} = 1.6928$ GPa and $t_{\text{LPL,target}} = 32.055$ yr.

The Weibull modulus k turns out to be decisive as it comes to predictability of both σ_{MAL} and t_{LPL}. Previously it was shown that for $k = 2$ the maximum allowable load σ_{MAL} is very well predictable, even for a short 'experimental program'. However, predictability of t_{LPL} required an unfeasibly extensive 'experimental program'. If the time-to-failure is much less variable described by say $k = 8$, overall predictability would increase so much that proper prediction of t_{LPL} becomes feasible (see Figure 2.5). On the other hand, if variability is much larger (say $k = 0.5$), then even predictability of σ_{MAL} is poor.

2.4.5 Comparison between MLE and LSM prediction routes

Not surprisingly, applying inverse regression on the load curve yields prediction sets for σ_{MAL} slightly wider than found using MLE. Besides, the LSM predictions are biased: for LSMa the bias is always positive (on average too optimistic values for σ_{MAL}), bias for LSMb may be positive or negative, depending on the 'experimental program' (see Figure 2.6). MLE predictions are also positively biased, however bias is lifted for a sufficiently large number of observations in the 'experimental program'. For LSM, bias is structural. All in all, both bias and wider prediction sets obtained for LSM require more conservative safety factors, but differences between MLE and LSM are minor. The present simulations therefore justify the application of LSM to obtain predictions for long-term time-to-failure, even if time-to-failure is Weibull distributed.

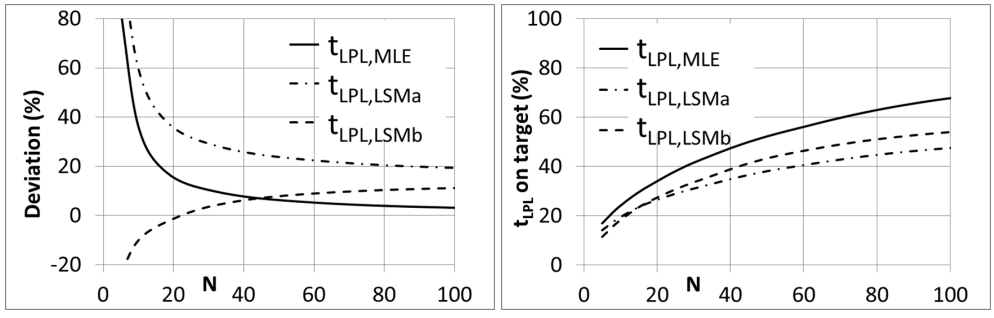

(a) bias of mean t_{LPL} with respect to target

(b) percentage of MC-simulations predicting t_{LPL} within 20% of target

Figure 2.6: *LSM and MLE estimated t_{LPL} for $k = 2$ and $\rho = 40$ for a power-law Coleman fiber ($S = 3$ GPa) and $\epsilon = 0.05$.*
Using $\mathbf{n} = (N,0,N,0,0)$ with variable N and $\sigma_{\text{obj}} = 1.655$ GPa ($t_{\text{LPL,target}} = 30$ yr).

2.4.6 Power-law versus exponential failure behavior

Experimental failure data usually do not allow for a justified choice for either a power-law or exponential relationship between time-to-failure and load, however their predictions for long-term time-to-failure are markedly different, the exponential model being the more conservative. The present Monte Carlo simulation procedure allows for calculation of prediction errors in case 'the wrong' model is chosen. That is: suppose the target fiber truly behaves according to the power-law model but its experimental data are (mis-)interpreted as if the fiber would behave according to the exponential model and the other way around. Figure 2.7 demonstrates the expected under- and overestimation of the maximum allowable load σ_{MAL}. Overestimation is most critical and should be bought off with a more conservative safety factor. Naturally, prediction errors of this type increase in case of further extrapolation (see Figure 2.8). The error fades for a widened span of support loads (see Figure 2.8 (left)).

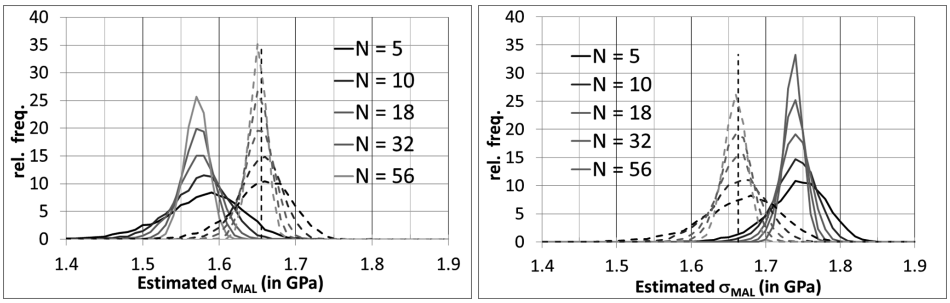

Figure 2.7: *MLE estimated σ_{MAL} for $k = 2$ and a Coleman fiber ($S = 3$ GPa) and $\epsilon = 0.05$. Using $\mathbf{n} = (N,0,N,0,0)$ with variable N and $t_{\mathrm{obj}} = 30$ yr.*
Left: power-law fiber with $\rho = 40$ ($\sigma_{\mathrm{MAL,target}} = 1.655$ GPa), assuming a power-law (dotted lines) or an exponential model (solid lines, underestimation).
Right: exponential fiber with $\beta = 18$ ($\sigma_{\mathrm{MAL,target}} = 1.663$ GPa), assuming an exponential (dotted lines) or a power-law model (solid lines, overestimation).

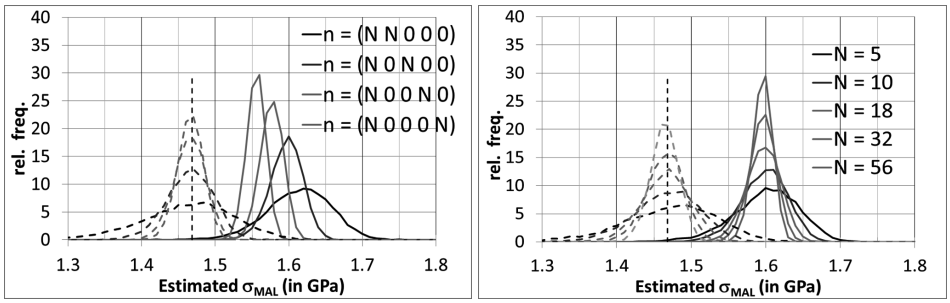

Figure 2.8: *MLE estimated σ_{MAL} for a target exponential Coleman fiber ($S = 3$ GPa, $\beta = 18$, $k = 2$) and $\epsilon = 0.05$, using $t_{\mathrm{obj}} = 1{,}000$ yr ($\sigma_{\mathrm{MAL,target}} = 1.468$ GPa), with variable support load span and $N = 20$ (left) or using $\mathbf{n} = (N,0,N,0,0)$ and variable N (right).*
Assuming an exponential (dotted lines) or a power-law model (solid lines).

2.5 Discussion and conclusions

The results of many experimental studies on the failure time of industrial products subjected to a certain loading (including axially stressed fibers) are described in terms of 'load curves', suggesting a linear relationship between the logarithm of the failure time and the load or the logarithm of the load. Both types of load curves can be inferred from Coleman's model after applying either the power-law or the exponential breakdown rule. For high performance fibers, time-to-failure is extremely sensitive to load. Predicting time-to-failure at low load boils down to predicting the load curve close to this low load. Due to its steepness, a small uncertainty in the load curve's position will have a large effect on the predicted time-to-failure. In fact, time-to-failure for a prescribed (low) fiber load turns out to be almost unpredictable in case a small but unknown error is inflicted upon this load. This conclusion at least holds for high performance fibers with Weibull distributed time-to-failure and Weibull modulus $k \leq 4$, like Twaron. The benefits of extending the 'experimental program' (more observations per support load and/or widening the span of the support loads by for instance adding experimental data with very long time-to-failure of say 10^4 hr or 1.14 yr) are rather limited. The lower prediction limit of time-to-failure remains undesirably variable, the main cause being the natural variability of the fiber itself. Examination and prediction of failure data of fibers or fiber reinforced products, exhibiting load-sensitive failure behavior and moderate time-to-failure variability should be carried out with caution. The common use of linear regression with its standard error analysis of predictions is likely to provide very unreliable results. Starting with an alleged probability distribution for fiber time-to-failure and using MLE, the accuracy of predictions is not expected to improve substantially.

From an engineering point of view, the unpredictability of long-term time-to-failure is not a hopeless dead-end. It is merely a matter of posing the right question. Instead of recovering the time-to-failure properties of a fiber subjected to some design loading one should focus on establising the (maximum) allowable load for some design time-to-failure. For very steep load curves, slightly reducing the fiber's load will firmly extend time-to-failure and thus shift the fiber into a safe operating window. The present study shows that the maximum allowable load to guarantee some prescribed (desired) product lifetime is well predictable. Both with MLE and LSM, the latter with inverse regression error analysis. Reliable predictions of the maximum allowable load do not require extensive 'experimental programs'. Short programs, with a limited number of relatively short time-to-failure observations are sufficient. Again, the most important parameter influencing prediction quality is the natural variability in fiber time-to-failure. For fibers with highly variable time-to-failure, prediction quality reduces and more conservative safety factors are necessary.

Most failure studies, aiming at the construction of a 'load curve' to describe product time-to-failure as function of applied load, focus on measuring the load curve's slope and intercept. We want to stress that natural product variability with respect to time-to-failure is also important.

This variability predominantly determines the feasibility of prediction of long-term time-to-failure and sets the size of the safety factor. Natural variability can be inferred from the sample standard deviation (LSM) or simply the Weibull modulus if time-to-failure is assumed to be Weibull distributed.

The necessity for an extensive 'experimental program' (e.g. including time-to-failure measurements up to 10^4 hr) for optimum accuracy of time-to-failure prediction is called into question. Numerical simulations in the present study do not confirm the importance of such a program. Prediction of time-to-failure at prescribed load is unreliable and prediction of maximum allowable load at prescribed time-to-failure is reliable (at least for the fiber properties studied), largely independent of the size of the 'experimental program'.

Still, long-term time-to-failure measurement can be very important for other reasons, for instance to disprove (or demonstrate) other failure mechanisms (other than creep rupture). A 'straight' load curve can bend downwards for long time-to-failure and evidence a different failure mechanism (e.g. by chemical attack).

There is yet another reason to add long-term time-to-failure measurements. In most situations there is no strong evidence for either a power-law or exponential relationship between time-to-failure and load and still either of these relationships is chosen to work with. Without claiming that long-term time-to-failure measurements can definitely determine the true relationship between time-to-failure and load (power-law or exponential), adding long-term time-to-failure measurements in the 'experimental program' will at least reduce prediction errors if the wrong relationship was chosen.

Chapter 3

Re-examination of moment expressions for truncated Weibull distributed variables

Abstract

This chapter provides an overview of moment expressions for both singly and doubly truncated Weibull distributed variables, also recovering some erroneous expressions which have penetrated the literature on this topic during the past years. Moment expressions for translated, left-truncated Weibull distributed variables, frequently used to describe residual lifetime, are summarized as well.

3.1 Introduction

Truncated Weibull distributions have found their way in various practical applications, e.g in hydrology [32], fatigue strength of composites [33], residual lifetime of equipment, components or materials [34], diameter distribution of pine trees in the Mediterranean region [35], wind speed [36], fire size distribution [37] and others. McEwen and Parresol [38] and Wingo [39] published papers on the moments of these distributions which have deservedly become frequently cited papers. In the vast literature on truncated Weibull distributions, some mistakes were introduced in moment expressions and copied by others. This may be confusing to the unsuspicious reader. In this chapter we correct some mistakes.

First we derive a general expression for the moments of the doubly truncated Weibull distribution. We start with the cumulative distribution function (cdf) of a 3-parameter Weibull distributed variable X:

$$F_X(x) = 1 - \exp\left(-\left(\frac{x-a}{b}\right)^c\right), \quad \text{for } x > a \geq 0.$$

Next, this distribution is doubly truncated by elimination of observations for X below t_1 (with $t_1 > a$) and above t_2 (with $t_2 > t_1$):

$$F_{X_d}(x) = \frac{F_X(x) - F_X(t_1)}{F_X(t_2) - F_X(t_1)}, \quad \text{for } t_1 < x < t_2. \tag{3.1}$$

The moments of a doubly truncated Weibull variable X_d follow from:

$$\begin{aligned} E[X_d^n] &= \int_{t_1}^{t_2} x^n \frac{d}{dx} F_{X_d}(x) dx = \frac{1}{F_X(t_2) - F_X(t_1)} \int_{t_1}^{t_2} x^n \frac{d}{dx} F_X(x) dx \\ &= P(u_1, u_2) \int_{u_1}^{u_2} \left(bu^{1/c} + a\right)^n \exp(-u) du \\ &= P(u_1, u_2) \sum_{k=0}^{n} \binom{n}{k} b^k a^{n-k} \left(\Gamma_{\text{lower}}(1 + k/c, u_2) - \Gamma_{\text{lower}}(1 + k/c, u_1)\right), \end{aligned} \tag{3.2}$$

where $u_1 = \left(\frac{t_1 - a}{b}\right)^c$, $u_2 = \left(\frac{t_2 - a}{b}\right)^c$, $P(u_1, u_2) = 1/\left(\exp(-u_1) - \exp(-u_2)\right)$ and the lower incomplete gamma function $\Gamma_{\text{lower}}(p, x) = \int_0^x u^{p-1} \exp(-u) du$. As a service to the reader, an overview of moment expressions for doubly and singly truncated Weibull distributed variables is provided at the end of this chapter. Here, expressions for the first moment or expectation ($n = 1$) and for vanishing location parameter ($a = 0$) are given separately for these are employed frequently in literature.

3.2 Erroneous moment expressions in literature

The majority of all literature on (the application of) truncated Weibull distributions refer to the paper of McEwen and Parresol [38]. Unfortunately, there is an error in their general expression for the moments of the doubly truncated Weibull distribution. Instead of:

$$P(u_1, u_2) = \frac{1}{\exp\left(-\left(\frac{t_1-a}{b}\right)^c\right) - \exp\left(-\left(\frac{t_2-a}{b}\right)^c\right)} \tag{3.3}$$

before the $\sum$-symbol in (3.2) they use (in their formula (14)):

$$\frac{\exp\left(\left(\frac{t_1-a}{b}\right)^c\right)}{1 - \exp\left(-\left(\frac{t_2-a}{b}\right)^c\right)}. \tag{3.4}$$

Note that the error neutralizes for the left-truncated Weibull distribution ($t_2 \to \infty$) as well as for the right truncated Weibull distribution ($t_1 = a$). In 1993, an erratum was published by McEwen and Parresol [40]. This short note is not well-known in the community, evidenced by the fact that the original error is still copied in modern literature [41, 42]. Moreover, we did not find a reference to the erratum anywhere.

We came across additional errors in more recent literature, some of them replicate in literature as well. Most troublesome are incorrect moment expressions, published without derivation, in reviews or surveys. Colleague scientists in various fields, considering the erroneous expressions as factual, may easily mutilate their own work. Besides, there is high probability that erroneous expressions spread out further in literature.

Next we will discuss (and correct) erroneous moment expressions we encountered.

- Murthy et al. [41] cite the following moment expression for the doubly truncated Weibull distribution:

$$E[X^n] = \frac{\exp\left(\left(\frac{b-\tau}{\alpha}\right)^\beta\right)}{1 - \exp\left(-\left(\frac{a-\tau}{\alpha}\right)^\beta\right)} \cdot \sum_{k=0}^{n} \binom{n}{k} \alpha^k \tau^{n-k} \cdot \left\{ \Gamma\left(1 + \frac{k}{\alpha}, \left(\frac{b-\tau}{\alpha}\right)^\beta\right) - \Gamma\left(1 + \frac{k}{\alpha}, \left(\frac{a-\tau}{\alpha}\right)^\beta\right) \right\}. \tag{3.5}$$

  In order to relate their and our nomenclature note that $a = \tau$, $b = \alpha$, $c = \beta$, $t_1 = a$ and $t_2 = b$. Apart from some minor mistakes, i.e. omission of brackets and lacking definition of their Γ-function, they apparently copied the mistake of McEwen and Parresol and also consequently interchanged a and b (our t_1 and t_2).
  We presume that Murthy et al. meant to use the upper incomplete gamma function in their expression: $\Gamma(p, x) = \Gamma_{\text{upper}}(p, x)$.

- Nadarajah and Kotz [42] also publish the general moment expression for a doubly truncated Weibull variable, only this time for the simpler case of vanishing location parameter ($a = 0$). Here, exactly the same mistakes were made as in Murthy et al.

- Zhang and Xie [43] provide expressions for the mean and variance of a right truncated Weibull variable:

$$\mu = \frac{\eta\Gamma(1+1/\beta)}{1-\exp\left(-u_T\right)}; \quad \sigma^2 = \frac{\eta^2\Gamma(1+2/\beta)}{1-\exp\left(-u_T\right)} - \mu^2 \quad \left(u_T = \left(\frac{T}{\eta}\right)^{\beta}\right).$$

  In order to relate their and our nomenclature note that $a = t_1 = 0$, $b = \eta$, $c = \beta$, $t_2 = T$. In these expressions the ordinary Γ-function should have been replaced by the lower incomplete gamma function: $\Gamma_{\text{lower}}(1 + 2/\beta, u_T)$. Lai [44] and Kantar and Usta [36] probably copied this mistake.

- Fu and Noche [45] give the following expression for the expectation of a left-truncated Weibull variable ($t_1 = t$ and $t_2 = \infty$):

$$E[X] = \exp\left(\left(\frac{t-a}{b}\right)^c\right) \cdot b\Gamma\left(1 + \frac{1}{c}, \left(\frac{t-a}{b}\right)^c\right).$$

  However, on the right-hand-side they should have added '+ a'. Besides, they forgot to define their $\Gamma(.)$, which must be the upper incomplete gamma function: $\Gamma(p, x) = \Gamma_{\text{upper}}(p, x)$ in order to be correct.

3.3 Overview of moment expressions for truncated Weibull variables

We use the doubly truncated Weibull variable X_d defined by the cdf in (3.1) as starting point. The general moment expression for X_d was derived in (3.2). The moment expressions for a left or lower truncated Weibull distributed variable X_l and a right or upper truncated Weibull distributed variable X_r are obtained by substituting $t_2 \to \infty$ or $t_1 = a$ respectively. Substituting both jointly recovers the moment expression for a standard (not truncated) Weibull distributed variable X.

$$\begin{aligned}
E[X_d^n] &= P(u_1,u_2)\sum_{k=0}^{n}\binom{n}{k}b^k a^{n-k}\left(\Gamma_{\text{lower}}(1+k/c,u_2)-\Gamma_{\text{lower}}(1+k/c,u_1)\right),\\
E[X_l^n] &= \exp(u_1)\sum_{k=0}^{n}\binom{n}{k}b^k a^{n-k}\Gamma_{\text{upper}}(1+k/c,u_1),\\
E[X_r^n] &= \frac{1}{1-\exp(-u_2)}\sum_{k=0}^{n}\binom{n}{k}b^k a^{n-k}\Gamma_{\text{lower}}(1+k/c,u_2),\\
E[X^n] &= \sum_{k=0}^{n}\binom{n}{k}b^k a^{n-k}\Gamma(1+k/c),
\end{aligned} \tag{3.6}$$

where $u_1 = \left(\frac{t_1-a}{b}\right)^c$, $u_2 = \left(\frac{t_2-a}{b}\right)^c$ and $P(u_1,u_2) = 1/\left(\exp(-u_1)-\exp(-u_2)\right)$.
$\Gamma_{\text{upper}}(p,x) = \int_x^\infty u^{p-1}\exp(-u)du$ and $\Gamma_{\text{lower}}(p,x) = \int_0^x u^{p-1}\exp(-u)du$ are the upper and lower incomplete gamma function respectively.
For vanishing location parameter $a = 0$ $\left(u_1 = \left(\frac{t_1}{b}\right)^c \text{ and } u_2 = \left(\frac{t_2}{b}\right)^c\right)$ the calculations simplify considerably:

$$\begin{aligned}
E[X_d^n] &= P(u_1,u_2)\cdot b^n\left(\Gamma_{\text{lower}}(1+n/c,u_2)-\Gamma_{\text{lower}}(1+n/c,u_1)\right),\\
E[X_l^n] &= \exp(u_1)\cdot b^n\,\Gamma_{\text{upper}}(1+n/c,u_1),\\
E[X_r^n] &= \frac{1}{1-\exp(-u_2)}\cdot b^n\,\Gamma_{\text{lower}}(1+n/c,u_2),\\
E[X^n] &= b^n\,\Gamma(1+n/c).
\end{aligned} \tag{3.7}$$

The first moments or expectations ($n = 1$) for arbitrary location parameter a are given by:

$$\begin{aligned}
E[X_d] &= a + P(u_1,u_2)\cdot b\left(\Gamma_{\text{lower}}(1+1/c,u_2)-\Gamma_{\text{lower}}(1+1/c,u_1)\right),\\
E[X_l] &= a + \exp(u_1)\cdot b\,\Gamma_{\text{upper}}(1+1/c,u_1),\\
E[X_r] &= a + \frac{1}{1-\exp(-u_2)}\cdot b\,\Gamma_{\text{lower}}(1+1/c,u_2),\\
E[X] &= a + b\,\Gamma(1+1/c).
\end{aligned} \tag{3.8}$$

The left-truncated Weibull distribution with vanishing location parameter ($a = 0$) is often used for describing residual lifetime [33, 34]. Since counting starts after reaching a certain

threshold value (t_1), preference is given to a translated, left-truncated Weibull distributed variable $Y_l = X_l - t_1$ with cdf:

$$F_{Y_l}(y) = 1 - \exp\left(\left(\frac{t_1}{b}\right)^c - \left(\frac{y+t_1}{b}\right)^c\right) \quad \text{for } y > 0. \tag{3.9}$$

Residual time-to-failure, introduced in Chapter 4, is also a translated, left-truncated Weibull distributed variable. For completeness we list the general moment expression for Y_l which is closely related to the one of X_l:

$$\begin{aligned} E[Y_l^n] &= \exp(u_1) \cdot \sum_{k=0}^{n} \binom{n}{k} b^k (-t_1)^{n-k} \Gamma_{\text{upper}}(1 + k/c, u_1), \\ E[Y_l] &= \exp(u_1) \cdot b\, \Gamma_{\text{upper}}(1 + 1/c, u_1) - t_1 \quad \text{for } n = 1, \end{aligned} \tag{3.10}$$

with: $u_1 = \left(\frac{t_1}{b}\right)^c$.

Chapter 4

A probabilistic approach on residual strength and damage buildup of high performance fibers

Abstract

This chapter is based on a paper by Knoester, Hulshof and Meester [46].
An elementary, probabilistic model for fiber failure, developed by Coleman in the fifties of the last century, predicts a Weibull distributed time-to-failure for fibers subject to a constant load. This has been experimentally confirmed, not only for fibers but for load bearing products in general. In this chapter we analyze residual strength, i.e. the strength after having survived a given load program. We demonstrate that the Weibull modulus, describing variability of time-to-failure, affects residual strength. It determines (a) how fast residual strength of fibers decays during their service life, (b) the residual strength variability, and (c) the fraction of surviving fibers during service life. Experiments show that residual strength of Twaron fiber (p-aramid fiber), exceeding predictions of Coleman's model, remains unrelentingly high (close to virgin strength) during service life.

4.1 Introduction

High performance fibers and fiber composites are well-known for their strength and high modulus properties, enabling competition with conventional steel wire solutions. For industrial products (ropes, pipes, optical fibers) manufactured from or reinforced with light-weight high-strength fibers, both strength and expected lifetime are important. Durability of fibers is threatened by its environment (e.g. chemical attack, high temperature, humidity, UV radiation) and internal damage buildup directly caused by tensioning the fibers.

Not only should materials survive their economical lifetime with high probability, but mechanical properties such as strength should also remain at a high level, for instance to be able to cope with peak stresses. Residual strength is therefore important as well.

In the present study, the focus is on residual strength of high performance fibers. Residual mechanical properties of fibers or fiber assemblages (such as in ropes or fiber reinforced pipes) are often investigated experimentally, simply because a theoretical framework is lacking. Our objective is to investigate if an existing classical model, developed by Coleman [9], is suitable to describe failure of Twaron yarns (in short: 'fibers'). Coleman's model is intended for single indivisible fibers. Note that the Twaron yarns we are interested in are in fact twisted bundles of filaments, and filaments can to some extent be considered as single fibers. Coleman [47, 48] and Phoenix [49] analyzed the failure behavior of bundles of single fibers. We choose not to consider our yarns as 'bundles of single fibers', mainly because time-to-failure of Twaron yarns at constant load is reasonably well described by the Weibull distribution, one of the features of the Coleman model. Besides, Twaron filaments are not amenable to experimental investigation, whereas yarns are mechanically tested all the time. The price we have to pay for separating a yarn from its constituents is that we will not easily be able to predict what will happen with the yarn's failure properties if we are going to change its construction (twist level, number of filaments, type of filaments).

In this chapter, we consider Coleman's model as a general toolkit, which may or may not be used for the failure of a load-bearing material or piece of equipment. For fibers subjected to a constant load, the model predicts a Weibull distribution for time-to-failure and allows for virtually any relationship between time-to-failure and load ('load curve'). The model covers both power-law and exponential load curves, i.e. linear relationships between the logarithm of time-to-failure and load or logarithm of load respectively. Such behavior is observed for many materials. It is tempting to investigate if Coleman's model is still applicable to these materials for arbitrary load programs. Another benefit of the model is that it captures the probabilistic nature of time-to-failure and strength, an important feature for materials exhibiting substantial scatter for these properties (such as high performance fibers).

Basically, Coleman proposed a time-to-failure distribution function for fibers subjected to an arbitrary load program. By analyzing both the constant load program and the linearly increasing load program, Phoenix [49,50] elaborated on this model and demonstrated that strength variability is intimately related to time-to-failure variability for fibers satisfying Coleman's model. Comparison of these variabilities obtained from measurements can thus be used to validate Coleman's model. Let us assume that measurements of both time-to-failure and strength fit reasonably well in the Coleman model. We propose a subsequent step to validate the model by comparison of predicted residual strength with measurements. This process is illustrated by measurements on Twaron para-aramid fiber. Experiments show that time-to-failure and strength measurements for this fiber fit Coleman's model, whereas residual strength measurements do not.

Coleman's model combines a deterministic damage buildup as function of a load program, and a probability of failure given the actual level of damage in the fiber. Residual strength solely depends on current damage level, not on the way the damage was built up. In Coleman's model there is ample freedom in specifying how fast and in what way damage builds up as a function of the load. In this chapter we first give an explicit expression for the probability distribution for residual strength in accordance with Coleman's model. Phoenix [50] earlier derived an approximate expression for residual strength distribution to predict median strength of proof-tested epoxy-impregnated graphite strands. We show that the residual strength of a Coleman fiber (that is, a fiber satisfying the Coleman model) is only slightly reduced if at all. Even if a load program has continued to such an extent that the probability of survival of fibers is minimal, the mean residual strength of surviving fibers has hardly changed with respect to the virgin fiber strength.

Coleman fibers are defined by three parameters, two of which describe the load sensitivity of time-to-failure. The third parameter is the load-independent Weibull modulus of time-to-failure, being a measure of the natural variability in time-to-failure. In Chapter 2 we showed that a large Weibull modulus (equivalent to a narrow time-to-failure distribution) is essential for reliable time-to-failure predictions. In this chapter, as was observed by Phoenix [50] earlier, we demonstrate that the Weibull modulus for time-to-failure is also pivotal for residual strength properties. The Weibull modulus k determines how the mean residual strength of surviving fibers evolves relative to the mean strength of virgin fibers as damage accumulates. It descends below virgin strength for $k > 1$ and ascends above virgin strength for $k < 1$. Also, the larger k, the narrower the width of the residual strength distribution. Although his focus was on fatigue of epoxy-graphite strands, Chou [51] explained that the mean residual strength of surviving proof-tested strands can be higher than the original strength by the phenomenon of weeding out weaker elements during fatigue proof-testing. They introduced a free model parameter i, similar to our k, to match theory with experimental data on residual strength. A prerequisite for their analysis is that the strands satisfy the so-called strength-fatigue life equal rank assumption (SLERA) [51,52]. Fibers satisfying Coleman's model, by definition also satisfy SLERA.

The chapter is built up as follows. In Section 4.2 we explain the model and introduce the concept of accumulated damage at the moment of breaking. Next, in Section 4.3 we derive distributions for residual strength and residual time-to-failure and we compare these with residual strength measurements of Twaron 2300 (p-aramid fiber). In Section 4.4 we end with conclusions on residual strength of Coleman fibers.

4.2 Model assumptions

A fiber breaks by creep rupture after accumulation of internal damage. Having survived a finite load program, the residual strength of a fiber is determined by the actual damage buildup in the fiber. Before focusing on the topic of residual strength, it is necessary to first define damage accumulation in 4.2.1. We adhere to the work of Coleman [9] and propose a simple model where damage accumulation rate is a function of actual load only. In 4.2.2 we show that the accumulated damage at the moment of breaking is a Weibull distributed random variable (denoted by Ω), closely related to random variables time-to-failure (T) and strength (S). In case a fiber has obtained a given damage level ω after having survived a preload program, the variable Ω is conveniently replaced by Ω_{res}, the residual accumulated damage at the moment of breaking. Ω_{res} is naturally related to residual time-to-failure and residual strength, and this will be the topic of Section 4.3.

4.2.1 Modeling damage accumulation

We describe fiber failure as a stochastic process: the fiber will not predictably break at a fixed moment during a given load program. Weibull [53], one of the pioneers in this field, proposed an exponential (Weibull) distribution for material strength loosely derived from the weakest link principle [54], which has been successfully applied and modified in numerous studies on material strength behavior [9, 55–60].

Coleman [9] was probably the first to extend this concept of strength by developing a stochastic description of time-to-failure for fibers subject to an arbitrary load program. His model comprises two distinct features:

1. deterministic damage buildup as function of the applied load program and

2. a probability of (instantaneous) failure for each amount of accumulated damage.

For the probability of failure, Coleman applied the weakest link hypothesis and some other, rather general and intuitive postulates of the theory of breaking kinetics. He argued that the probability of failure should follow an exponential distribution, which, under certain conditions, reduces to the well-known Weibull distribution for time-to-failure. Knoester et. al [12] proposed an alternative derivation based on the Poisson process to arrive at the same result.

In Coleman's model the damage function $\omega(t)$ quantifies the accumulated damage (*amount of breakdown* in his words) as a result of a so-called load program $\sigma(\cdot)$ to which a fiber is subjected during time interval $(0, t)$. The so-called *breakdown rule* tells us how to calculate $\omega(\cdot)$ from a given load program $\sigma(\cdot)$. It is assumed that damage growth rate only depends on the actual load and not on the already accumulated damage level. If it is further assumed that the initial amount of damage (for $t = 0$) vanishes. More precisely, Coleman postulates the following damage

function:

$$\omega(t) = \int_0^t \kappa(\sigma(x))dx, \tag{4.1}$$

where $\kappa(\cdot)$ is the *the breakdown rule function* which remains to be specified.

Let T denote the moment of breaking of a fiber. Following the analysis and nomenclature of Coleman, the distribution function of T is given by:

$$F_T(t) = 1 - \exp\left\{-\ell(\omega(t))^k\right\}, \tag{4.2}$$

where k is the so called *shape parameter*, or *shape factor*, and ℓ is the length parameter. In this chapter the time-to-failure distribution function will be used in conjunction with two different families for the breakdown rule function κ, namely *power law*,

$$\kappa(s) = \gamma s^\rho,$$

and *exponential*,

$$\kappa(s) = \alpha \exp(\beta s).$$

4.2.2 Accumulated damage at the moment of breaking

Let Ω be the accumulated damage at the moment of breaking, that is, $\Omega = \omega(T)$. Writing $g(x) = 1 - \exp(-\ell x^k)$, we have $F_T(t) = g(\omega(t))$, and since g is strictly increasing it follows that

$$\begin{aligned} F_\Omega(x) &= P(\Omega \le x) = P(\omega(T) \le x) \\ &= P(T \le \omega^{-1}(x)) = F_T(\omega^{-1}(x)) \\ &= g(\omega(\omega^{-1}(x)) = g(x). \end{aligned}$$

Hence Ω has a Weibull distribution with Weibull modulus k and scale factor $\omega_0 = \ell^{-1/k}$ (written as $\Omega \sim W(k, \omega_0)$) with distribution function

$$F_\Omega(x) = 1 - \exp\left(-\left(\frac{x}{\omega_0}\right)^k\right). \tag{4.3}$$

Within the Coleman model, equation (4.3) is universally valid for any breakdown rule function $\kappa(\cdot)$ and any load program $\sigma(\cdot)$. More general, equation (4.3) is derived from (4.2) for any invertible damage function ω. The concept Ω as the 'damage at breaking' turns out to be very helpful in formally deriving probability distributions for residual mechanical properties. It allows a natural definition of residual time-to-failure and strength in the framework of the Coleman model (see Section 4.3).

A constant load program $\sigma(t) = \sigma$ with constant σ represents classic time-to-failure experiments. For these experiments, time-to-failure is the time the fiber can withstand load σ before it

breaks. For a constant load program in combination with an arbitrary breakdown rule function, we simply have

$$\Omega = \omega(T) = \kappa(\sigma)T. \tag{4.4}$$

It follows that $T \sim W(k, t_0)$ with $t_0 = \omega_0/\kappa(\sigma)$.

If a fiber is subjected to a constant load rate program $\sigma(t) = \dot{\sigma}t$ with constant load rate $\dot{\sigma}$, and breaks after time T, the *fiber strength* S is defined as $S = \dot{\sigma}T$ (for a given rate $\dot{\sigma}$). In this case, the accumulated damage at the moment of breaking depends on the breakdown rule function, as follows:

$$\Omega = \begin{cases} \frac{\gamma}{(\rho+1)\dot{\sigma}} S^{\rho+1} & \text{power-law,} \\ \frac{\alpha}{\beta\dot{\sigma}} \left(\exp(\beta S) - 1\right) & \text{exponential.} \end{cases} \tag{4.5}$$

Only for the power-law breakdown rule function, strength S is Weibull distributed $S \sim W(k(\rho + 1), s_0)$ with $s_0 = \left(\frac{\omega_0(\rho+1)\dot{\sigma}}{\gamma}\right)^{1/(\rho+1)}$. Formulas (4.4) and (4.5) show a direct relationship between lifetime and strength.

4.3 Residual strength and residual lifetime

If a single fiber survives a load program $\sigma(t)$ for a given time interval $[0, t^*]$, it will have acquired an accumulated amount of damage following from the damage function in equation (4.1). The overall damage buildup is denoted $\omega^* = \omega(t^*)$ which is subsequently the *initial* amount of damage prior to the next load program. If this next program is a constant load program then the observed time-to-failure is in fact the residual time-to-failure given an initial amount of damage of ω^*. A similar definition for residual strength holds in case the next load program would have been a constant load rate program.

Residual strength is a profoundly important engineering property of fiber reinforced materials and fiber composites, expressing to what extent one can still rely on the fiber product once it has already served part of its economic lifetime. In many studies, residual strength of materials is investigated in conjunction with fatigue loading [33, 51, 52, 61, 62].

In this section, we first derive a distribution for residual strength as predicted by the Coleman model (see 4.3.1). For convenience residual strength is scaled with the strength of the virgin fiber. The residual strength distribution depends primarily on the Weibull modulus of the time-to-failure distribution. In 4.3.2 we obtain residual strength experimentally for Twaron 2300.

4.3.1 Theoretical distribution functions

We introduce a new random variable, the residual damage Ω_{res}. It represents the extra amount of damage, on top of ω^*, at the moment of breaking, conditioned on the event that the virgin fiber did survive the preload program which led to a damage level of ω^* in the first place. Residual strength Ω_{res} turns out to be a translated, left-truncated Weibull distributed variable (compare with equation (3.9)):

$$\begin{aligned} F_{\Omega_{\text{res}}}(x) &= P(\Omega_{\text{res}} \leq x | \Omega > \omega^*) = \frac{P(\Omega_{\text{res}} \leq x \cap \Omega > \omega^*)}{P(\Omega > \omega^*)} \\ &= \frac{P(\omega^* < \Omega \leq x + \omega^*)}{1 - P(\Omega \leq \omega^*)} = \frac{F_\Omega(x + \omega^*) - F_\Omega(\omega^*)}{1 - F_\Omega(\omega^*)} \\ &= 1 - \exp\left(\left(\frac{\omega^*}{\omega_0} \right)^k - \left(\frac{x + \omega^*}{\omega_0} \right)^k \right), \quad \text{for } x > 0. \end{aligned} \tag{4.6}$$

This can be exploited to easily derive residual time-to-failure T_{res} at constant load σ or residual strength S_{res} at constant load rate $\dot{\sigma}$ similar to (4.4) and (4.5) respectively. Given Ω_{res}, T_{res} and S_{res} follow from:

$$\Omega_{\text{res}} = \int_0^{T_{\text{res}}} \kappa(\sigma) dx = \kappa(\sigma) T_{\text{res}}, \tag{4.7}$$

$$\Omega_{\text{res}} = \int_0^{S_{\text{res}}/\dot{\sigma}} \kappa(\dot{\sigma} x) dx = \begin{cases} \frac{\gamma}{(\rho+1)\dot{\sigma}} S_{\text{res}}^{\rho+1} & \text{power-law,} \\ \frac{\alpha}{\beta\dot{\sigma}} \left(\exp(\beta S_{\text{res}}) - 1 \right) & \text{exponential.} \end{cases} \tag{4.8}$$

Clearly, residual time-to-failure T_{res} is also a translated, left-truncated Weibull distributed variable. Our focus is on scaled residual time-to-failure $U_{\text{res}} = T_{\text{res}}/\overline{T}$ and scaled residual strength $V_{\text{res}} = S_{\text{res}}/\overline{S}$, with $\overline{T}$ the mean time-to-failure of the virgin material corresponding to load level σ and $\overline{S}$ the mean strength of the virgin material corresponding to load rate $\dot{\sigma}$. It is emphasized that the distribution functions of U_{res} and V_{res} are conditional. They apply to the subset of fibers which have survived the preload. In Appendix D the distribution functions for U_{res} and V_{res} are derived:

$$F_{U_{\text{res}}}(u) = 1 - \exp\left((\hat{\omega}^*)^k - (u\Gamma_k + \hat{\omega}^*)^k \right), \tag{4.9}$$

$$F_{V_{\text{res}}}(v) = 1 - \exp\left((\hat{\omega}^*)^k - \left(\left(v\Gamma_{k(\rho+1)} \right)^{\rho+1} + \hat{\omega}^* \right)^k \right) \quad \text{power-law,} \tag{4.10}$$

$$F_{V_{\text{res}}}(v) = 1 - \exp\left((\hat{\omega}^*)^k - \left(\frac{1}{\eta} \left(e^{vL(0;k;\eta)} - 1 \right) + \hat{\omega}^* \right)^k \right) \quad \text{exponential,} \tag{4.11}$$

where $L(y;a,b) = \int_y^\infty \ln\left(b(z^{1/a} - y^{1/a}) + 1\right) \exp(y - z)\, dz$, $\Gamma_x = \Gamma(1 + 1/x)$, $\hat{\omega}^* = \omega^*/\omega_0$ and $\eta = \beta\dot{\sigma}\omega_0/\alpha$. Note that for $k = 1$ both U_{res} and V_{res} are independent of the initial amount of damage $\hat{\omega}^*$. For this special case, T and T_{res} are identically exponentially distributed (just as Ω and Ω_{res}).

Hence the distribution of U_{res} depends only on k and is independent of constant load σ. The distribution of V_{res} depends on two parameters (k and ρ for the power-law breakdown rule function; k and η for the exponential breakdown rule function). For the power-law breakdown rule, V_{res} is independent of load rate $\dot{\sigma}$. Residual time-to-failure and residual strength depend on ω^*, but the particular preload program which has led to ω^* is of no interest. Relations for $\overline{U}_{\text{res}}$ and $\overline{V}_{\text{res}}$ as functions of $\hat{\omega}^*$ are derived in Appendix D.

In Figure 4.1 the course of mean scaled residual strength ($\overline{V}_{\text{res}}$) as function of damage accumulation is visualized. For $k = 1$, the distribution function for the scaled residual strength is independent of the accumulated damage ω^* and $\overline{V}_{\text{res}} = 1$. For $k > 1$, $\overline{V}_{\text{res}}$ decays in time. For $k < 1$, $\overline{V}_{\text{res}}$ exceeds 1 and climbs with accumulated damage. These phenomena are explained by Chou [51], as follows. There are two competing mechanisms influencing residual strength.

1. Relatively weak fibers are weeded out quite early during a load program, and the subset of much stronger surviving fibers, belonging to the high-end of the fiber strength distribution, push-up mean residual strength.

2. Simultaneously, during loading, the mechanical properties of the surviving fibers degrade causing the mean residual strength to reduce.

For a narrow time-to-failure distribution (large k) relatively few fibers fail during the early stages of a load program and, as a consequence, degradation in the large subset of surviving fibers is felt stronger, causing a reduced mean residual strength of this subset. In the nomenclature of Chou, this situation is labeled ‘strong degradation’. For a wide time-to-failure distribution (small k) the first mechanism dominates (‘weak degradation’). For $k = 1$ both mechanisms are balanced.

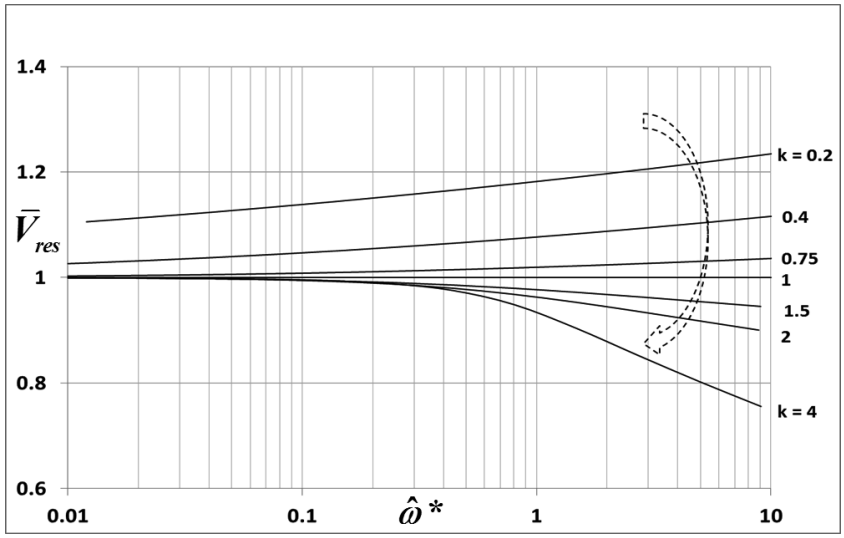

Figure 4.1: *Mean scaled residual strength* $\overline{V}_{\text{res}}$ *for the power-law breakdown rule as function of* $\hat{\omega}^*$ *and* k *(while* $\rho + 1 = 30$*). For the distribution of* V_{res} *see equation* (4.10)*.*

Phoenix [50] analyzed residual strength (non-scaled) after a constant preload. He found the same dependency of residual strength on Weibull modulus k as described above. Differences in residual strength (for different values of k) getting larger for higher preload level and/or longer preload duration. Translated to the present scaled analysis, note that in both cases ω^* is increased and Phoenix' findings are in agreement with Figure 4.1.

The width of the scaled residual strength distribution also depends on the accumulated damage ω^* (see Figure 4.2). Here we plot prediction intervals, or 'high probability intervals', for residual strength as function of ω^*. The boundaries of the prediction intervals (ν_1, ν_2) are obtained from $F_{V_{\text{res}}}(\nu_1) = \epsilon$ and $F_{V_{\text{res}}}(\nu_2) = 1 - \epsilon$ with $\epsilon = 0.025$ and $\epsilon = 0.05$ for the 95% and 90% prediction interval respectively. Generally, the larger k, the narrower the distribution of V_{res}.

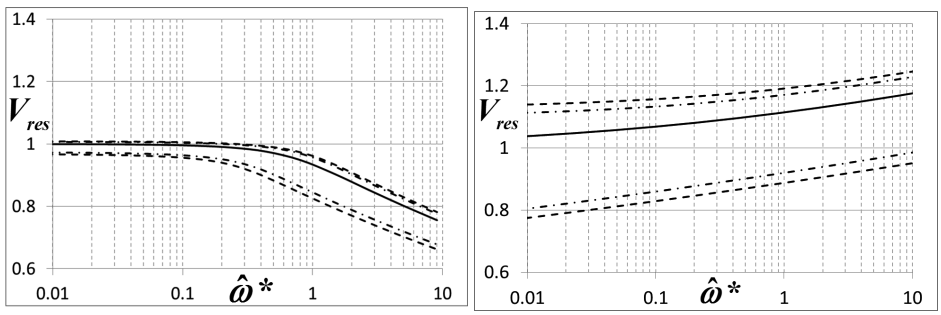

(a) $k = 4; \rho + 1 = 30$ (b) $k = 0.4; \rho + 1 = 20$

Figure 4.2: *95% and 90% prediction intervals for scaled residual strength (see text) as function of* $\hat{\omega}^*$*. Solid line represents* $\overline{V}_{\text{res}}$*.*

4.3.2 Fitting p-aramid fibers to Coleman

This section describes residual strength experiments on Twaron 2300 (p-aramid) fibers. We used Twaron 2300 fibers with a nominal density of 1680 dtex and 1000 filaments per fiber. All tested fiber specimens were twisted with 80 twists per meter. For details on the failure behavior of twisted and flat Twaron fibers, i.e. the relationship between time-to-failure and load, the reader is referred to Knoester et. al. [63].

Before turning to residual strength, we first concentrate on time-to-failure and strength. To avoid confusion with residual strength we will henceforth use 'virgin strength' to denote the fiber's strength. A total of 150 fiber specimens (obtained from the same production spool) were tested on a Zwick Z010 tensile tester (load capacity 5 kN) with gauge length 500 mm. For 75 specimens we measured time-to-failure T: the time lapse of fibers subjected to $\sigma_p = 324$ N until failure. For the other 75 specimens we measured virgin strength S: maximum observed load for fibers subjected to load rate $\dot{\sigma} = 50$ N/s (= 0.418 GPa/s) until failure. The time-to-failure and virgin strength measurements resulted in $\overline{T} = 43.7$ min and $\overline{S} = 391.7$ N. The scaled time-to-failure $U = T/\overline{T}$ and scaled virgin strength $V = S/\overline{S}$ measurements are plotted in Figure 4.3. Apparently the theoretical predictions of Coleman i.c.w. the power-law breakdown rule for various values of k and $k(\rho + 1)$ agree nicely with the observed scaled time-to-failure U and virgin strength V. It is noted that U and V solely depend on k and $k(\rho + 1)$ respectively.

We measured residual strength for 300 fiber specimens obtained from the same Twaron 2300 spool. The objective is to test if this Twaron fiber fits into the residual strength distribution derived from the Coleman model. The experimental procedure is simple. The fiber specimens were subjected to a constant preload $\sigma_p = 324$ N for a fixed time t_i, with $t_i = 15, 25, 35$ or 45 min. (75 randomly chosen specimens for each t_i). At the start of each experiment, load is quickly raised to σ_p with a fixed rate of 50 N/s, then the timer is started and the load is kept constant until $t = t_i$. If the fiber has survived the preload, residual strength is measured by immediately further raising the load (at rate 50 N/s) until failure. The load at the moment of breaking is the residual strength.

Comparison of measured residual strength with theoretical predictions (see equation (4.10)) requires Coleman parameters k, ρ (assuming power-law breakdown rule function) associated with this Twaron 2300 fiber. Weibull modulus $k = 4.1$ was obtained from a Weibull plot of the present time-to-failure measurements. This parameter is known to be sensitive to 'outliers'. The Coleman parameter ρ (slope of the power-law load curve) was approximated by $\rho + 1 \sim 36$ for this particular Twaron 2300 quality. For standard Twaron 2300, Knoester et al [63] give $\rho + 1 \sim 40$. In the present analysis, we reckoned with a range of ρ-values ($30 \leq \rho + 1 \leq 40$) while comparing theoretical distributions with measurements. Alternatively, we tried to describe Twaron 2300 with the Coleman model in combination with the exponential breakdown rule function. Additional to k we need parameter $\eta = f(\alpha, \beta)$ in equation (4.11). The exponential load curve for this Twaron 2300 spool yields $\beta = 14.4$ and $\eta = 8.5e20$ whereas standard Twaron

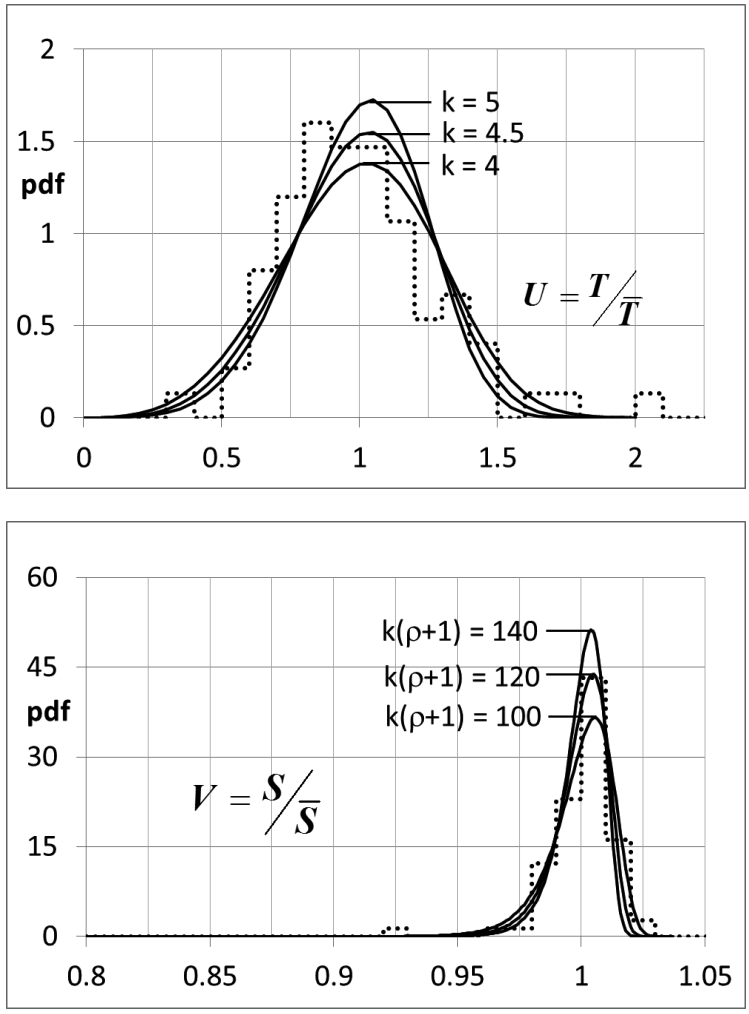

Figure 4.3: *Predicted probability distribution of scaled time-to-failure U (top) and scaled strength V (bottom) compared to Twaron 2300 measurements (dotted bars).*

2300 is associated with $\beta = 15.5$ and $\eta = 1.5e22$ [63]. If β is varied down to $\beta = 13.5$ one has to reckon with lower values of η as well ($\eta = 2e19$). The parameter η can also be obtained from the virgin strength measurements in the present study. Taking the mean of both sides of equation (4.5), we find that $E[(\exp(\beta S) - 1)] = \frac{\beta\dot{\sigma}}{\alpha}\,\overline{\Omega} = \eta\Gamma_k$. Therefore, we estimate η from:

$$\eta = \Gamma_k^{-1}\left(\overline{\exp(\beta S) - 1}\right), \tag{4.12}$$

where for S the virgin strength measurements are used. For $\beta = 14.4$, equation (4.12) results in $\eta = 4e20$.

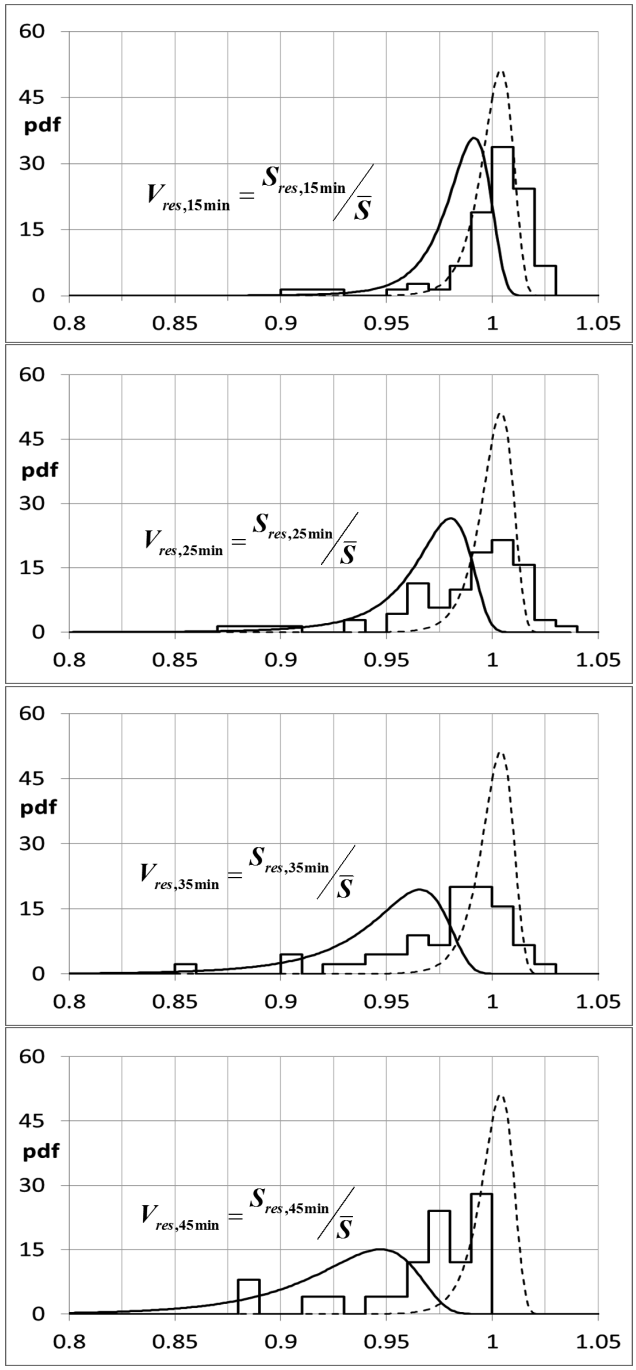

Figure 4.4: *Probability distribution function of scaled residual strength predicted by the Coleman model ($k = 4$ and $\rho + 1 = 35$, solid curves) and Twaron 2300 measurements (bars). Residual strength distributions apply to fibers having survived 15, 25, 35, 45 min at preload 324 N. A total of $n = 74, 70, 45, 25$ Twaron fibers survived the preload respectively. Reference dashed lines: scaled virgin strength $V = S/\overline{S}$.*

Predictions for the scaled residual strength depend on two model parameters: $(k, \rho + 1)$ (power-law) and (k, η) (exponential). Residual strength data in Figure 4.4 show that Twaron 2300 fiber seems to have a systematically higher residual strength than predicted by the Coleman model. The 'distance' between the Coleman model and the measurements is more convincingly displayed by comparison of the distribution functions in Figure 4.5.

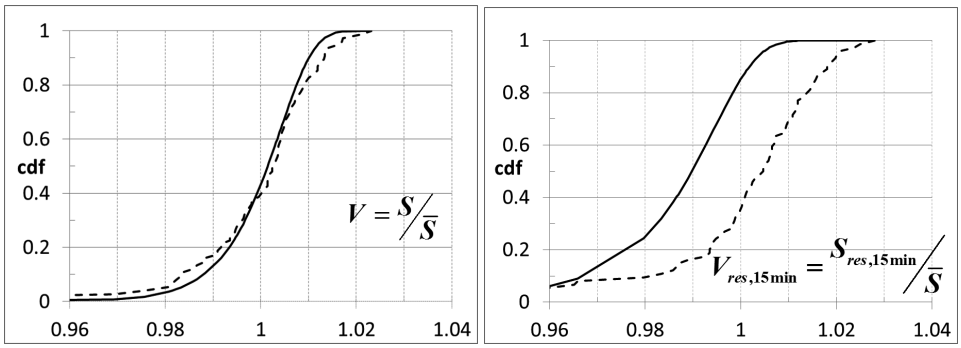

(a) virgin strength (b) residual strength (after 15 minutes preload)

Figure 4.5: *Comparison between the cumulative distribution function cdf for scaled strength predicted by the Coleman model ($k = 4$ and $\rho + 1 = 35$, solid curves) compared to the empirical distribution function recovered from scaled strength measurements (dashed curves).*

To produce quantitative evidence for the assertion that residual strength of Twaron is not properly described by the Coleman model, the non-parametric (one sample) Kolomogorov-Smirnov test (KS test) is used to either reject or not reject a reference distribution underlying the measured sample distribution. The KS statistic χ is the maximum (vertical) distance between the empirical distribution function based on the set of measured (residual) strengths, and the (residual) strength distribution as derived from the Coleman model (= reference distribution). For example, the maximum vertical distance between the curves in Figure 4.5 is 0.094 (for V) and 0.518 (for $V_{res,15min}$). For $n = 75$ observations and a 5% significance level the critical value for the KS statistic is 0.157. This implies that Coleman's V-distribution cannot be rejected as parent distribution for the virgin strength observations whereas for residual strength after 15 minutes Coleman's distribution must be rejected. Table 4.1 shows that for $(k = 4, \rho + 1 = 35)$ (power-law) and $(k = 3, \eta = 4e20)$ (exponential) the Coleman model cannot be rejected as reference distribution for both the virgin strength and time-to-failure measurements. However, residual strength measurement do not fit into the model for these model parameters. We found no parameter combinations for which time-to-failure, virgin strength and all four residual strengths cannot be rejected as originating from their respective reference distributions. The capability of the KS test to reject the reference distribution for the residual strength measurements is by virtue of a large sample size n. For example, $n = 10$ corresponds to $\chi_c = 0.489$ and $\chi_c = 0.409$ at significance level 1% and 5% respectively. Furthermore, χ_m tends to decrease as n decreases.

	χ_c = critical value of the KS statistic (n=sample size) (at the 1% / 5% significance level)	χ_m = KS statistic from measurements (power-law) ($k = 4; \rho + 1 = 35$)	χ_m = KS statistic from measurements (exponential) ($k = 3; \eta = 4e20$)
time-to-failure	0.188 / 0.157 (n=75)	0.080 NR / NR	0.108 NR / NR
virgin strength	0.188 / 0.157 (n=75)	0.094 NR / NR	0.128 NR / NR
res. strength (15 min)	0.189 / 0.158 (n=74)	0.518 R / R	0.268 R / R
res. strength (25 min)	0.195 / 0.163 (n=70)	0.435 R / R	0.279 R / R
res. strength (35 min)	0.243 / 0.203 (n=45)	0.434 R / R	0.423 R / R
res. strength (45 min)	0.317 / 0.264 (n=25)	0.391 R / R	0.721 R / R

Table 4.1: *Kolmogorov-Smirnov test results. Critical values for the KS statistic, dependent on sample size n, are at the 1% or 5% significance level. NR= H_0 hypothesis Not Rejected; R= H_0 hypothesis Rejected. H_0 hypothesis: measurements originate from reference distribution.*

So for $n = 10$, the KS test would not have been able to reject Coleman's model as underlying model for the residual strength measurements.

The outcome of the KS test strongly depends on the model parameters used for the reference distribution. For various combinations of model parameters we computed the p-value: the probability of obtaining the measured KS statistic (χ_m) or an even larger value on condition that measurement data indeed originate from the reference distribution (H_0 hypothesis is true). Or: p-value $= P(\chi \geq \chi_m \mid H_0 \text{ is true})$. These p-values are plotted in Figure 4.6 and Figure 4.7. Clearly, a similar outcome of the KS test as in Table 4.1 is found for a whole range of model parameters: $2.5 \leq k \leq 6.5$, $75 \leq k(\rho + 1) \leq 175$ (power-law) and $2.5 \leq k \leq 3.5$, $2e19 \leq \eta \leq 2e22$ (or: $13.5 \leq \beta \leq 15.5$) (exponential).

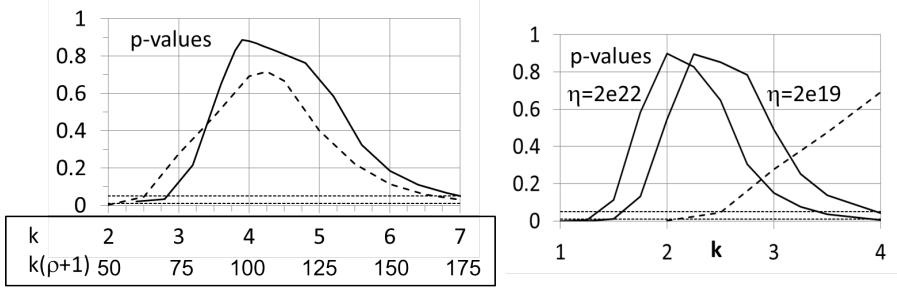

Figure 4.6: *p-values of time-to-failure (dashed lines) and virgin strength (solid lines) (left power-law; right exponential); dotted horizontal lines indicate significance levels of 0.05 and 0.01.*

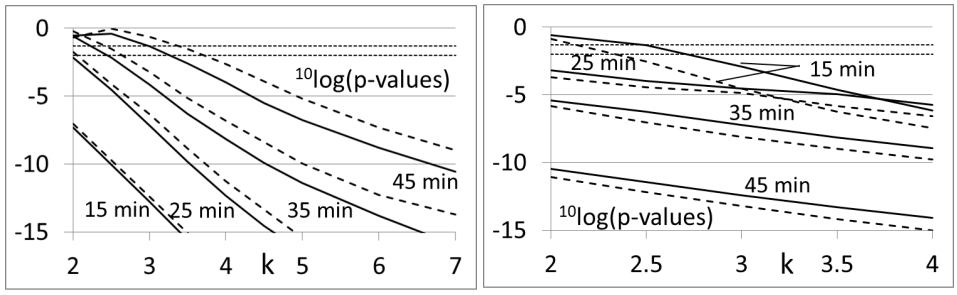

Figure 4.7: ^{10}*log(p-values) of residual strength after 15, 25, 35 and 45 minutes (left power-law,* $\rho + 1 = 40$ *dashed lines,* $\rho + 1 = 35$ *solid lines; right exponential,* $\eta = 2e19$ *solid lines,* $\eta = 2e22$ *dashed lines); dotted horizontal lines indicate significance levels of 0.05 and 0.01.*

In empirical and modeling studies, the variability of residual strength is commonly ignored. Instead, the mean residual strength is plotted as a function of scaled time [33,51,61,64]. In Figure 4.8 the decay of $\overline{V}_{\text{res}}$ as damage builds up is plotted for the Coleman model and compared with the Twaron 2300 measurements. Whereas residual strength of Coleman fibers (and Twaron 2300) remains close to their virgin strength, the fraction of surviving fibers n_s decreases significantly as damage builds up (see Figure 4.9). For ropes and fiber reinforced products constructed from a large number of continuous fibers, the gradual loss of the weakest fibers fraction by breaking is probably more serious than the strength deterioration of the surviving ones [62].

The decay of n_s in Figure 4.9 is predicted by Coleman for a constant load program using scaled time $\xi = t/\overline{T}$:

$$n_s = 1 - P(\Omega \leq \omega^*) = \exp\left(-\left(\hat{\omega}^*\right)^k\right) = \exp\left(-\left(\xi\Gamma_k\right)^k\right). \tag{4.13}$$

Here the identity $\hat{\omega}^* = \xi\Gamma_k$ readily follows from:

$$\hat{\omega}^* = \frac{\omega^*}{\omega_0} = \frac{\kappa(\sigma)\xi\overline{T}}{\omega_0} = \xi\Gamma_k. \tag{4.14}$$

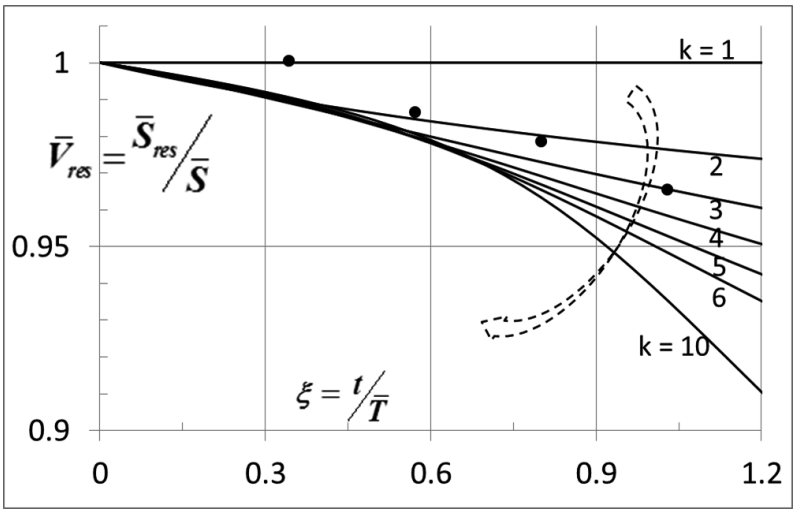

Figure 4.8: *Mean residual strength* $\overline{V}_{\text{res}}$ *(equation* (D.10) *in appendix D;* $\eta = 10^{20}$*) as function of* $\xi = t/\overline{T}$ *during a constant load program with mean time to failure* $\overline{T}$*. Twaron 2300 measurements are represented by the solid dots.*

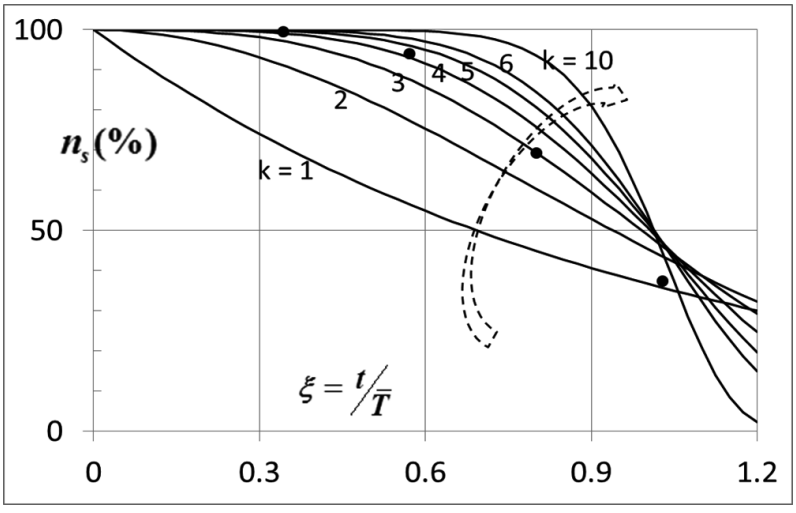

Figure 4.9: *Surviving fiber fraction* n_s *(equation* (4.13)*) as function of* $\xi = t/\overline{T}$ *during a constant load program with mean time to failure* $\overline{T}$*. Twaron 2300 measurements are represented by the solid dots.*

4.4 Discussion and Conclusions

For obvious reasons it is useful to be able to predict fiber failure during an arbitrary load program. Coleman developed a model for the time-to-failure distribution for single fibers. Both virgin strength and failure time of fibers subjected to a constant load are easily measured in practice. For many fibers, or other load carrying materials, it is possible to select Coleman model parameters in order to get model predictions in accordance with measurements. Yet this does not mean that Coleman's model correctly predicts failure time for any load program.

In this chapter we investigated how residual strength measurements can add to the confidence that the Coleman model properly describes failure behavior also for complex loading. Here residual strength stands for the fiber's strength after it has been subjected to a constant load for a certain period of time (proof testing). First we formulated the residual strength distribution based on Coleman's model for time-to-failure. Here, the random variable representing damage-at-the-moment of breaking turned out to be a useful concept. We showed that time-to-failure variability, expressed in terms of its Weibull modulus k, determines different modes in residual strength behavior. Weak degradation for $k < 1$: the mean residual strength of surviving fibers exceeds mean virgin fiber strength. Strong degradation for $k > 1$ corresponds to a strictly decreasing mean residual strength. It is time-to-failure variability rather than virgin strength variability that sets residual strength behavior.

For a wide range of k-values, residual strength of a Coleman fiber remains close to its virgin strength, i.e for $0.4 < k < 4$ and the period of constant load not exceeding time-to-failure ($\hat{\omega}^* \leq 1$) the mean residual strength of a Coleman fiber is within 10% of its virgin strength (see Figure 4.1). If a proof-tested fiber has residual strength considerably deviating from its virgin strength, it will not be possible to describe its failure behavior in terms of the Coleman model. Oppositely, if measured residual strength remains close to virgin strength it will be difficult to deny that Coleman's model is applicable to the fiber's failure behavior. Many repetitive measurements are then necessary to prove statistically significant distance between the model predictions and the observations (provided there is such a distance).

We found that time-to-failure and virgin strength measurements of Twaron 2300 do fit into the Coleman model after choosing appropriate Coleman model parameters. Furthermore, residual strength of proof-tested Twaron 2300 p-aramid fiber was shown to stay close to its virgin level, even if the fraction of fibers surviving the proof test is small. This property is not unique for p-aramid fibers but also holds for nylon [62]. Using various selections of model parameters - in accordance with time-to-failure and virgin strength measurements - and employing large numbers of repetitive residual strength measurements, we demonstrated that the Coleman model statistically significantly underpredicts the residual strength of Twaron 2300. We therefore conclude that failure of Twaron 2300 fiber cannot be fully described by the Coleman model.

A better agreement between model and experiments might be obtained for more complex models. Coleman's model described in this chapter is in fact the simplest approach proposed by

Coleman [9], where damage buildup is a sole function of current load level. Coleman sketches model extensions for which damage buildup is also dependent of, for instance, current damage level or the current load rate. Apart from heuristic modeling, failure of Twaron fibers can also be addressed from a mechanistic point of view, by looking at what is happening inside the fiber. Twaron fibers are (twisted) bundles of filaments and fiber damage can be associated with local filament breaks. The load of broken filaments is locally taken over by its neighbors. The way load is shared between surviving filaments determines how local fiber damage propagates through the bundle and thus determines fiber failure. If time-to-failure of single filaments is Weibull distributed, the strength and lifetime of bundles of filaments will not be adequately described by the Weibull distribution [65]. The empirical distribution of residual strength of Twaron bundles, as obtained in the present study, could provide mechanistic clues as to how load is shared within the bundles. One of the reviewers of our paper [46] pointed out that measuring residual strength either directly following a preload or after a short moment of unloading after the preload could affect residual strength (whereas it should not according to the Coleman model). If residual strength is indeed different for both procedures, this could be connected to redistribution of stress around broken filaments during this short moment of unloading. Measuring residual strength using both procedures could therefore provide clues for the mechanism of fiber (or: bundle of filaments) failure.

Mechanical reliability of fiber assemblages (i.e. ropes, fiber reinforced pipes etc.) requires that the residual strength is retained as much as possible throughout the lifetime of the product particularly if the fiber product is periodically subjected to peak stresses. Since damage builds up during a load program, fiber reinforced products should be replaced timely and their economic lifetime is limited. For p-aramid fibers, residual strength is very high, even far beyond their scheduled economic lifetime. Breaking of fibers in fiber reinforced materials, even if breaking weakens the material only locally because of load sharing between the fibers, must therefore be taken more seriously than strength erosion of non-broken fiber segments.

Chapter 5

Probabilistic lifetime models for materials subjected to high-low and low-high single step loading

Abstract

Load induced cumulative damage growth is a key element in modeling lifetime of load-bearing materials and structures carrying day-to-day loads. The concept of damage accumulation was originally introduced for fatigue related failure, but is also successfully applied to describe creep rupture caused by for example constant load or step-wise constant load. For a step-wise constant load program, it is common practice to calculate the Life Fraction by adding up the normalized times at each constant load in the program, with normalization done by the mean time-to-failure at that load. If the Life Fraction is unity at failure, the material is said to satisfy the Life Fraction Rule (LFR), equivalent to Palmgren-Miner's rule for fatigue. The far majority of models for lifetime of load-bearing materials is deterministic. Inspired by popular deterministic models, we introduce probabilistic models both for materials satisfying the LFR and for materials not satisfying the LFR. Our models calculate the Life Fraction distribution in case of single step constant load programs and, after tuning them with data from constant load experiments, very few model parameters are needed. Theory is illustrated by experiments on Twaron p-aramid yarn. We show that failure of these yarns subjected to single step constant load programs does not satisfy the Life Fraction Rule. In fact, failure of these yarns cannot be described by any model based on classic damage theory, where damage is a non-decreasing function of time during yarn loading.

5.1 Introduction

Failure of materials or fibers subjected to some load program is often described in terms of a damage function. Damage builds up during loading and at some critical damage level, failure is expected. The concept of damage is rather common in material failure theory, despite the fact that it is a virtual property (it can not be measured). The usefulness of damage pertains to it being a simple scalar, disconnected from the load program which has inflicted the damage, providing information on how far the material specimen is away from failure. The introduction of damage in failure theory dates back to the work of Kachanov [66], though he used 'continuity' $\Psi = 1 - D$ instead of damage D. He introduced a scalar field variable Ψ describing the (local) deterioration of material on micro-structural level. Damage and damage theory has since then attained a lot of attention in engineering literature.

A more empirical approach started with the work of Palmgren [67] in fatigue analysis, in which the concept of damage is disengaged from load-induced material changes. Suppose a material is subjected to various types of cycles in random order. Now, damage buildup is simply expressed as the linear sum of normalized cycle numbers per cycle type that the material has endured. For each cycle type, normalization is done with respect to the total number of cycles required for failure of the material. Miner [68] proposed an engineering rule, known as Palmgren-Miner's rule, for materials that fail at the moment this linear sum adds up to unity. This methodology also works for other failure mechanisms such as creep rupture, where materials are exposed to one or more constant loads. Stigh [69] describes an analog of Palmgren-Miner's rule for creep rupture and calls it the Life Fraction Rule. For a step-wise constant load program, it is common practice to calculate the Life Fraction by adding up the normalized times at each constant load in the program, with normalization done by the mean time-to-failure at that load. If the Life Fraction is unity at failure, the material is said to satisfy the Life Fraction Rule (LFR) (see Section 5.2).

This work has become known under the terminology 'linear damage theory' since damage contributions of various loads (or load cycles in case of fatigue) are added together linearly to obtain the overall damage level. A necessary prerequisite for this methodology is that damage builds up linearly during a constant load and that load order is irrelevant for damage accumulation. Many materials are known not to satisfy the LFR (or Palmgren-Miner's Rule). The word 'linear' may cause confusion for such materials because one may think that this implies that damage builds up in some nonlinear way during constant load. This need not be the case. To avoid this confusion, we will refer to materials satisfying the LFR as 'regular' materials. We reserve the term 'linear' for the property of linear damage buildup during a constant load program. Linearity is model property rather than a material property. We will show that a model for material failure behavior can be both nonlinear and regular. It can also be both non-regular and linear.

Damage buildup is often described in terms of a damage evolution law: a differential equation for the rate of damage buildup ($\dot{\omega}$) as function of current damage level (ω) and current load

(σ), i.e. $\dot{\omega} = f(\omega, \sigma)$. Stigh [69] points out that, in order to get deviation from the LFR, a non-separable damage evolution law is required and, vice versa, regular behavior induces a separable evolution law ($\dot{\omega} = f(\omega)h(\sigma)$). This is true only if the critical damage, i.e. the damage required for failure, is load-independent. Christensen [70] proposes a load-dependent critical damage. He uses a separable damage evolutions law, constructed from kinetic crack growth theory, and ends up with non-regular material behavior.

Modeling variability in time-to-failure at constant load is of major importance for synthetic yarns. Application of damage theory, often analyzed deterministically, should therefore be extended to encompass material variability. Christensen [71] stresses the need for probabilistic treatment of both creep rupture and fatigue data since the mean values of time-to-failure and fatigue life are almost meaningless without also recording their spread. Coleman [9] suggested a cumulative distribution function (cdf) for time-to-failure in case of an arbitrary load program. Phoenix [50] perceives that Coleman's model, general as it may be, leads to regular material failure behavior. In Section 5.3 we show that Coleman's model is in fact part of a class of regular models sharing a separable damage evolution law and a load-independent failure criterion. Coleman's model additionally assumes a Weibull distributed time-to-failure at constant load. Christensen [72] also models time-to-failure probabilistically and focuses on a failure mechanism based on kinetic crack growth, and applies his theory on failure of fiber-reinforced composites. He derives time-to-failure variability from the much smaller strength variability and ends up with a result which is largely similar to the findings of Phoenix [49] using Coleman's model. Christensen's work is not confined to Weibull distributed time-to-failure (as is the case for Coleman's model) but it does not address complex load programs.

We are not aware of any existing probabilistic model in the literature capable of handling non-regular failure behavior, i.e. failure for which loading order affects the time-to-failure of the specimen under consideration. In this chapter we construct two such probabilistic models for non-regular material failure behavior using damage theory. The first model (model A in Section 5.4) is based on the notion of Christensen discussed earlier. Here, the critical damage level required for failure depends on the current load. If the current load is large, a relatively low level of damage in the material is already sufficient for (instantaneous) failure. The second model (model B in Section 5.5) is based on the concept of power-law damage growth during constant load put forward by Marco and Starkey [11] (with the exponent a function of load). This leads to a non-separable damage evolution law and the model pairs nonlinearity with non-regularity. For both models we examine the Life Fraction distribution in case of a single step constant load program. During such program fibers are sequentially loaded to two loads σ_1 and σ_2, with a rapid load switch $\sigma_1 \rightarrow \sigma_2$ at a specified time. Single step constant load programs will be abbreviated by SSP. Our probabilistic models are constructed to analyze failure during an SSP, however, both models hold promise of generalization to more complex load programs. We focus our analysis on associate Low-High and High-Low single step constant load programs: SSPs using the same load levels σ_1 and σ_2 but in reversed order ('associate SSP'). The distribution functions

for the Life Fraction are expressed in terms of a measurable but unspecified time-to-failure distribution. We also present the Life Fraction distribution in more detail in case of Weibull distributed time-to-failure. The focus on single step constant load programs greatly reduces the number of model parameters. Insofar as possible, we tune remaining parameters with (constant load) time-to-failure measurements.

Crack growth and Marco-Starkey power-law damage growth, sources of inspiration for model A and model B respectively, have been proposed as failure mechanism for a variety of materials. Even if either of these models fits observations successfully, it is practically impossible to confirm whether the physical background of the model makes sense or that the 'success' of the model is based on mathematical curve fitting. Our probabilistic models provide easy tools to validate model consistency and herewith gain confidence in the physical background of the models. For materials which indeed fail due to crack growth one may observe failure of specimen fractions at the moment of the load switch of an SSP, according to model A. Yet, in that case there must also be non-zero periods devoid of failure following the load switch in the associate SSP. Model B offers the opportunity to validate power-law behavior in damage growth by simply measuring the time-to-failure variability at the Low and High loads used in the SSP. These do not only predict if the lifetime of Low-High or High-Low SSPs is prolonged, but also to which extent.

As illustration of the theoretical work, we obtained empirical distributions for the Life Fraction of Twaron 2300 yarns, subjected to various single step constant load programs (see Section 5.6). Twaron demonstrates non-regular failure behavior but can not be captured by either of the non-regular models analyzed in this chapter.

5.2 The Life Fraction Rule and regular material failure behavior

One of the most simple engineering rules used for capturing failure behavior is the so-called Life Fraction Rule. Suppose a material or fiber is sequentially subjected to a series of constant loads with instantaneous intermediate load switches. Suppose further that the material fails during the n^{th} load. The Life-Fraction L is a random variable defined as the sum of scaled residence times:

$$L = \sum_{i=1}^{n} \frac{t_i}{\bar{T}_i}, \tag{5.1}$$

where t_i and $\bar{T}_i$ are the residence time and the mean time-to-failure respectively corresponding to the i^{th} load σ_i. The definition for L is easily generalized for arbitrary load program $\sigma(\cdot)$ [69, 70]:

$$L = \int_0^T \frac{dx}{\bar{T}(\sigma(x))}, \tag{5.2}$$

where T is the failure time while exposed to load program $\sigma(t)$ and $\bar{T}(\sigma)$ is the mean time-to-failure at constant load σ. Models for which the distribution of L is independent of the load program will henceforth be denoted as regular. Note that regularity implies that L is independent of the order of loading, for instance in a stepwise constant load program. For a constant load program at arbitrary load σ it is easy to see that

$$E[L] = 1, \tag{5.3}$$

because $L = T/\bar{T}(\sigma)$. For regular models, the distribution of L is independent of the load and equation (5.3) is thus satisfied for any load program (not only for constant load programs). Generally, an experimentally tested material is said to satisfy the Life Fraction Rule (LFR) if equation (5.3) holds for the applied load program. Regularity therefore implies the LFR.

The Life Fraction Rule is often interpreted deterministically. Residence times are then scaled with a scalar time-to-failure T and the LFR reduces to $L = 1$. Equation (5.3) is a straightforward generalization taking into account the probabilistic nature of time-to-failure explicitly (also see Shimokawa [73]).

5.3 A class of regular models

In this section a class of models is defined based on two assumptions: 1) a separable damage evolution law and 2) a load-independent failure criterion. Stigh [69] analyzed such models and he used a scalar 'damage-at-the-moment-of-breaking' as failure criterion, being independent of load. Here, we replace this scalar by a load independent distribution of the damage at the moment of breaking (Ω) and construct a class of probabilistic models. Similar to the work of Stigh, we prove regularity for these models. We briefly discuss the 'load curves' associated with these models. i.e. time-to-failure at constant load as function of this constant load. At the end of this chapter, apart from the two assumptions above, we additionally assume Weibull distributed time-to-failure. This subclass of regular models turns out to be the same as proposed by Coleman [9] earlier.

We will now construct a class of failure models predicting the stochastic time-to-failure of fibers (or materials in general) subjected to an arbitrary load program. The models predict regular failure behavior, so they satisfy the Life Fraction Rule, despite the fact that damage buildup can be highly nonlinear.

The models are founded on the following two assumptions:

- Assumption 1
  Damage growth during an arbitrary load program $\sigma(t)$ is controlled by a separable damage evolution law of the form:
  $$\dot{\omega}(t) = \frac{\kappa(\sigma(t))}{f(\omega(t))}, \quad \omega(0) = 0. \tag{5.4}$$
- Assumption 2
  Ω is a random variable describing the damage level at which fibers break and is independent of the load program.

Integration of the damage evolution law, bearing in mind the definition of Ω, leads to the following relationship between time-to-failure T and damage-at-break Ω:

$$\int_0^{\Omega} f(z)dz = \int_0^{T} \kappa(\sigma(\tau))d\tau. \tag{5.5}$$

Since Ω is a load independent random variable, the right-hand-side of equation (5.5) must be load independent as well. For convenience we replace the left-hand-side by a load independent random variable X:

$$X = \int_0^{T} \kappa(\sigma(\tau))d\tau. \tag{5.6}$$

Clearly, for a constant load program $\sigma(t) = \sigma$, equation (5.6) reduces to:

$$X = \kappa(\sigma)T, \text{ so } \bar{T} = \frac{\bar{X}}{\kappa(\sigma)}. \tag{5.7}$$

We use this result in equation (5.2) to obtain:

$$L = \int_0^T \frac{dx}{\bar{T}(\sigma(x))} = \frac{1}{\bar{X}} \int_0^T \kappa(\sigma(x))dx = \frac{X}{\bar{X}}. \tag{5.8}$$

For this class of models, the Life Fraction Rule holds since $E[L] = E[X/\bar{X}] = 1$. Moreover, the materials described by this class of models demonstrate regular failure behavior because the distribution of L does not depend on the load program. Repeated measurement of L, using arbitrary load program should always render the same distribution. The distribution of L can also be obtained from constant load experiments since $L = X/\bar{X} = T/\bar{T}$ (see equation (5.7)).

We will henceforth use the shorthand CRM for the Class of Regular Models, produced by the two assumptions described above. A model of the CRM is set after specification of $\kappa(\cdot)$, $f(\cdot)$ and random variable Ω. If two models of the CRM, say $(\kappa_1, f_1, \Omega_1)$ and $(\kappa_2, f_2, \Omega_2)$, satisfy $\kappa_1 = \kappa_2$ and $\int_0^{\Omega_1} f_1(z)dz = \int_0^{\Omega_2} f_2(z)dz$ then clearly these models lead to the same distribution of time-to-failure T (for arbitrary load program). However, damage buildup during a constant load program will be different for both models. For any model of the CRM (κ, f, Ω) there is an associate linear model $(\kappa, 1, X = \int_0^{\Omega} f(z)dz)$, also in the CRM, rendering the same L and T, however this time with linear damage buildup during a constant load program. Apparently, the way damage builds up during a constant load program is irrelevant. Palmgren-Miner's rule, as archetype of regular material behavior, is associated with 'linear damage accumulation' all through the literature on this subject. Our analysis shows that 'linear damage accumulation' is not a prerequisite for satisfying Palmgren-Miner's rule. This is also true for a completely deterministic interpretation of Palmgren-Miner's rule. Crucial in this discussion is that the damage function $\omega(t)$ itself is insufficient to determine T; it can only do so in combination with Ω:

$$\Omega = \int_0^T \omega(z)dz. \tag{5.9}$$

Next we investigate the load curve, i.e. the functional relationship between the logarithm of time-to-failure and applied load in case of a constant load program. The equality $X = \kappa(\sigma)T$ (equation (5.7)) with X independent of load σ represents linear scalability of the time-to-failure distributions belonging to constant load programs. It readily follows for all models of the CRM that $\ln(T) = \ln(X) - \ln(\kappa(\sigma))$. The shape of the load curve depends on function $\kappa(\cdot)$. Two commonly encountered types of load curves, power-law and exponential, can be recovered by substitution of $\kappa(\sigma) = a\sigma^b$ or $\kappa(\sigma) = a\exp(b\sigma)$ respectively. Apparently, $\text{Var}[\ln(T)] = \text{Var}[\ln(X)]$ is independent of load. This can readily be verified experimentally.

For regular behavior, the assumptions given earlier in this chapter are sufficient. For some materials there is experimental evidence of Weibull distributed time-to-failure at constant load. A special subclass of the CRM is arrived at if it is additionally assumed that:

- Assumption 3
  Time-to-failure at constant load σ is Weibull distributed, say $T \sim W(k, t_0(\sigma))$, and the shape factor k is independent of load.

Now random variable X (equation (5.7)) is also Weibull distributed: $X \sim W(k, x_0 = \kappa(\sigma)t_0(\sigma))$, with x_0 independent of load σ. From equation (5.6) we can construct the distribution function of T for arbitrary load program:

$$\begin{aligned} F_T(t) &= P(T \leq t) = P\left(X \leq \int_0^t \kappa(\sigma(\tau))d\tau\right) \\ &= 1 - \exp\left(-\left(x_0^{-1}\int_0^t \kappa(\sigma(\tau))d\tau\right)^k\right). \end{aligned} \tag{5.10}$$

The model depicted in equation (5.10) was already proposed by Coleman [9] in 1958 and later studied by Phoenix [49,50] and Knoester et al [12,46]. This model will henceforth be denoted the 'Coleman model'. Note that the Life Fraction L is also Weibull distributed and only depends on the Weibull shape factor k: $L \sim W(k, \Gamma_k^{-1})$. Note also that the assumption that k is independent of load in Assumption 3 is essential. If k would have been load dependent then surely the distribution of L is load dependent as well, refuting regularity.

In practice, many materials show non-regular behavior. At least this holds for fatigue, where Palmgren-Miner's rule (the 'fatigue analog' of the LFR) is often found to give non-conservative results, i.e. predicting a lifetime longer than observed experimentally (Paepegem [74]). Constant load programs are not suited to investigate non-regularity since for such programs we find $E[L] = E[T/\bar{T}] = 1$ for any material. Single step constant load programs (SSPs), the simplest type of load program after constant load programs, turn out to be very well suited to measure material regularity. Non-regular materials show either prolonged or reduced lifetime for High-Low or Low-High SSPs or both. For non-regular materials, Life-Fraction L will depend on the load program. In Sections 5.4 and 5.5 we analyze two non-regular models and their distributions of the Life-Fraction L. For one of the models the random variable representing damage at the moment of breaking Ω is not load independent anymore (Section 5.4). For the other model, the damage evolution law is non-separable (Section 5.5).

5.4 Non-regular model A: Damage-at-break inversely proportional to actual load

In this chapter a class of non-regular models is introduced for failure of fibers by creep rupture, which will be denoted by 'model A'. Similar to the class of regular models (CRM) discussed previously, for model A we assume the existence of a damage function. Contrary to the CRM, the critical damage level (= damage at the moment of breaking) is considered load-dependent, which violates the second assumption put forward in the previous chapter. Christensen [70] suggested that a fiber subjected to a high load only needs relatively little accumulated damage in order to break. Subjected to a low load, the fiber must first build up considerable internal damage before it breaks. Translated to the nomenclature in Section 5.3, the damage-at-break random variable Ω is considered load-dependent. This notion gives rise to deviation from the Life Fraction Rule. We will show that the failure time of High-Low SSPs is prolonged and for Low-High SSPs the failure time is shortened, that is: if 'damage-at-break' (failure criterion) is inversely proportional to applied load.

First we construct a class of models for time-to-failure T for fibers subjected to a constant load program (see 5.4.1). Then the model is extended to accommodate single step constant load programs in 5.4.2. The primary focus in this section is to obtain a distribution function for Life Fraction L. We derive distribution functions for L expressed in the distribution of time-to-failure T (at constant load). The latter can easily be measured experimentally, but remains unspecified at first. Since time-to-failure of Twaron yarn is adequately described by a Weibull distribution, we later reformulate the distribution of L accordingly (see 5.4.2). In Section 5.6 we compare theory with measurements on Twaron yarn.

Model A only applies to constant load and single step constant load programs. In case theory and measurements compare well for these loadings, it is tempting to investigate if and how model A can be extended to more complex load programs. We will briefly describe such an extension in 5.4.3, however the focus of this chapter remains solely on single step load programs.

5.4.1 Constant load program

Suppose damage buildup during a constant load program is linear in time, load dependent and therefore a special case of equation (5.4):

$$\omega(t) = \kappa(\sigma)t, \text{ or: } \dot{\omega} = \kappa(\sigma) = \text{constant}. \tag{5.11}$$

Apparently, if T_i is the time-to-failure distribution at constant load σ_i, then the damage-at-break distribution Ω_i associated with σ_i simply follows from:

$$\Omega_i = \kappa(\sigma_i)T_i. \tag{5.12}$$

Next, deviating from the CRM, we assume the existence of a load independent random variable Ω with cdf $F_\Omega(\cdot)$ from which Ω_i for arbitrary constant load σ_i can be derived:

$$\Omega_i = \Omega / f(\sigma_i). \tag{5.13}$$

Clearly:

$$T_i = \Omega / \kappa_n(\sigma_i) \quad \text{with} \quad \kappa_n(\sigma_i) = \kappa(\sigma_i) f(\sigma_i). \tag{5.14}$$

Equation (5.14) is considered as a class of probabilistic models for time-to-failure T_i at arbitrary constant load σ_i. Specific models in this class follow if function $\kappa_n(\cdot)$ and a distribution for Ω are prescribed. After inclusion of equation (5.11) into these models, extension to single step constant load programs is possible (next section) and we will show that non-regular material behavior is retrieved.

Similar to the regular models (CRM) discussed previously, there is linear scalability for time-to-failure at constant load: $F_{T_i}(t) = F_\Omega\left(\kappa_n(\sigma_i)t\right)$. As a consequence, the load curves of materials satisfying model A cannot be distinguished from the load curves predicted by the models of the CRM. Still we like to draw attention to the fact that the combination of a power function for $f(\cdot)$, say $f(x) = x^m$ and an exponential $\kappa(x) = \alpha e^{\beta x}$ (or vice versa) results in a mixed form of load curve:

$$\ln T_i = \ln \Omega - \ln \alpha - m \ln \sigma_i - \beta \sigma_i. \tag{5.15}$$

This load curve form is identical to the Eyring-Tobolsky model (see Henderson [6]). It is emphasized that equation (5.15) can also be obtained for material behavior corresponding to the CRM by choosing an appropriate $\kappa(\cdot)$ function.

Before we analyze single step constant load programs, it is convenient to introduce scaled time-to-failure and scaled damage-at-break by:

$$U = \frac{T_i}{\overline{T_i}} = \frac{\Omega}{\overline{\Omega}}. \tag{5.16}$$

Scaled time-to-failure U applies to constant load programs only and is independent of load.

5.4.2 Single step constant load program (SSP)

Next we turn to an SSP and extend the above model as to predict the Life Fraction L for this type of load program. We plan to subject fibers sequentially to two loads σ_1 and σ_2. The load switches rapidly from σ_1 to σ_2 at a specified time τ_1. Naturally, a fiber may already have failed prior to the load switch. We add two new elements to extend the model. Damage buildup before and after the load switch are similar to as if the fiber would have been been subjected to a constant load (without load switch). Secondly, the damage level at the start of load σ_2 is the same as the final damage at $t = \tau_1$ at load σ_1.

It is convenient to compare our SSP experiment with a single constant load program (at load σ_2 only). We will denote the former experiment 'Experiment A' and the latter 'Experiment B'.

In case the fiber survived load σ_1 in Experiment A, the damage has accumulated to $\omega = \kappa(\sigma_1)\tau_1$. Let τ_2 be the corresponding time during Experiment B at which the fiber has accumulated the same amount of damage, then:

$$\omega = \kappa(\sigma_1)\tau_1 = \kappa(\sigma_2)\tau_2 \quad \text{or} \quad \tau_2 = \frac{\kappa(\sigma_1)}{\kappa(\sigma_2)}\tau_1. \tag{5.17}$$

In scaled form:

$$\omega^* = \frac{u_1}{f(\sigma_1)} = \frac{u_2}{f(\sigma_2)} \quad \text{with: } \omega^* = \frac{\omega}{\overline{\Omega}}, u_1 = \frac{\tau_1}{\overline{T}_1} \text{ and } u_2 = \frac{\tau_2}{\overline{T}_2}. \tag{5.18}$$

In equation (5.17) it was tacitly assumed that the load switch itself does not add to the damage accumulation. $\overline{T}_1$ and $\overline{T}_2$ represent mean time-to-failure corresponding to constant loads σ_1 and σ_2.

As a result of the model choices we made, the course of Experiment A after $t = \tau_1$ up to failure is identical to the course of Experiment B after $t = \tau_2$. In both cases we start with accumulated damage level ω and continue the experiment up to failure at constant load σ_2. The distribution of the Life Fraction L is conditional, depending on the moment of failure (i.e. before or after the load switch):

$$\begin{aligned} L &= \frac{T_1}{\overline{T}_1} = U \qquad \text{up to load switch,} \\ L &= \frac{\tau_1}{\overline{T}_1} + \frac{T_2 - \tau_2}{\overline{T}_2} = U + (1-\alpha)u_1 \text{ after load switch,} \end{aligned} \tag{5.19}$$

using $u_2 = \alpha u_1$ with $\alpha = \frac{f(\sigma_2)}{f(\sigma_1)}$. However, there is a complicating factor. The situation of Experiment A at $t = \tau_1$ is not entirely the same as Experiment B at $t = \tau_2$. This can best be understood by imagining that each of the Experiments is performed on all members of some large, representative set of fibers. The fraction of failed fibers in Experiment A during $[0, \tau_1)$ equals $n_1 = F_{T_1}(\tau_1) = F_U(u_1)$ and the fraction of failed fibers in Experiment B during $[0, \tau_2)$ equals $n_2 = F_{T_2}(\tau_2) = F_U(u_2)$. Generally, n_1 and n_2 are not the same.

Case $\alpha > 1$. ($f(\sigma_2) > f(\sigma_1)$)

Clearly $n_2 > n_1$ for this case, i.e. in Experiment A there are more surviving fibers at $t = \tau_1$ than at $t = \tau_2$ during Experiment B. As a matter of fact, the surplus number of surviving fibers in Experiment A will momentarily break during the load switch. After all, the probability of failure during the load switch is:

$$P(T_1 > \tau_1 \cap T_2 \leq \tau_2) = P\left(u_1 < U \leq u_2\right) = n_2 - n_1. \tag{5.20}$$

If we make the intuitive assumption that the required damage-at-break decreases with increasing (actual) load then clearly $f(\sigma_2) > f(\sigma_1)$ iff $\sigma_2 > \sigma_1$. So, for a Low-High SSP, the model predicts a non-zero fraction of fibers to fail during the load switch (again: without taking into account a damage contribution due to the load switch itself).

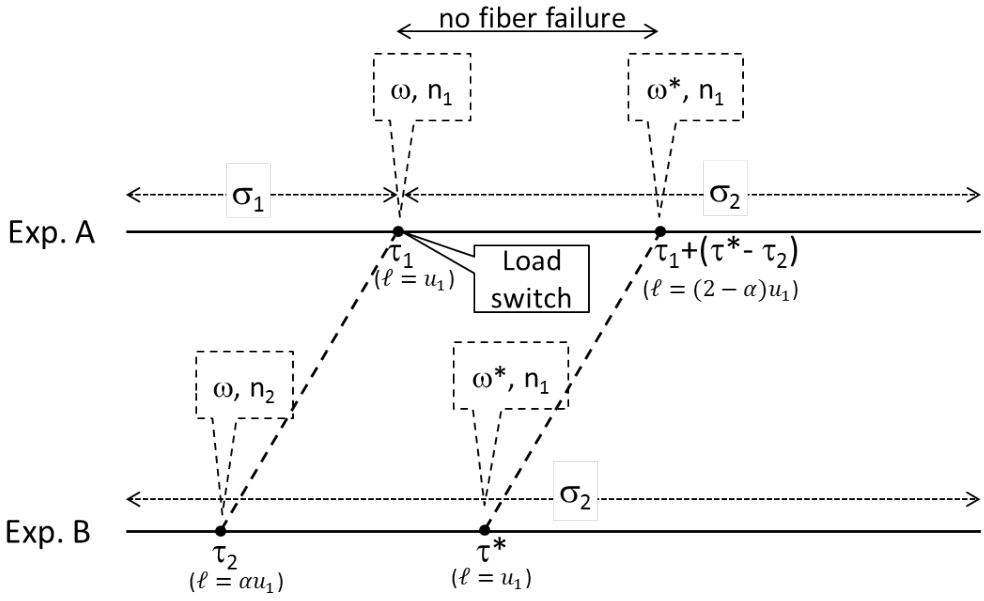

Figure 5.1: *Comparison of Experiment A and B for case* $0 < \alpha < 1$. *For some specific times the damage* ω *and failed fiber fraction* n *are given:* $\omega = \kappa(\sigma_1)\tau_1 = \kappa(\sigma_2)\tau_2$, $\omega^* = \kappa(\sigma_2)\tau^*$, $n_1 = F_{T_1}(\tau_1) = F_{T_2}(\tau^*)$, $n_2 = F_{T_2}(\tau_2)$. *For each time the corresponding current Life Fraction* ℓ *is given between brackets.*

Case $0 < \alpha < 1$. $(f(\sigma_2) < f(\sigma_1))$

There are less surviving fibers at $t = \tau_1$ for Experiment A than at $t = \tau_2$ during Experiment B. The fraction surviving fibers for Experiment A, e.g. $1 - n_1$, must be the strongest cohort of all fibers tested. It makes sense to assume that, starting with the same set of fibers, the fraction of fibers demonstrating the longest time-to-failure in Experiment A would also exhibit the longest time-to-failure in any other load-bearing experiment. We will call this assumption the Equal Rank Assumption or ERA, following the well-known (Strength-Lifetime Equal Rank Assumption) [51, 52]. The surviving fiber fraction $1 - n_1$ in Experiment A will also have the longest times-to-failure in case they would have been subjected to σ_2 only (Experiment B). During Experiment B, this cohort starts breaking at time $t = \tau^*$ satisfying:

$$F_{T_2}(\tau^*) = n_1 \quad \Rightarrow \frac{\tau^*}{\bar{T}_2} = \frac{\tau_1}{\bar{T}_1}. \tag{5.21}$$

Translated back again to Experiment A, this means that as from the load switch at time $t = \tau_1$ no fiber failures are expected during a time period of length $(\tau^* - \tau_2)$, i.e. from time $t = \tau_1$ until $t = \tau_1 + (\tau^* - \tau_2)$. Equivalently, there will be no observation of a Life Fraction in between $L = u_1$ (for failure at $t = \tau_1$) and $L = \tau_1/\bar{T}_1 + (\tau^* - \tau_2)/\bar{T}_2 = (2 - \alpha)u_1$ (at time $t = \tau_1 + (\tau^* - \tau_2)$). The situation is graphically elucidated in Figure 5.1.

Next, we derive the distribution function for the Life Fraction L, defined in equations (5.19) (also see Figure 5.2). Clearly, the distribution function of L can be expressed in terms of the distribution function of U, however, one should reckon with the stipulations outlined above.
Case $\alpha > 1$

$$\begin{aligned}
\ell < u_1: \quad F_L(\ell) &= P(L \le \ell) = P(U \le \ell) = F_U(\ell) \\
\ell = u_1: \quad F_L(\ell) &= P(L \le u_1) = P(L = u_1) + P(L < u_1) \\
&= P(u_1 < U < \alpha u_1) + P(U < u_1) \\
&= F_U(\alpha u_1) \\
\ell > u_1: \quad F_L(\ell) &= P(L \le \ell) = P(L \le u_1) + P(u_1 < L < \ell) \\
&= F_U(\alpha u_1) + P(\alpha u_1 < U < \ell - (1-\alpha)u_1) \\
&= F_U(\ell - (1-\alpha)u_1) \qquad (5.22)
\end{aligned}$$

Case $0 < \alpha < 1$

$$\begin{aligned}
\ell \le u_1: \quad F_L(\ell) &= P(L \le \ell) = P(U \le \ell) = F_U(\ell) \\
u_1 < \ell < (2-\alpha)u_1: \quad F_L(\ell) &= P(L \le \ell) = P(L \le u_1) + P(u_1 < \ell < (2-\alpha)u_1 l) \\
&= P(L \le u_1) = F_U(u_1) \\
\ell \ge (2-\alpha)u_1: \quad F_L(\ell) &= P(L \le \ell) = P(L \le u_1) + P((2-\alpha)u_1 < L \le \ell) \\
&= P(U \le u_1) + P(u_1 < U < \ell - (1-\alpha)u_1) \\
&= F_U(\ell - (1-\alpha)u_1) \qquad (5.23)
\end{aligned}$$

Expressions for the expectation of L are given below:
Case $\alpha > 1$

$$\begin{aligned}
E[L] &= \int_0^{u_1} x f_U(x)dx + u_1 P(L = u_1) + \int_{u_1}^{\infty} x f_U(x - (1-\alpha)u_1)dx \\
&= 1 + u_1 \left(1 - F_U(u_1)\right) - \alpha u_1 \left(1 - F_U(\alpha u_1)\right) - \int_{u_1}^{\alpha u_1} x f_U(x)dx, \qquad (5.24)
\end{aligned}$$

using $\bar{U} = 1$ and $P(L = u_1) = P\left(u_1 < U \le \alpha u_1\right)$.
Note that $E[L] < 1$ for all u_1 because $\int_{u_1}^{\alpha u_1} x f_U(x)dx \ge u_1 \left(F_U(\alpha u_1) - F_U(u_1)\right)$.
Case $0 < \alpha < 1$

$$\begin{aligned}
E[L] &= \int_0^{u_1} x f_U(x)dx + \int_{(2-\alpha)u_1}^{\infty} x f_U(x - (1-\alpha)u_1)dx \\
&= 1 + (1-\alpha)u_1 \left(1 - F_U(u_1)\right). \qquad (5.25)
\end{aligned}$$

Clearly, $E[L] > 1$ for all u_1 in this case.

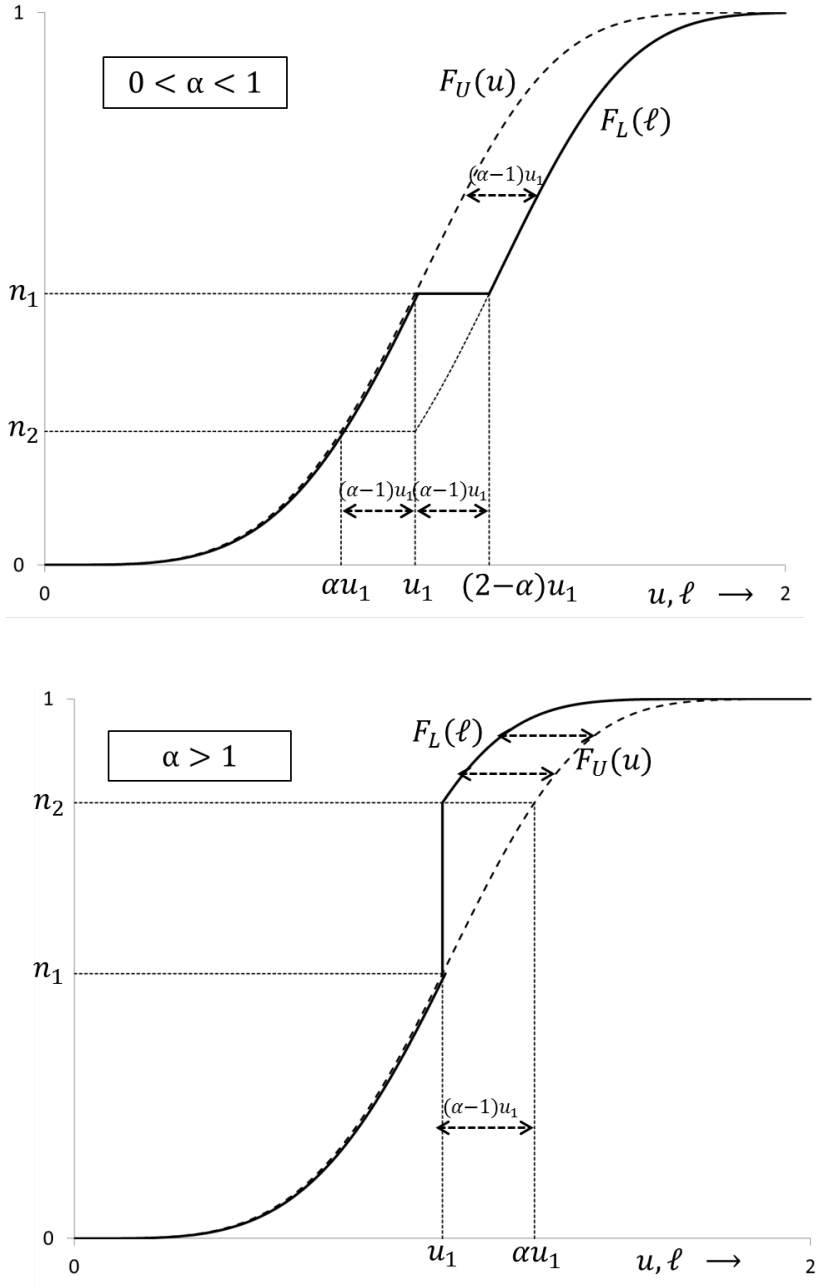

Figure 5.2: $F_L(\ell)$ *(solid curves) for both cases* $0 < \alpha < 1$ *and* $\alpha > 1$ *as derived from* $F_U(u)$ *(dashed curves).*

Weibull distributed time-to-failure

If we assume that time-to-failure at constant load is Weibull distributed, then scaled time-to-failure $U = T/\bar{T}$ is also Weibull distributed and depends on one parameter k only (the Weibull modulus of time-to-failure):

$$F_U(u) = 1 - \exp\left\{-\left(u\Gamma_k\right)^k\right\} \text{ with: } \Gamma_k = \Gamma(1 + 1/k). \tag{5.26}$$

In Section 5.3 we outlined that the distribution of the Life Fraction L for any model from the class of regular models (CRM) and for any load program is identical to the distribution for scaled time-to-failure: $F_L(\ell) = F_U(\ell)$. For model A applied to SSPs, the distribution function of L (and $E[L]$) are obtained after substitution of equation (5.26) into equations (5.22) to (5.25):
Case $\alpha > 1$

$$\begin{aligned} \ell < u: \quad F_L(\ell) &= 1 - \exp\left\{-\left(\ell\Gamma_k\right)^k\right\}, \\ \ell \geq u: \quad F_L(\ell) &= 1 - \exp\left\{-\left(\left(\ell - (1-\alpha)u\right)\Gamma_k\right)^k\right\}, \end{aligned} \tag{5.27}$$

$$\begin{aligned} E[L] &= 1 + u\exp\left\{-\left(u\Gamma_k\right)^k\right\} - \alpha u\exp\left\{-\left(\alpha u\Gamma_k\right)^k\right\} + \\ &\quad \frac{\Gamma_{\text{lower}}\left(1 + 1/k, (u\Gamma_k)^k\right)}{\Gamma_k} - \frac{\Gamma_{\text{lower}}\left(1 + 1/k, (\alpha u\Gamma_k)^k\right)}{\Gamma_k}, \end{aligned} \tag{5.28}$$

with $\Gamma_{\text{lower}}(p, x)$ the lower incomplete Gamma function defined by:

$$\Gamma_{\text{lower}}(p, x) = \int_0^x z^{p-1}\exp(-z)dz. \tag{5.29}$$

Case $0 < \alpha < 1$

$$\begin{aligned} \ell \leq u: \quad F_L(\ell) &= 1 - \exp\left\{-\left(\ell\Gamma_k\right)^k\right\}, \\ u < \ell < (2-\alpha)u: \quad F_L(\ell) &= 1 - \exp\left\{-\left(u\Gamma_k\right)^k\right\}, \\ \ell \geq (2-\alpha)u: \quad F_L(\ell) &= 1 - \exp\left\{-\left(\left(\ell - (1-\alpha)u\right)\Gamma_k\right)^k\right\}, \end{aligned} \tag{5.30}$$

$$E[L] = 1 + (1-\alpha)u\exp\left\{-\left(u\Gamma_k\right)^k\right\}. \tag{5.31}$$

The distribution of L depends on two model parameters: k and α. The time-to-failure distribution at constant load (σ_1 and/or σ_2) delivers an estimate for k, for example from the classic Weibull plot. The other parameter α can then be used to fit the experimental data of the SSP experiments. For material behavior consistent with model A, it must be possible to describe associate High-Low and Low-High SSPs by a single α and its reciprocal value. Note in this respect that $\alpha = \frac{f(\sigma_2)}{f(\sigma_1)}$ with $f(\cdot)$ an unknown function. In Figure 5.3 the average Life Fraction is plotted for associate High-Low and Low-High SSPs.

In this Figure we adopted the assumption that $f(\cdot)$ is a positive, increasing function. This choice corresponds to the theory of Christensen [70]. For a High-Low SSP ($\sigma_1 > \sigma_2$ and

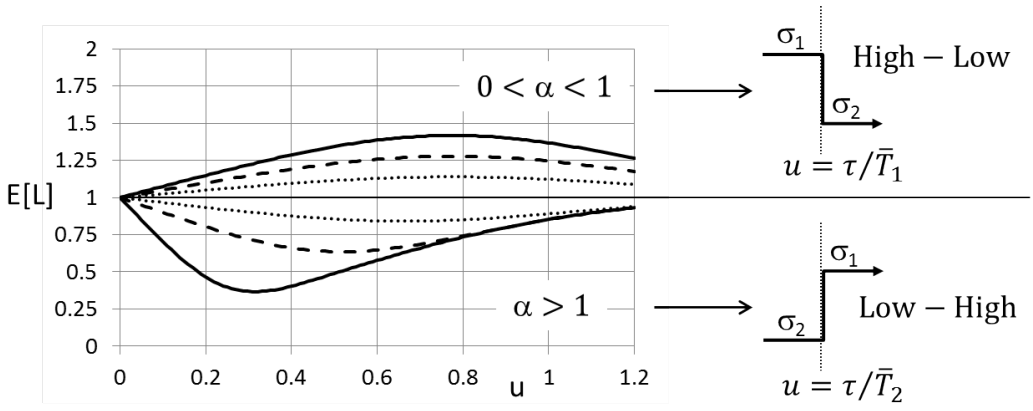

Figure 5.3: *Mean value of Life Fraction L corresponding to model A, for a single step constant load program as function of the scaled time at load switch u for $k = 3$ and various couples of $(\alpha, 1/\alpha)$. Solid curves: $(0.25, 4)$; dashed curves: $(0.5, 2)$; dotted curves: $(0.75, 4/3)$. Connection to High-Low and Low-High SSP valid for an increasing function $f(\cdot)$ (see text).*

$0 < \alpha < 1$) we showed earlier that $E[L] > 1$ and so its lifetime is prolonged. Clearly, the associate Low-High SSP corresponding to $\alpha > 1$ has a shortened lifetime $E[L] < 1$. Still, the assumption of $f(\cdot)$ being an increasing function is not needed for the mathematical analysis. In principle, $f(\cdot)$ may also be decreasing, ultimately giving opposite model predictions. Anyway, for monotonous $f(\cdot)$, associate High-Low and Low-High SSP experiments should always render opposite material behavior. If one experiment corresponds to $E[L] > 1$ then the associate experiment must correspond to $E[L] < 1$.

Figure 5.3 shows that maximum deviation from regular behavior (maximum or minimum values for $E[L]$) for associate Low-High and High-Low programs is not found at the same scaled time u:

$$\text{maximum } E[L] \text{ is found for} \quad u_{\max} = \Gamma_k^{-1} \cdot \left(\frac{1}{k}\right)^{1/k} \quad (0 < \alpha < 1), \tag{5.32}$$

$$\text{minimum } E[L] \text{ is found for} \quad u_{\min} = \Gamma_k^{-1} \cdot \left(\frac{\ln \alpha}{\alpha^k - 1}\right)^{1/k} \quad (\alpha > 1). \tag{5.33}$$

Apparently, $u_{\max}$ is independent of α and $u_{\min} < u_{\max}$ for all $\alpha > 1$.

5.4.3 Arbitrary load program

How can model A be generalized to encompass an arbitrary load program $\sigma_p(t)$? A straightforward generalization of damage accumulation is obtained from equation (5.11):

$$\omega(t) = \int_0^t \kappa(\sigma_p(x))dx. \tag{5.34}$$

For all regular models in the CRM, the probability of fiber failure depends solely on the accumulated damage. For model A, this probability also depends on the current load level the fiber is subjected to, effectuated by a load-dependent damage-at-break variable (see equation (5.13)):

$$\Omega_i = \Omega / f(\sigma_i). \tag{5.35}$$

Here, Ω_i is the damage-at-break distribution of fibers breaking at a load level of σ_i. We propose that the damage-at-break distribution continuously changes with changing load and herewith becomes a function of time t: $\Omega_t = \Omega / f(\sigma_p(t))$. For a constant load program at load σ_i we have $P(T < \tau) = P(\Omega_i \leq \omega(\tau))$. Here, $\Omega_i = \Omega / f(\sigma_i)$ is fixed in time and $\omega(\cdot)$ is non-decreasing. Thus, probability $P(\Omega_i \leq \omega(t))$ is a non-decreasing function of t (as it should). For arbitrary load program $\sigma_p(t)$, probability $P(\Omega_t \leq \omega(t))$ can locally be decreasing. Therefore, in order to compute $P(T < \tau)$ we need to check $P(\Omega_t \leq \omega(t))$ for the whole history of the load program up to the current moment τ, i.e.

$$\begin{aligned} F_T(\tau) &= P(T \leq \tau) = \max\left\{P\left(\Omega_t \leq \omega(t)\right); 0 < t \leq \tau\right\} \\ &= \max\left\{P\left(\Omega \leq f(\sigma_p(t)) \cdot \omega(t)\right); 0 < t \leq \tau\right\} \\ &= P\left(\Omega \leq \max\left\{f(\sigma_p(t)) \cdot \omega(t); 0 < t \leq \tau\right\}\right). \end{aligned} \tag{5.36}$$

If load program $\sigma_p(\cdot)$, break-down rule function $\kappa(\cdot)$ and function $f(\cdot)$ are prescribed, equation (5.36) is a recipe for the construction of the time-to-failure distribution T corresponding to $\sigma_p(\cdot)$ (see Figure 5.4). To this end, Ω can be estimated by measuring the time-to-failure distribution T_i at arbitrary constant load σ_i, after all: $\Omega = f(\sigma_i)\,\kappa(\sigma_i)T_i = \kappa_n(\sigma_i)T_i$. Thus:

$$F_T(\tau) = F_{T_i}\left(\max\left\{\frac{f(\sigma_p(t)) \cdot \omega(t)}{\kappa_n(\sigma_i)}; 0 < t \leq \tau\right\}\right). \tag{5.37}$$

Finally, according to model A the Life Fraction for load program $\sigma_p(t)$ follows from:

$$L = \int_0^T \frac{dx}{\bar{T}(\sigma_p(x))} = \frac{1}{\bar{\Omega}} \int_0^T \kappa_n(\sigma_p(x))dx = \frac{1}{\bar{T}_i} \int_0^T \frac{\kappa_n(\sigma_p(x))}{\kappa_n(\sigma_i)}dx, \tag{5.38}$$

where time-to-failure T_i at arbitrary constant load σ_i is again taken as reference.

Comparison of the theoretically obtained distribution of L in equation (5.38) with observed Life Fractions from measurements is not trivial, simply because it is not evident how to calculate the Life Fraction from an experiment using arbitrary load program $\sigma_p(t)$. Calculation of L for an SSP relies on the (accurate) knowledge of the mean times-to-failure at the loads applied in the

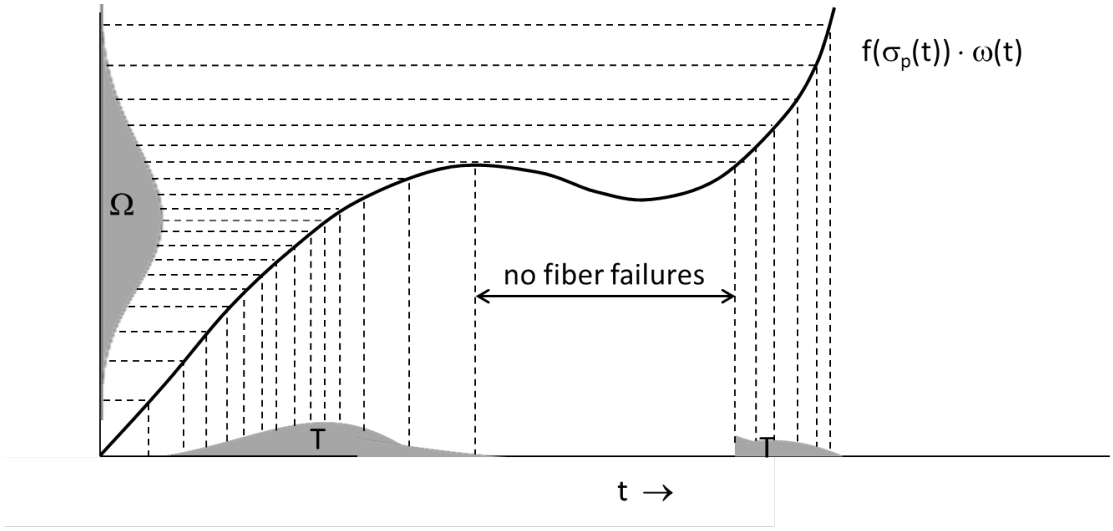

Figure 5.4: *Example time-to-failure density in two parts corresponding to load program $\sigma_p(t)$ caused by a temporarily declining $f(\sigma_p(t)) \cdot \omega(t)$.*

SSP. For an arbitrary load program, mean time-to-failure is required for the whole interval of loads that the arbitrary load program runs through. If measurements at various constant loads are properly described by a load curve, e.g.

$$\overline{logT} = A - B\sigma, \tag{5.39}$$

then $\bar{T} = \gamma \cdot 10^{\overline{logT}}$ can be substituted in the definition of L (equation (5.2)) to find:

$$L = \frac{1}{\gamma} \int_0^T 10^{(B\sigma_p(x)-A)} dx. \tag{5.40}$$

Here γ depends on the actual distribution of time-to-failure. For Weibull distributed time-to-failure with Weibull modulus k it follows that $\gamma = \Gamma_k \, e^{\zeta/k}$ with $\zeta = 0.577215$ the Euler-Mascheroni constant (see Appendix A.4). Comparison of the theoretical Life Fraction (5.38) with 'experimentally observed' Life Fractions according to equation (5.40) validates model A. However, it is much easier to compare observed time-to-failure with its theoretical distribution in equation (5.37).

5.5 Non-regular model B: Power-law damage accumulation

In this section we introduce a second class of non-regular models for failure of fibers, which we denote by 'model B'. Model B is inspired by the Marco-Starkey model, well-known in fatigue analysis (for a review see Fatemi [75]). For model B damage-at-break is fixed, but damage in a fiber subjected to a constant load builds up as a power-law function in time, with the power a function of the load level. Now the first assumption in Section 5.3 is violated (separable damage evolution law).

First we construct a class of models for time-to-failure T of fibers subjected to a constant load program (see 5.5.1) which is extended to accommodate SSPs in 5.5.2. Again the focus is on the Life Fraction L. The distribution of L is expressed in terms of the distributions of scaled times-to-failure at the load levels used in the SSP. Then, to enable comparison with measurements on Twaron yarns in Section 5.6, a distribution function for L is derived which is consistent with a Weibull distributed time-to-failure at constant load. Model B only applies to constant load programs and SSPs. We will briefly describe how the model can be extended to an arbitrary load program in 5.5.3.

5.5.1 Constant load program

The first element of the model is that damage buildup during a constant load program is described by a load-dependent power-law relationship:

$$\omega(t) = (\kappa(\sigma)t)^{\alpha(\sigma)}, \tag{5.41}$$

with both $\kappa(\cdot)$ and $\alpha(\cdot)$ positive functions of load σ. For arbitrary constant load σ_i, this enables the construction of the damage-at-break variable Ω_i via $\Omega_i = (\kappa_i T_i)^{\alpha_i}$, where T_i is the time-to-failure distribution at load σ_i, $\kappa_i = \kappa(\sigma_i)$ and $\alpha_i = \alpha(\sigma_i)$. The second element of the model, similar to the regular models, assumes that damage-at-break is in fact load independent. Thus there is a damage-at-break distribution Ω with distribution function $F_\Omega()$ such that $\Omega_i = \Omega$ for arbitrary load σ_i. Now, time-to-failure distribution T_i is linked to Ω via:

$$T_i = \Omega^{1/\alpha_i}/\kappa_i. \tag{5.42}$$

The combined equations (5.41) and (5.42) form a class of models for time-to-failure T_i and damage accumulation at arbitrary constant load σ_i. Specific models in this class follow if functions $\kappa(\cdot)$, $\alpha(\cdot)$ and a distribution for Ω are prescribed. The following scaling rule applies:

$$F_{T_i}(t) = P(T_i \le t) = P\left((\kappa_i T_i)^{\alpha_i} \le (\kappa_i t)^{\alpha_i}\right) = F_\Omega\left((\kappa_i t)^{\alpha_i}\right). \tag{5.43}$$

Taking the logarithm of equation (5.42) yields the following prediction for the load curve: $\ln T = \ln \Omega/\alpha(\sigma) - \ln(\kappa(\sigma))$. Variability of $\ln T$ satisfies $\mathrm{Var}[\ln T] = \mathrm{Var}[\ln \Omega]/\alpha^2(\sigma)$ and is

therefore load dependent. Load dependent variability of $\ln T$ contradicts regular behavior. The way time-to-failure scales with load depends on $\kappa(\sigma)$. Via this function, all kinds of load curves (e.g. power-law, exponential) can be retrieved in the same way as for regular models.

Also for this model we introduce scaled time-to-failure and scaled damage-at-break:

$$U_i = \frac{T_i}{\bar{T}_i} \text{ and } U = \frac{\Omega}{\bar{\Omega}} \quad \text{so:} \quad F_{T_i}(\tau) = F_{U_i}(u) = F_U(\xi_i u^{\alpha_i}), \tag{5.44}$$

with: $u = \tau/\bar{T}_i$ and $\xi_i = (\overline{\Omega^{1/\alpha_i}})^{\alpha_i}/\bar{\Omega} = 1/\overline{U_i^{\alpha_i}}$. Similar to the regular models and model A, function κ_i does not affect scaled time-to-failure U_i in any way. Note that the scaled time-to-failure distributions U_i and U_j are related to each other:

$$U_j = \left(\frac{\xi_i}{\xi_j}\right)^{1/\alpha_j} U_i^{\alpha_i/\alpha_j} = a_{ij} U_i^{b_{ij}}. \tag{5.45}$$

We will consider a_{ij} and b_{ij} as known constants, they can be estimated once the time-to-failure distributions T_i and T_j are determined experimentally.

5.5.2 Single step constant load program (SSP)

For a single step constant load program (SSP), the fiber is first preloaded at load σ_1 during time τ_1. In case of survival, the load is then switched to σ_2 and the experiment is continued until failure. We add two new elements to model B in order to be able to apply it to SSPs. Damage buildup before and after the load switch are similar to as if the fiber would have been been subjected to a constant load (without load switch). Secondly, the damage level at the start of load σ_2 is the same as the final damage at $t = \tau_1$ at load σ_1, therefore:

$$\omega = (\kappa_1 \tau_1)^{\alpha_1} = (\kappa_2 \tau_2)^{\alpha_2}, \tag{5.46}$$

where τ_2 is the virtual time at the moment of load switching as if the fiber had been subjected to load σ_2 right from the start of the experiment. Here it was tacitly assumed that the load switch itself does not add to the damage accumulation. Equation (5.46) can be rewritten in scaled form:

$$\xi_1 u_1^{\alpha_1} = \xi_2 u_2^{\alpha_2} \text{ or: } u_2 = a_{12} u_1^{b_{12}} \text{ with: } u_i = \frac{\tau_i}{\bar{T}_i}; \tag{5.47}$$

therefore we find:

$$\begin{aligned} n_1 &= P(T_1 \le \tau_1) = F_{U_1}(u_1) = F_U(\xi_1 u_1^{\alpha_1}) \\ &= F_U(\xi_2 u_2^{\alpha_2}) = F_{U_2}(u_2) = P(T_2 \le \tau_2) = n_2. \end{aligned} \tag{5.48}$$

The fraction of failed fibers n_1 at time $t = \tau_1$ during the SSP is thus the same as the fraction of failed fibers n_2 at time $t = \tau_2$ during a constant load program at load σ_2. The procedures in case of $n_1 \neq n_2$ as explained for model A (see 5.4.2) are unnecessary for model B.

Again, the distribution of the life Fraction L is conditional, depending on the moment of failure (i.e. before or after the load switch):

$$\begin{aligned} L &= \frac{T_1}{\bar{T}_1} = U_1 \qquad \text{up to load switch,} \\ L &= \frac{\tau_1}{\bar{T}_1} + \frac{T_2 - \tau_2}{\bar{T}_2} = U_2 + \beta_{12} \text{ after load switch,} \end{aligned} \tag{5.49}$$

with $\beta_{12} = u_1 - u_2 = u_1 - a_{12}u_1^{b_{12}}$. The scalar u_1 is prescribed: τ_1 is an input variable of the experimental program and $\bar{T}_1$ can be measured separately. Scalar u_2 is a function of u_1, so both u_1 and u_2 can be considered as known. Factually, β_{12} is a constant, however dependent on the scaled moment of load switch u_1 so it can be expressed as function:

$$\beta_{ij}(x) = x - a_{ij}x^{b_{ij}}. \tag{5.50}$$

The subscript $\{ij\}$ reminds us that β also depends on the load levels σ_1 and σ_2 and their ordering. Using equations (5.49), the distribution function of L and its expectation follow from:

$$\begin{aligned} \ell \le u_1: \quad F_L(\ell) &= P(L \le \ell) = P(U_1 \le \ell) = F_{U_1}(\ell), \\ \ell > u_1: \quad F_L(\ell) &= P(L \le \ell) = P(L \le u_1) + P(u_1 < L < \ell) \\ &= F_{U_1}(u_1) + P(u_1 - \beta_{12}(u_1) < U_2 < \ell - \beta_{12}(u_1)) \\ &= F_{U_1}(u_1) - F_{U_2}(u_2) + F_{U_2}(\ell - \beta_{12}(u_1)) = F_{U_2}(\ell - \beta_{12}(u_1)), \end{aligned} \tag{5.51}$$

$$\begin{aligned} E[L] &= \int_0^{u_1} x f_{U_1}(x)dx + \int_{u_1}^{\infty} x f_{U_2}(x - \beta_{12}(u_1))dx \\ &= 1 + \beta_{12}(u_1)(1 - F_{U_1}(u_1)) + \int_0^{u_1} x f_{U_1}(x)dx - \int_0^{u_2} x f_{U_2}(x)dx \\ &= 1 + \beta_{12}(u_1)(1 - F_{U_1}(u_1)) + \int_0^{u_1} \beta_{12}(x) f_{U_1}(x)dx. \end{aligned} \tag{5.52}$$

The cumulative distribution function of L is visualized in Figure 5.5 for cases $\beta_{12}(u_1) > 0$ and $\beta_{12}(u_1) < 0$ separately. Both $F_L(\cdot)$ and $E[L]$ can be expressed in terms of the measurable distributions of U_1 and U_2. More important is the stochastic ordering of L relative to U_1. In the bottom panel of Figure 5.5 the SSP starts of with the load having the lowest variability (equivalent to steepest cumulative distribution function). For this case L is first order dominant over U_1 ($L \succeq U_1$) because $F_{U_1}(x) \ge F_L(x)$ for all $x > 0$ and the inequality is strict for some interval in x. This implies that $E[L] > E[U_1] = 1$. Contrary, if the load having the highest variability is the first load of the program (see top panel of Figure 5.5) then U_1 is first order dominant over L and $E[L] < 1$. These conclusions always hold, irrespective of the moment of load switching represented by u_1. Apparently, it is the variability of time-to-failure associated with a load and not the load level itself which is decisive. So the model does not actually make predictions for a High-Low or Low-High SSP. Here model B essentially deviates from the Marco-Starkey model [11, 75], where the order of load levels is held responsible for the Life Fraction (also see discussion and conclusions in Section 5.7).

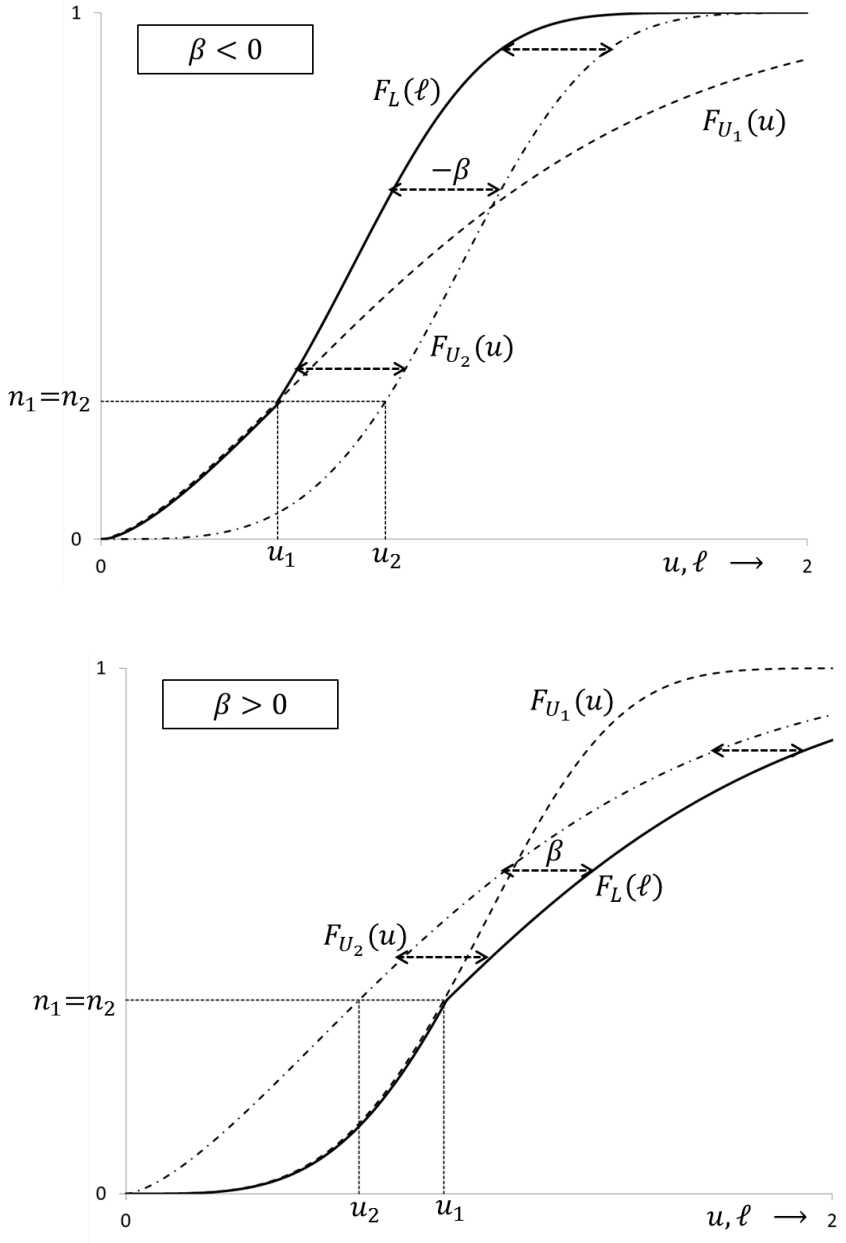

Figure 5.5: $F_L(\ell)$ *(solid curves) for cases* $\beta = \beta_{12}(u_1) > 0$ *and* $\beta = \beta_{12}(u_1) < 0$ *as derived from* $F_{U_1}(u)$ *and* $F_{U_2}(u)$ *(dashed curves).*

Weibull distributed time-to-failure

Suppose time-to-failure T_i at constant load σ_i is Weibull distributed. Then the damage-at-break Ω (see equation (5.42)) is also Weibull distributed. If $\Omega \sim W(k, \omega_0)$, then $T_i \sim W(k\alpha_i, \omega_0^{1/\alpha_i}/\kappa_i)$ with $\alpha_i = \alpha(\sigma_i)$ and $\kappa_i = \kappa(\sigma_i)$. Clearly, $U_i = T_i/\bar{T}_i \sim W\left(k\alpha_i, \Gamma_{k\alpha_i}^{-1}\right)$ with $\Gamma_{k\alpha_i} = \Gamma(1 + 1/(k\alpha_i))$, so:

$$F_{U_i}(u) = 1 - \exp\left\{-\left(u\Gamma_{k\alpha_i}\right)^{k\alpha_i}\right\}. \tag{5.53}$$

A first clue for the validity of model B is therefore the observation that the Weibull modulus of (scaled) time-to-failure is a function of load. Factually, equation (5.53) replaces equation (5.26). From equation (5.45) we know that:

$$U_2 = a_{12}U_1^{b_{12}} \quad \text{with: } a_{12} = \Gamma_{k\alpha_1}^{\alpha_1/\alpha_2}/\Gamma_{k\alpha_2} \text{ and } b_{12} = \alpha_1/\alpha_2. \tag{5.54}$$

Here we used $a_{12} = \left(\frac{\xi_1}{\xi_2}\right)^{1/\alpha_2} = \left(\frac{\overline{U_2^{\alpha_2}}}{\overline{U_1^{\alpha_1}}}\right)^{1/\alpha_2}$ and $\overline{U_i^{\alpha_i}} = \Gamma_{k\alpha_i}^{-\alpha_i} \cdot \Gamma_k$.
The distribution function for L and an expression for its mean $E[L]$ follow after substitution of equations (5.53) and (5.54) into (5.51) and (5.52):

$$\begin{aligned} \ell \le u: \quad F_L(\ell) &= 1 - \exp\left\{-\left(\ell\Gamma_{k\alpha_1}\right)^{k\alpha_1}\right\}, \\ \ell > u: \quad F_L(\ell) &= 1 - \exp\left\{-\left(\left(\ell - \beta(u)\right)\Gamma_{k\alpha_2}\right)^{k\alpha_2}\right\}, \end{aligned} \tag{5.55}$$

$$\begin{aligned} E[L] &= 1 + \beta(u)\exp\left\{-\left(u\Gamma_{k\alpha_1}\right)^{k\alpha_1}\right\} + \frac{\Gamma_{lo}\left(1 + 1/(k\alpha_1), \left(u\Gamma_{k\alpha_1}\right)^{k\alpha_1}\right)}{\Gamma_{k\alpha_1}} \\ &\quad - \frac{\Gamma_{lo}\left(1 + 1/(k\alpha_2), \left((u - \beta(u))\Gamma_{k\alpha_2}\right)^{k\alpha_2}\right)}{\Gamma_{k\alpha_2}}, \end{aligned} \tag{5.56}$$

with $\beta(u) = u - a_{12}u^{b_{12}}$. The distribution function of L depends on 2 model parameters $k\alpha_1$ and $k\alpha_2$. (Note that both a_{12} and b_{12} depend on $k\alpha_1$ and $k\alpha_2$). Measurement of the time-to-failure distributions of U_1 and U_2 allows estimation of the model parameters. This means that there are no unknown parameters left to fit measurements obtained for single step constant load programs. These measurements can thus directly be used to falsify or support the validity of the model.

In Figure 5.6, $E[L]$ is plotted for associate SSPs going from the first load with low variability (large α_1) to the second load with high variability (small α_2) and vice versa. If we step from load σ_1 with Weibull modulus $k_1 = k\alpha_1$ to load σ_2 with Weibull modulus $k_2 = k\alpha_2$, then $E[L]$ attains a maximum value (if $k_1 > k_2$) or minimum value (if $k_1 < k_2$) for scaled time $u_{\text{ext},12}$ given by:

$$u_{\text{ext},12} = \left(\frac{1}{a_{12}b_{12}}\right)^{1/(b_{12}-1)}. \tag{5.57}$$

Associate SSPs do not attain their maximum and minimum values for $E[T]$ at the same scaled time because $u_{\text{ext},12}/u_{\text{ext},21} = b_{12} = \alpha_1/\alpha_2 \neq 1$. Here $u_{\text{ext},21}$ is defined as in equation (5.57), with switched subscripts, using $b_{21} = 1/b_{12}$ and $a_{21} = a_{12}^{-1/b_{12}}$.

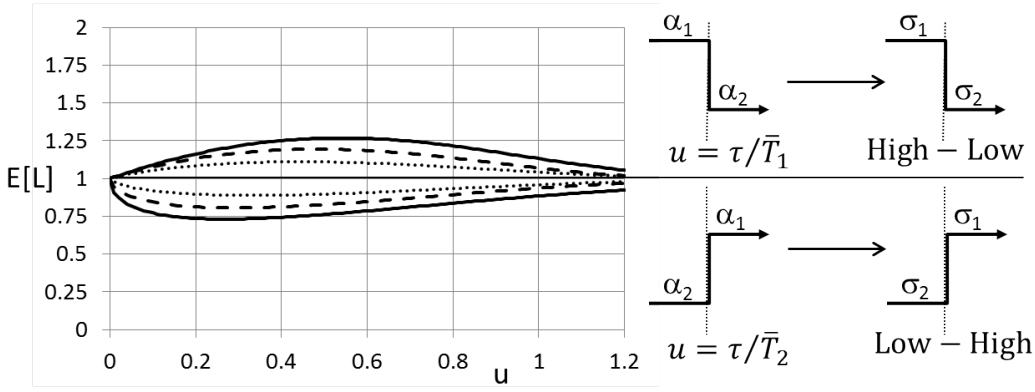

Figure 5.6: *Mean value of Life Fraction L, according to model B, for associate single step constant load programs as function of the scaled time at load switch u for various couples of $(k\alpha_1, k\alpha_2)$, $(k\alpha_2, k\alpha_1)$.*
Solid curves: (2,4), (4,2); dashed curves: (3,5), (5,3); dotted curves: (3,4), (4,3).

For Twaron yarn, time-to-failure variability does not vary significantly with load. If there is a difference in variability at all, it seems that the lower the load the larger the time-to-failure variability. Therefore, we made the connection: (low load, high variability) and (high load, low variability). This enables to present model predictions in terms of High-Low and Low-High SSPs. But it should be remembered that we made a connection between load level and time-to-failure variability observed for Twaron yarn. For other materials this connection may be the other way around. In fact, Marco and Starkey [11] claim life time prolongation for Low amplitude - High amplitude fatigue programs.

5.5.3 Arbitrary load program

As we did earlier for model A (see 5.4.3), we like to investigate briefly if and how model B can be generalized to arbitrary load programs. For this purpose we propose the following non-separable damage evolution law which is a straightforward extension of equation (5.41):

$$\dot{\omega}(t,\sigma) = \alpha(\sigma)\kappa(\sigma)\left(\omega(t;\sigma)\right)^{1-1/\alpha(\sigma)} \text{ with: } \omega(0;\sigma) = 0. \tag{5.58}$$

Integration of equation (5.58) in case of constant load σ, thus treating $\alpha(\sigma)$ and $\kappa(\sigma)$ as constants, readily leads to equation (5.41), the starting point of analysis for model B. Unlike equation (5.41) we here prefer to write $\omega(t;\sigma)$ instead of $\omega(t)$ to emphasize that the damage function depends on the load program. One of the features of model B is the existence of a fixed random variable Ω representing the damage-at-break. Presently, we assume that Ω not only applies to constant load and single step constant load programs but to any load program. Now, the following formal

relationship between Ω and time-to-failure T corresponding to program $\sigma_p(t)$ holds:

$$\Omega = \omega(T; \sigma_p). \tag{5.59}$$

For practical computation of T, we first have to measure the time-to-failure distribution T_i corresponding to some constant load σ_i. If it is appreciated that Ω applies to both this constant load σ_i and our arbitrary load program $\sigma_p(t)$, we find:

$$(\kappa_i T_i)^{\alpha_i} = \omega(T_i; \sigma_i) = \Omega = \omega(T; \sigma_p), \tag{5.60}$$

where $\kappa_i = \kappa(\sigma_i)$ and $\alpha_i = \alpha(\sigma_i)$. The above equality allows us to formulate the distribution function of T in terms of the distribution function of T_i:

$$\begin{aligned} F_T(\tau) &= P(T \leq \tau) = P(\omega(T; \sigma_p) \leq \omega(\tau; \sigma_p)) \\ &= F_{T_i}\left(\frac{(\omega(\tau; \sigma_p))^{1/\alpha_i}}{\kappa_i} \right), \end{aligned} \tag{5.61}$$

since $\omega(t; \sigma_p)$, to be found by integration of equation (5.58), is non-decreasing. Naturally, model predictions are only possible if functions $\kappa(\cdot)$ and $\alpha(\cdot)$ are prescribed.

For the Life Fraction associated to load program $\sigma_p(t)$ we use equation (5.2):

$$L = \int_0^T \frac{dx}{\bar{T}(\sigma_p(x))}, \tag{5.62}$$

where T is obtained from equation (5.61). Evaluation of this equation is only possible after evaluation of the mean times-to-failure at any constant load that load program $\sigma_p(t)$ runs through. Contrary to model A, this will only work if the type of distribution for time-to-failure is prescribed. If we assume time-to-failure Weibull distributed, we can adopt the analysis in 5.5.2 and express mean time-to-failure at any arbitrary constant load σ_j in terms of mean time-to-failure of a single, prescribed constant load σ_i:

$$\bar{T}_j = d_{ij} \bar{T}_i^{b_{ij}} \quad \text{with: } b_{ij} = \frac{\alpha_i}{\alpha_j},\ d_{ij} = \left(\frac{\kappa_i}{\Gamma_{k\alpha_i}} \right)^{b_{ij}} \frac{\Gamma_{k\alpha_j}}{\kappa_j}, \tag{5.63}$$

where $\Gamma_x = \Gamma(1 + 1/x)$. Using this result in equation (5.62), the Life Fraction corresponding to arbitrary load program $\sigma_p(t)$ can be evaluated in terms of a single (measured) $\bar{T}_i$:

$$L = \int_0^T \frac{dx}{\bar{T}(\sigma_p(x))} = \int_0^T \frac{C^{1/(\alpha(\sigma_p(x)))}}{\Gamma(1 + 1/(k\alpha(\sigma_p(x))))} \kappa(\sigma_p(x)) dx, \tag{5.64}$$

where constant $C = \left(\frac{\Gamma_{k\alpha_i}}{\kappa_i \bar{T}_i} \right)^{\alpha_i}$. Similar to model A, the validity of model B for an arbitrary load program can not be checked with help of Life Fraction L. That should be done by comparing observed failure time with equation (5.61).

5.6 Experiments on Twaron fiber subjected to single step-load programs

In this section we discuss failure measurements on Twaron fiber subjected to single step constant load experiments. We will show that Twaron fiber does not behave as a regular material and that both non-regular models (A and B), analyzed in this chapter, do not properly describe the failure behavior of Twaron fiber either. Under certain conditions, the time-to-failure properties of Twaron fiber seem to improve during loading. This phenomenon can not be explained by any model which is based on a non-decreasing damage function.

Twaron 2300 yarns (produced by Teijin Aramid) were subjected to single step constant load programs up to failure. We computed the Life Fraction for these measurements, with 50 repetitions per experiment set-up, and constructed empirical distribution functions (edf's) of L. These empirical distributions will be compared to theoretical distributions of L. We used Twaron 2300 fibers with a nominal density of 1680 dtex and 1000 filaments per fiber. All tested fiber specimens were twisted with 80 twists per meter. For details on the failure behavior of twisted and flat Twaron fibers, i.e. the relationship between time-to-failure and load, the reader is referred to Knoester et. al. [63].

All single step constant load programs were constructed with two load levels: $\sigma_1 = 300$ N and $\sigma_2 = 325$ N. With these loads, we defined Low-High ($\sigma_1 \rightarrow \sigma_2$) and associate High-Low ($\sigma_2 \rightarrow \sigma_1$) single step constant load programs using fixed moments of load switching.

A total of $6\text{x}50 = 300$ fiber specimens (obtained from the same production spool) were tested on a Zwick Z010 tensile tester (load capacity 5 kN) with gauge length 500 mm. For $2\text{x}50 = 100$ specimens we measured time-to-failure T_1 and T_2 at constant load σ_1 and σ_2 respectively. On average, time-to-failure at these loads was found to be 11.0 hr (σ_1) and 36.9 min (σ_2). A total of $4\text{x}50 = 200$ specimens were subjected to single step constant load programs, divided in the following 4 experiment set-ups:

- SSP1: 1 hr at $\sigma_1 = 300$ N, then switching to $\sigma_2 = 325$ N,
- SSP2: 5 hr at $\sigma_1 = 300$ N, then switching to $\sigma_2 = 325$ N,
- SSP3: 20 min at $\sigma_2 = 325$ N, then switching to $\sigma_1 = 300$ N,
- SSP4: 35 min at $\sigma_2 = 325$ N, then switching to $\sigma_1 = 300$ N.

We executed the measurements in 50 consecutive series of 6 experiments each. Per series, we had 2 time-to-failure measurements and 4 different single step constant load experiments. For each series, the experiments were executed in random order. In 5.6.1 time-to-failure measurements are presented and discussed. Single step constant load measurements are discussed and compared with models associated with regular and non-regular material behavior in 5.6.2 and 5.6.3 respectively.

5.6.1 Time-to-failure measurements

In Figure 5.7 the empirical distribution functions (edf's) of scaled time-to-failure (e.g. $T/\bar{T}$) are plotted for the time-to-failure measurements at 300 N and 325 N. Applying a two-sample Kolmogorov-Smirnov test, we can not reject the null hypothesis (H_0) that the measured scaled time-to-failure distributions are in fact random drawings from the same underlying distribution. The maximum vertical distance between the edf's in Figure 5.7 was estimated $D_{measured} = 0.16$ corresponding to a p-value of 0.51. The critical distance at significance level $\alpha = 0.05$ is $D_{critical} = 0.27$ (for two samples with sample size $n_1 = n_2 = 50$).

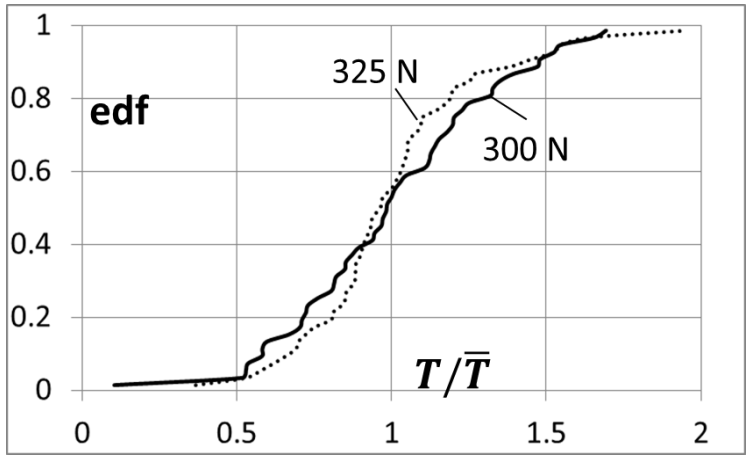

Figure 5.7: *Empirical distribution functions of scaled time-to-failure.*

We conjecture that time-to-failure of Twaron yarn (at constant load) can well be described by a Weibull distribution. To justify our assumption, we constructed Weibull plots of the measurements at $\sigma_1 = 300$ N and $\sigma_1 = 325$ N (see Figure 5.8). Let $\{t_i\}$ $(i = 1, 2, \cdots n)$ be the ordered set of measured time-to-failure data at constant load. If the data are truly Weibull distributed, then $\ln(-\ln(1 - F(t_i)))$, with $F(t_i) = (i - 0.3)/(n + 0.4)$ the empirical distribution function, is linearly related to $\ln(t_i)$:

$$\ln(-\ln(1 - F(t))) = k \ln(t) - k \ln(t_0), \tag{5.65}$$

with k the Weibull modulus and t_0 the scale factor. From Figure 5.8 we deduce that time-to-failure can reasonably well be described by the Weibull distribution. The Weibull plots predict slightly different Weibull moduli: $k = 3.5$ for load $\sigma_1 = 300$ N and $k = 4$ for load $\sigma_1 = 325$ N. Note that these estimates for the Weibull modulus are quite sensitive to outliers in the tails of the distribution.

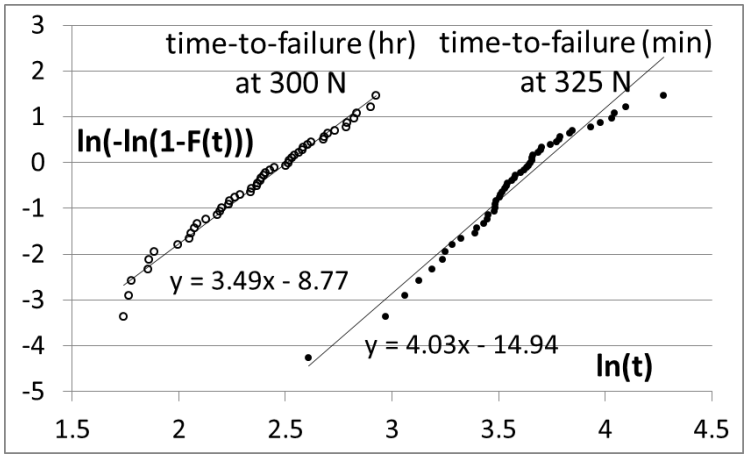

Figure 5.8: *Weibull plots of time-to-failure measurements. For the plot corresponding to a load of 300 N one outlier ($t = 1.1$ hr) was removed.*

5.6.2 Testing the validity of regular models for Twaron yarn

All models within the class of regular models (CRM) discussed in Section 5.3 require that the distribution $T/\bar{T}$ is the same for any load. After all, from equation (5.7) we find that $T/\bar{T} = X/\bar{X}$ and X a load independent random variable. In the previous section, we could not reject the hypothesis that the time-to-failure measurements at both loads are random drawings from the same underlying distribution. Therefore, the time-to-failure measurements do not deny the validity of the CRM. We now assume that all measurements of the scaled time-to-failure, both at 300 N and 325 N, indeed originate from the same distribution. We therefore add these measurements together and build an overall empirical distribution function from the ordered set of 100 time-to-failure measurements. Supported by the Weibull plots in Figure 5.8, we also assume that time-to-failure is Weibull distributed. Scaled time-to-failure is therefore also Weibull distributed and $T/\bar{T} \sim W(k, \Gamma_k^{-1})$. Using one-sample Komogorov-Smirnov testing, the overall empirical distribution function cannot be distinguished from Weibull for a broad range of Weibull moduli ($2.4 < k < 6.6$). In Figure 5.9 the overall edf is plotted together with Weibull distributions for $k = 2.5$, $k = 6.5$ and $k = 4.4$, the latter resulting in the best fit according to Kolmogorov-Smirnov.

For all models in the CRM and any load program, the distribution of the Life Fraction L equals the distribution of the scaled time-to-failure $T/\bar{T}$. To investigate the validity of the CRM for Twaron yarn, the measured distributions for the Life Fraction for the various step load programs (SSP1 to SSP4) are compared to the Weibull distribution $W(k, \Gamma_k^{-1})$ for a broad range of Weibull moduli $2.5 < k < 6.5$ (see Figure 5.10). It is clear that the measured Life Fractions for SSP1, i.e. '300 N (1 hr) $\rightarrow$ 325 N', are not in accordance with $W(k, \Gamma_k^{-1})$ for any $k > 0$. Using one-sample Kolmogorov-Smirnov testing, we found that the measurements for the SSP2 series do not obey the CRM predictions either. The sample mean and sample variance

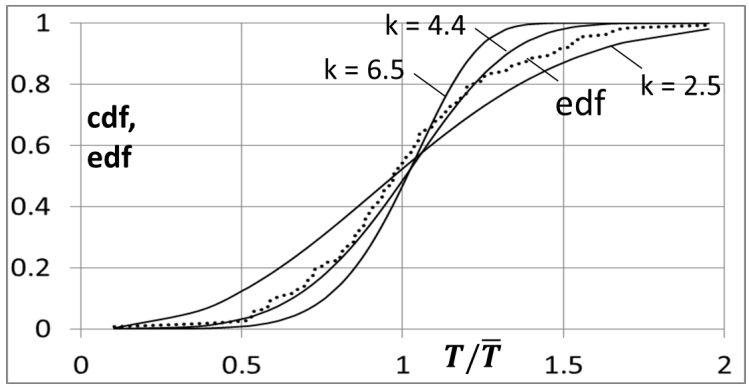

Figure 5.9: *Comparison of the overall set of scaled time-to-failure measurements at 300 N and 325 N (dotted line) with Weibull distributions $W(k, \Gamma_k^{-1})$ (solid curves: $k = 2.5$, 4.4 and 6.5).*

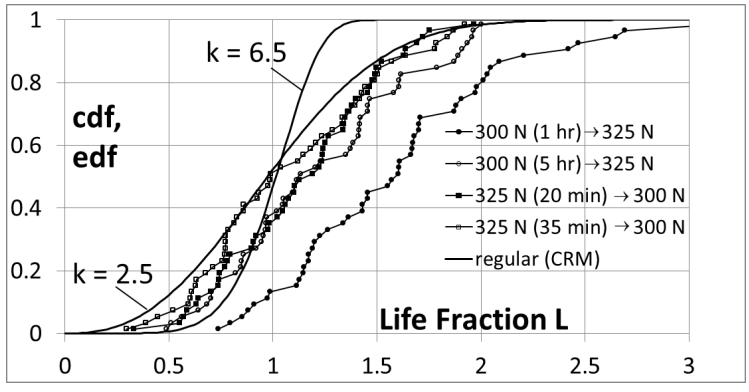

Figure 5.10: *Comparison of the Life Fraction distributions observed for the single step constant load programs (dotted lines) with Weibull distributions $W(k, \Gamma_k^{-1})$ (solid curves: $k = 2.5$ and 6.5)*

of the measured Life Fraction L are listed in Table 5.1. The sample mean should be close to unity for regular material behavior. The sample variance for the SSPs is significantly larger than the sample variance of $T/\bar{T}$ (0.085 and 0.11 for 325 N and 300 N respectively). We conclude that the Life Fraction measurements reject regular models (CRM) as valid description of the failure behavior of Twaron yarns. This conclusion is not limited to the subclass of the CRM with Weibull distributed time-to-failure. Irrespective of the underlying distribution, the edf built from 100 scaled time-to-failure measurements does not match with the edf's observed for the single step constant load programs.

	300 N (1 hr) ↓ *325 N (SSP1)*	*300 N (5 hr)* ↓ *325 N (SSP2)*	*325 N (20 min)* ↓ *300 N (SSP3)*	*325 N (35 min)* ↓ *300 N (SSP4)*
$\overline{L} = \frac{1}{n}\sum_1^n L_i$	1.59	1.21	1.14	1.07
$S^2 = \frac{1}{n-1}\sum_1^n \left(L_i - \overline{L}\right)^2$	0.28	0.19	0.14	0.18
LCL	1.44	1.09	1.04	0.96
UCL	1.74	1.33	1.24	1.19
u	0.091	0.45	0.54	0.95

Table 5.1: *Overview of characteristics of the Life Fraction observations for the single step constant load programs: $\overline{L}$, S^2: sample mean and sample variance; LCL / UCL: Lower and Upper Confidence Limit of the 95% Confidence Interval on the (true) mean of the Life Fraction; u: scaled time at load switch.*

5.6.3 Testing the validity of non-regular models (A and B) for Twaron yarn

In this section we show that the measured Life Fraction distributions of Twaron yarns subjected to single step constant load programs are incompatible with both non-regular models (model A and model B).

In Figure 5.11 the confidence interval on the unknown distribution mean $\mu = E[L]$ per series of measurements is plotted (for $\alpha = 0.05$). For the construction of the confidence intervals we used the central limit theorem, a valid approximation for large sample size n, hence:

$$\sqrt{n}\,\frac{\overline{L} - \mu}{\sigma} \sim N(0,1), \tag{5.66}$$

with the standard deviation σ approximated by the sample standard deviation

$$s = \sqrt{\frac{1}{n-1}\sum_1^n \left(L_i - \overline{L}\right)^2}. \tag{5.67}$$

The borders of the confidence intervals, LCL and UCL, together with the scaled time at the load switch (u) are tabulated in Table 5.1. From this table it is clear that, on average, the lifetime is prolonged relative to regular models at least for SSP1 to SSP3. For SSP4 such inference can not be made because the confidence interval on the distribution mean contains unity.

For the class of non-regular models denoted 'model A', the distribution of Life Fraction L depends on two parameters: k and α. An increase of the Life Fraction relative to regular behavior (i.e. $E[L] > 1$) can only be obtained for $0 < \alpha < 1$. From equation (5.25) we find for any $0 < \alpha < 1$:

$$1 < E[L] < 1 + u. \tag{5.68}$$

The area $E[L] > 1 + u$ is a 'forbidden zone': observed material behavior in this area can not be explained by model A. From Figure 5.11 it is clear that the Low-High SSP1 series ('300 N (1 hr) $\rightarrow$ 325 N') is well within the 'forbidden zone'. Furthermore, since the Low-High programs

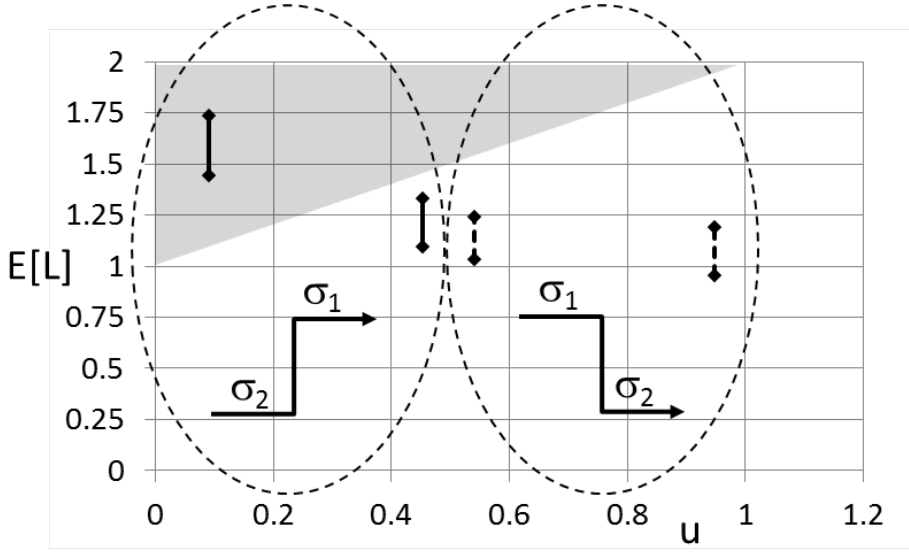

Figure 5.11: *Confidence intervals on the true mean of the Life Fraction constructed from the measurements of the Low-High programs (solid arrows) and the High-Low programs (dashed arrows). Gray area represents 'forbidden zone' (explained in text) defined by* $E[L] > 1 + u$.

demonstrate extension of lifetime, model A would consequently predict lifetime shortening for associate High-Low programs which is contrary to the observations of SSP3 ('325 N (20 min) $\rightarrow$ 300 N'). Model A is clearly unfit to explain the measurements.

Application of the class of non-regular models denoted 'model B' to single step constant load programs requires evaluation of one single parameter β. This parameter is a function of the scaled time of the load switch, i.e. $\beta = \beta(u)$ with $u = \tau/\overline{T}$ and $\overline{T}$ the average time-to-failure of the first load.

$$\beta(u) = u - a_{12}u^{b_{12}} \text{ with: } a_{12} \text{ and } b_{12} \text{ positive constants.} \tag{5.69}$$

It readily follows that $\beta(u) < u$. We use this result in equation (5.52) to obtain:

$$\begin{aligned} E[L] &= 1 + \beta(u)(1 - F_{U_1}(u)) + \int_0^u \beta(x) f_{U_1}(x) dx \\ &< 1 + u(1 - F_{U_1}(u)) + u \int_0^u f_{U_1}(x) dx \\ &= 1 + u, \end{aligned} \tag{5.70}$$

for arbitrary u and U_1. U_1 is the scaled time-to-failure distribution corresponding to the first load of the program. Apparently, the 'forbidden zone' $E[L] > 1 + u$ applies to both model A and model B. The validity of these models to explain Twaron yarn failure behavior is therefore rejected for the same reasons.

It is not surprising that $E[L] = 1 + u$ is found as upper boundary for both models. Imagine that damage buildup during the first load is negligible. Then at the moment of load switch

at scaled time u, the residual time-to-failure at the second load should almost be equal to the virgin time-to-failure at this load. Therefore, the expected Life Fraction of the complete single step constant load program reads $E[L] = 1 + u$. In other words, the latter equation is exactly true in case of no damage buildup during the first load. This boundary applies to any model which is based on a damage function, where damage is a non-decreasing function of time during loading. The failure behavior of Twaron yarns thus requires a fundamentally different approach of modeling.

We conclude with some final remarks on the series '300 N (1 hr) $\rightarrow$ 325 N', which clearly lies within the forbidden zone. Since there were no broken specimens during the 1hr preload at 300 N, it makes sense to compare residual time-to-failure at 325 N with the virgin time-to-failure distribution. The residual time-to-failure at 325 N of the preloaded specimens outperforms time-to-failure at 325 N of virgin specimens. This of course is consistent with the series being in the forbidden zone. In the top panel of Figure 5.12, the observed distribution function of virgin time-to-failure at 325 N is compared to observed residual time-to-failure distributions at that same load after a preload at 300 N during 1 hr and 5 hr respectively. A two-sample Kolmogorov-Smirnov test indisputably shows that the distribution of virgin time-to-failure lies above (and to the left of) that of residual time-to-failure after a 1 hr preload at 300 N. The preload thus extends the time-to-failure relative to virgin fibers. If the Equal Rank Assumption (ERA) holds, lifetime extension is most manifest for specimens that already have the longest virgin time-to-failure. Recall that the ERA, earlier discussed in 5.4.2, claims that the order of failure of a set of specimens will be the same for any load program. For an extended preload of 5 hr degradation sets in, but it is noticeable that the strongest cohort of the specimens (say the 20% specimens with the longest time-to-failure) still is on par with virgin material.

The residual time-to-failure distribution at 325 N after a preload at 300 N seems to keep its Weibull character evidenced by acceptable Weibull plots in the bottom panel of Figure 5.12. However, the preload seems to widen the residual time-to-failure distribution at 325 N, the more so for longer duration at the preload (300 N). In this respect note the decreasing slope of the Weibull plots as preload duration is increased.

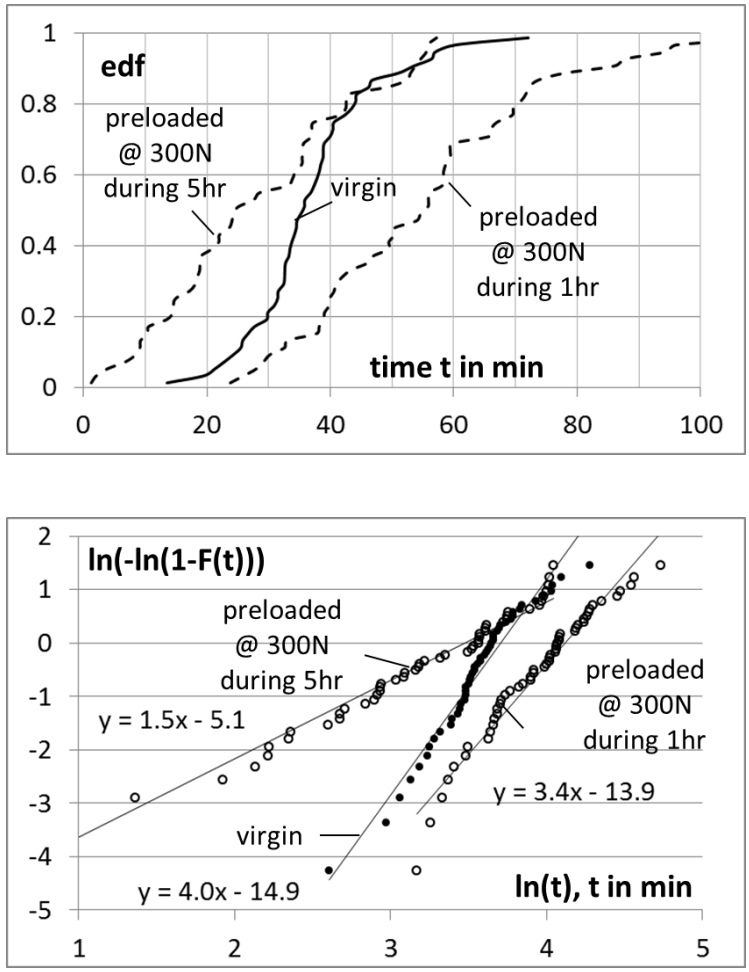

Figure 5.12: *Empirical distribution functions (top) and Weibull plots (bottom) of the (virgin) time-to-failure at 325 N (solid line / solid dots) and residual time-to-failure at 325 N after a 1 hr or 5 hr preload at 300 N (dashed lines / open dots).*

5.7 Discussion and conclusions

The expected lifetime of stressed fibers, or load-bearing materials in general, is an important industrial property. This property is often investigated by subjecting fibers to a constant load up to failure. Additionally, single step constant load programs are used to determine if loading order affects lifetime. These experiments may or may not confirm the Life Fraction Rule (analogous to Palmgren-Miner's Rule in fatigue experiments), which claims that fractions of spent lives on certain constant loads can simply be added together to predict failure.

In this chapter we introduced and analyzed three classes of probabilistic models, formulated in the framework of damage theory. Though the nature of the damage itself remains unspecified, the models prescribe how damage builds up during loading and lead to fiber failure if some critical damage level is reached. For the three classes of models we derived the Life Fraction L in case of a single step constant load program (in short: SSP), i.e. a load program with a single load switch from one constant load to another. One class of models shows 'regular' behavior, i.e. satisfies the Life Fraction Rule or $E[L] = 1$ for any load program. The other two classes of models are non-regular and loading order affects Life Fraction L. For all models it was found that variability in L is closely related to variability in (scaled) time-to-failure (at constant load). If L is measured experimentally with the objective to discriminate between regular and non-regular behavior, one should take into account time-to-failure variability for a proper judgment. It is emphasized that models which produce $E[L] = 1$, associated to regular material behavior, need not be based on the assumption that damage accumulates linearly in time during a constant load program. Indeed, models proposing a nonlinear damage buildup can still have regular material behavior. This legitimizes that we introduced new terminology 'regular' and 'non-regular' for $E[L] = 1$ and $E[L] \neq 1$ respectively instead of using the more common, but also confusing terminology 'linear' and 'nonlinear' material behavior.

Single step constant load programs are particularly useful to investigate materials' failure behavior because they are experimentally easy and effects of loading order on survival time are well observable. Contrary to more complex programs, the number of required model parameters to describe materials' response to SSPs is minimal, at least for the models analyzed in this chapter. In Chapter 4 we discussed residual strength measurements on Twaron yarn (using a complex load program) and found that the Coleman model (subclass of the CRM) is unfit to describe the measurement data for two specific choices for model function $\kappa(\cdot)$ (introduced in equation (5.4)). Based on these results only, it cannot be excluded that another, more exotic choice for $\kappa(\cdot)$ would nicely explain the measurements while not contradicting the (constant load) time-to-failure measurements. The single step constant load experiments in this chapter show that the Coleman model does not describe Twaron yarn failure for any $\kappa(\cdot)$.

The class of non-regular models (model A) inspired by crack growth theory obtains non-regularity by the assumption that the critical damage level (inducing failure) is load dependent. Specific properties of model A, e.g. failure of specimen fractions during the load switch of an

SSP and periods devoid of failure following the load switch in the associate SSP, must hold for materials which indeed fail due to crack growth. To validate if materials' failure follows crack growth theory, we recommend to subject these materials to SSP experiments. At least one should observe that the lifetime of High-Low SSPs extends whereas the lifetime of Low-High SSPs shortens.

The second class of non-regular models (model B) is inspired by the work of Marco and Starkey and uses power-law damage growth in time during constant load program (with the power a function of load): $\omega(t) \sim t^{\alpha(\sigma)}$. It was proposed as model to explain non-regular behavior of materials subjected to the fatigue analog of SSPs, without being able to actually determine damage growth in a material during such fatigue experiment. For many materials the lifetime of Low-High fatigue experiments is prolonged and vice versa, suggesting a decreasing function $\alpha(\cdot)$ of load σ. However, for some materials the opposite behavior is observed. Whilst the Marco-Starkey model is largely empirical, model B for the first time offers the opportunity to validate this power-law behavior in damage growth by simply measuring the time-to-failure variability at the Low and High loads used in the SSP. These do not only explain if the lifetime of Low-High of High-Low SSPs is prolonged, but also to which extent. If the observed variability does not match the observed non-regularity for SSPs, then clearly the cause of the non-regularity must be something else than the power-law model assumption put forward by Marco and Starkey.

Theoretical Life Fraction L is compared with experimental work on Twaron yarns exposed to several series of SSPs. Twaron yarn failure behavior cannot be captured by any of the models analyzed in this chapter. For one of the experimental series we observed improvement of yarn failure properties after being subjected to a preload. This series is in the so-called 'forbidden zone' (see 5.6.3) and thus can never be explained by any model based on damage theory, where the damage accumulation rate is a non-negative function of current damage level / load level. A proper model for the failure of Twaron yarns must therefore be fundamentally different from the models analyzed in this chapter.

Ultimately, mechanical properties of fibers can only be understood by analyzing their structure and morphology. Fiber loading causes structural changes, but not necessarily damages the structure. Modulus and stress-strain characteristics of p-aramid fibers do change as a consequence of loading [76]. Mechanical properties of textile fibers can be improved by 'mechanical conditioning' [77]. It is therefore tempting to qualify the preload that led to improved mechanical properties of Twaron yarn as some kind of 'mechanical conditioning'. The more so because a heat treatment, while moderately tensioning the fibers, is actually used to enhance mechanical properties of aramid yarn as part of the production process. Twaron is a fully crystalline material and the chains lay highly oriented along the fiber axis. Orientation is brought about during spinning, as the liquid crystalline spinning dope is pressed through tiny holes of a spinneret. The morphology of Twaron fiber and the way it adjusts to external loading in terms of elastic and plastic deformation was modeled theoretically by Baltussen and Northolt [4]. During loading, shearing between chains is inevitable, and hydrogen bonds between the chains may break as a

result.This could be characterized as damage buildup. Simultaneously, the average orientation of the chains increases, i.e. a further alignment of the polymer chains with the fiber axis is established, which is believed to improve the fiber's mechanical properties. Structural changes in aramid fiber, induced by loading, are probably too complex in order to be captured by a model based on one-way damage theory.

The measurements on Twaron yarn indicate that there might very well be multiple processes at work simultaneously, both improving and deteriorating the capability of the yarn to withstand external load. In fact, we have reason to believe that virgin yarns which already have a high load-bearing capability benefit most from preload. This again conditional to the Equal Rank Assumption (ERA), which hypothesizes that the rank of breaking of a set of specimens will be the same for any load program. The ERA was anyway needed to sensibly apply model A to single step constant load programs.

The analysis in this chapter is not only applicable to the creep failure of statically loaded materials but also to fatigue failure. We refer to the work of Christensen to fully appreciate the correspondence between these two areas of research.

Appendix A

Weibull, Gumbel and Lognormal distribution

A.1 Weibull distribution

The random variable X has a Weibulll distribution function with shape parameter k and scale parameter t_0 if

$$F_X(x) = 1 - \exp\left(-\left(\frac{x}{t_0}\right)^k\right). \tag{A.1}$$

For a Weibull distributed stochastic variable X the shorthand $X \sim W(k, t_0)$ is used.

A.2 Gumbel distribution

The random variable X has a Gumbel distribution function with location parameter a and scale parameter b if

$$F_X(x) = 1 - \exp\left(-\exp\left(\frac{x-a}{b}\right)\right). \tag{A.2}$$

For a Gumbel distributed stochastic variable X the shorthand $X \sim G(a, b)$ is used.

A.3 Lognormal distribution

Let $Y = \ln X$ be normally distributed: $Y \sim N(\mu, \sigma^2)$. By definition, X satisfies the lognormal distribution $X \sim LN(\mu, \sigma^2)$ given by:

$$\begin{aligned} F_X(x) &= F_Y(\ln x) = \frac{1}{2}\left(1 + \text{erf}\left(\frac{\ln x - \mu}{\sigma\sqrt{2}}\right)\right), \\ f_X(x) &= \frac{d}{dx}F_X(x) = \frac{1}{x\sigma\sqrt{2\pi}}\exp\left(-\left(\frac{\ln x - \mu}{\sigma\sqrt{2}}\right)^2\right). \end{aligned} \tag{A.3}$$

If $Z = \log_{10} X \sim N(\mu, \sigma^2)$ then $Y = \ln X \sim N\left(\mu \ln 10, (\sigma \ln 10)^2\right)$ and $X \sim LN\left(\mu \ln 10, (\sigma \ln 10)^2\right)$.

The mean, standard deviation, median and mode of the above three distributions are summarized in Table A.1.

	Weibull	Gumbel	Lognormal
mean	$t_0\Gamma(1+1/k)$	$a - \zeta b$	$e^{\mu+\frac{1}{2}\sigma^2}$
standard deviation	$t_0\sqrt{\Gamma(1+2/k) - (\Gamma(1+1/k))^2}$	$(\pi b)/\sqrt{6}$	$\sqrt{(e^{\sigma^2}-1)}*$ $e^{\mu+\frac{1}{2}\sigma^2}$
median	$t_0(\ln 2)^{1/k}$	$a + b\ln(\ln 2)$	e^{μ}
mode	$t_0((k-1)/k)^{1/k}$	a	$e^{\mu-\sigma^2}$

Table A.1: *Characteristics of the Weibull, Gumbel and Lognormal distributions. $\zeta \simeq 0.577215$ is the Euler-Mascheroni constant.*

A.4 Gumbel distributed $Y = \ln X$ for Weibull distributed X

If X is Weibull distributed variable with shape parameter k and scale parameter t_0, then the distribution function for $Y = \ln X$ is given by

$$F_Y(y) = F_X(e^y) = 1 - \exp\left(-\left(\frac{e^y}{t_0}\right)^k\right) = 1 - \exp\left(-\exp\left(ky - k\ln t_0\right)\right). \tag{A.4}$$

Clearly, Y is a Gumbel distributed variable: $Y \sim G\left(\ln t_0, \frac{1}{k}\right)$. The other way around, if $Y \sim G(a, b)$ then $X = e^Y \sim W\left(\frac{1}{b}, e^a\right)$.
It is noted that $\overline{X}$ and $\overline{\ln(X)}$ differ by a constant, be it a constant dependent on shape parameter k:

$$\overline{\ln(X)} = \overline{Y} = \ln(t_0) - \zeta/k = \ln(\overline{X}/\Gamma_k) - \zeta/k = \ln(\overline{X}) - f(k), \tag{A.5}$$

with $\Gamma_k = \Gamma(1+1/k)$ and $f(k) = \ln(\Gamma_k) + \zeta/k$, therefore $\overline{X} = \Gamma_k e^{\zeta/k} e^{\overline{\ln(X)}}$.
In case $Y = \log_{10}(X)$ it readily follows that $Y \sim G\left(\log_{10}(t_0), \frac{1}{k\ln 10}\right)$ and

$$\overline{\log_{10}(X)} = \overline{Y} = \log_{10}(t_0) - \zeta/(k\ln 10) = \log_{10}(\overline{X}/\Gamma_k) - \zeta/(k\ln 10) = \log_{10}(\overline{X}) - f(k), \tag{A.6}$$

with $f(k) = \log_{10}(\Gamma_k) + \zeta/(k\ln 10)$, therefore $\overline{X} = \Gamma_k e^{\zeta/k} 10^{\overline{\log_{10}(X)}}$.

Appendix B

Maximum Likelihood Estimation

In this Appendix the maximum likelihood estimation procedure is outlined for the estimation of parameters a, b, c of a Weibull distributed variable $Z \sim W(c, w)$ with $w = \frac{\ell^{-1/c}}{e^{a+bv}}$. For properly chosen parameters a, b, c and function v of load or load rate, Z represents time-to-failure or strength depending on load program and breakdown rule function, see Table B.1.

	power-law breakdown rule function	exponential breakdown rule function
constant load	$T \sim W(k, t_0)$ $t_0 = \ell^{-1/k}\gamma^{-1}\sigma^{-\rho}$ $Z = T \quad v = \ln\sigma$ $a = \ln\gamma \quad \gamma = e^a$ $b = \rho \quad \rho = b$ $c = k \quad k = c$	$T \sim W(k, t_0)$ $t_0 = \ell^{-1/k}\alpha^{-1}e^{-\beta\sigma}$ $Z = T \quad v = \sigma$ $a = \ln\alpha \quad \alpha = e^a$ $b = \beta \quad \beta = b$ $c = k \quad k = c$
constant load rate	$S \sim W(k(\rho+1), s_0)$ $s_0 = \left(\ell^{-1/k}\gamma^{-1}(\rho+1)\dot{\sigma}\right)^{1/(\rho+1)}$ $Z = S \quad v = \ln\dot{\sigma}$ $a = \frac{1}{\rho+1}\ln\left(\frac{\gamma}{\rho+1}\right) \quad \gamma = -\frac{1}{b}e^{-\frac{a}{b}}$ $b = -\frac{1}{\rho+1} \quad \rho = -\frac{1}{b} - 1$ $c = k(\rho+1) \quad k = -bc$	

Table B.1: *Time-to-failure and strength distribution expressed in terms of variable* $Z \sim W(c, w)$ *with* $w = \frac{\ell^{-1/c}}{e^{a+bv}}$.

For $j = 1, 2, \ldots, m$, let z_{ij} ($i = 1, 2, \ldots, n_j$) represent n_j observations of Weibull distributed variable $Z_j \sim W(c, w_j)$ (scale parameter w_j depends on load σ_j or load rate $\dot{\sigma}_j$). The pdf of Z_j is given by:

$$f_{Z_j}(z) = \left(\frac{c}{w_j}\right)\left(\frac{z}{w_j}\right)^{c-1} \exp\left(-\left(\frac{z}{w_j}\right)^{c}\right); w_j = \frac{\ell^{-1/c}}{e^{a+bv_j}}, \tag{B.1}$$

with $v_j = v(\sigma_j)$ or $v_j = v(\dot{\sigma_j})$. All observations z_{ij} are either times-to-failure or strengths, but not a mixture of both. There simply must be a unique recipe how to back transform estimators for a, b and c into estimators for the Coleman parameters (see Table B.1).

Using the maximum likelihood estimation technique, estimators for a, b and c are obtained by maximizing the likelihood function L defined by:

$$\begin{aligned} \ln L &= \sum_{j=1}^{m}\sum_{i=1}^{n_j} \ln\left(f_Z(z_{ij})\right) \\ &= n\left\{\ln(c\ell) + ac + bc\bar{v} + (c-1)\overline{\ln z} - \frac{\ell}{n}\sum_{j=1}^{m}\sum_{i=1}^{n_j} q_{ij}^{c}\right\}, \end{aligned} \tag{B.2}$$

with $q_{ij} = e^{a+bv_j} z_{ij}$, $n = \sum_{j=1}^{m} n_j$, $\bar{v} = \frac{1}{n}\sum_{j=1}^{m} n_j v_j$ and $\overline{\ln z} = \frac{1}{n}\sum_{j=1}^{m}\sum_{i=1}^{n_j} \ln z_{ij}$. The partial derivatives of $\ln L$ are

$$\begin{aligned} \frac{\partial \ln L}{\partial a} &= cn - c\ell\sum_{j=1}^{m}\sum_{i=1}^{n_j} q_{ij}^{c}, \\ \frac{\partial \ln L}{\partial b} &= cn\bar{v} - c\ell\sum_{j=1}^{m}\sum_{i=1}^{n_j} q_{ij}^{c} v_j, \\ \frac{\partial \ln L}{\partial c} &= \frac{n}{c} + na + nb\bar{v} + n\,\overline{\ln z} - \ell\sum_{j=1}^{m}\sum_{i=1}^{n_j} q_{ij}^{c}\ln q_{ij}. \end{aligned}$$

Enforcing vanishing partial derivatives results in the following three requirements for the ML estimators $\hat{a}$, $\hat{b}$ and $\hat{c}$:

$$\begin{aligned} \frac{\ell}{n}\sum_{j=1}^{m}\sum_{i=1}^{n_j} \hat{q}_{ij}^{\hat{c}} &= 1, \\ \frac{\ell}{n}\sum_{j=1}^{m}\sum_{i=1}^{n_j} \hat{q}_{ij}^{\hat{c}} v_j &= \bar{v}, \\ \frac{\ell}{n}\sum_{j=1}^{m}\sum_{i=1}^{n_j} \hat{q}_{ij}^{\hat{c}} \ln z_{ij} &= \frac{1}{\hat{c}} + \overline{\ln z}, \end{aligned} \tag{B.3}$$

with $\hat{q}_{ij} = e^{\hat{a}+\hat{b}v_j} z_{ij}$. In the last requirement $\ln \hat{q}_{ij} = \hat{a} + \hat{b}v_j + \ln z_{ij}$ was substituted and subsequently the first two requirements were used. Equations (B.3) need to be solved numerically to obtain $\hat{a}$, $\hat{b}$ and $\hat{c}$.

Analysis is continued to find the variance-covariance matrix of the ML estimators. The Hessian matrix J is composed of the second order derivatives of $\ln L$:

$$-J = -\begin{pmatrix} \frac{\partial^2 \ln L}{\partial a^2} & \frac{\partial^2 \ln L}{\partial a \partial b} & \frac{\partial^2 \ln L}{\partial a \partial c} \\ \frac{\partial^2 \ln L}{\partial a \partial b} & \frac{\partial^2 \ln L}{\partial b^2} & \frac{\partial^2 \ln L}{\partial b \partial c} \\ \frac{\partial^2 \ln L}{\partial a \partial c} & \frac{\partial^2 \ln L}{\partial b \partial c} & \frac{\partial^2 \ln L}{\partial c^2} \end{pmatrix} = n \begin{pmatrix} c^2\, A_0 & c^2\, B_0 & A_0 + A_1 - 1 \\ c^2\, B_0 & c^2\, C_0 & B_0 + B_1 - \bar{v} \\ A_0 + A_1 - 1 & B_0 + B_1 - \bar{v} & \frac{1}{c^2}\,(1 + A_2) \end{pmatrix},$$

with $A_0 = \frac{\ell}{n} \sum_{j=1}^{m} \sum_{i=1}^{n_j} q_{ij}^c$, $A_1 = \frac{\ell}{n} \sum_{j=1}^{m} \sum_{i=1}^{n_j} q_{ij}^c \ln q_{ij}^c$, $A_2 = \frac{\ell}{n} \sum_{j=1}^{m} \sum_{i=1}^{n_j} q_{ij}^c \left(\ln q_{ij}^c\right)^2$, $B_0 = \frac{\ell}{n} \sum_{j=1}^{m} \sum_{i=1}^{n_j} q_{ij}^c v_j$, $B_1 = \frac{\ell}{n} \sum_{i=1}^{n_j} q_{ij}^c \ln q_{ij}^c v_j$ and $C_0 = \frac{\ell}{n} \sum_{j=1}^{m} \sum_{i=1}^{n_j} q_{ij}^c v_j^2$.
Fisher information matrix equals minus the expectation of the Hessian matrix $I = -E\,[J]$, or:

$$I = n \begin{pmatrix} c^2 & c^2 \bar{v} & (1-\zeta) - \ln \ell \\ c^2 \bar{v} & c^2 \overline{v^2} & ((1-\zeta) - \ln \ell)\, \bar{v} \\ (1-\zeta) - \ln \ell & ((1-\zeta) - \ln \ell)\, \bar{v} & \frac{1}{c^2}\left(\frac{\pi^2}{6} + ((1-\zeta) - \ln \ell)^2\right) \end{pmatrix},$$

with determinant: $\det(-E\,[J]) = n^3 \frac{c^2 \pi^2}{6} \left(\overline{v^2} - \bar{v}^2\right)$ and $\zeta \simeq 0.577215$ the Euler-Mascheroni constant. Here it was used that:

$$\begin{aligned} E\left[Z_j^c\right] &= \omega_j^c\, \Gamma(2) = \omega_j^c, \\ E\left[Z_j^c \ln Z_j^c\right] &= \omega_j^k \ln \omega_j^k\, \Gamma(2) + \omega_j^k\, \Gamma'(2) = \omega_j^k \left(\ln \omega_j^k + (1-\zeta)\right), \\ E\left[Z_j^c \left(\ln Z_j^c\right)^2\right] &= \omega_j^k \left(\ln \omega_j^k\right)^2\, \Gamma(2) + 2\omega_j^k \ln \omega_j^k\, \Gamma'(2) + \omega_j^k\, \Gamma''(2) \\ &= \omega_j^k \left(\ln \omega_j^k + (1-\zeta)\right)^2 + \omega_j^k \left(\frac{\pi^2}{6} - 1\right), \end{aligned}$$

with Γ-function $\Gamma(x) = \int_0^\infty u^{x-1} \exp(-u) du$
and its first two derivatives $\frac{d^p}{dx^p}\Gamma(x) = \int_0^\infty u^{x-1} \exp(-u) \left(\ln u\right)^p du$ $(p = 1, 2)$.
It was found that [29] $\Gamma'(2) = 1 - \zeta$ and $\Gamma''(2) = (1-\zeta)^2 + \frac{\pi^2}{6} - 1$. The latter result was evaluated with Matcad.

The variance-covariance matrix $G = I^{-1}$ is the inverse of the information matrix [30, 31]. In the optimum point determined by $\hat{c}$ matrix G reads:

$$G = \frac{1}{n\hat{c}^2} \begin{pmatrix} \frac{\overline{v^2}}{\overline{v^2} - \bar{v}^2} + \frac{6((1-\zeta) - \ln \ell)^2}{\pi^2} & -\frac{\bar{v}}{\overline{v^2} - \bar{v}^2} & -\frac{6\hat{c}^2((1-\zeta) - \ln \ell)}{\pi^2} \\ -\frac{\bar{v}}{\overline{v^2} - \bar{v}^2} & \frac{1}{\overline{v^2} - \bar{v}^2} & 0 \\ -\frac{6\hat{c}^2((1-\zeta) - \ln \ell)}{\pi^2} & 0 & \frac{6\hat{c}^4}{\pi^2} \end{pmatrix}. \qquad \text{(B.4)}$$

Note that the ML estimators $\hat{b}$ and $\hat{c}$ are uncorrelated. Backtransformation from ML estimators $\hat{b}$ and $\hat{c}$ to estimators for the Coleman parameters $\hat{\rho}$, $\hat{k}$ or $\hat{\beta}$, $\hat{k}$ is discussed in Appendix C. Only if $\hat{b}$ and $\hat{c}$ were obtained via constant load experiments then clearly $\hat{\rho}$, $\hat{k}$ (power-law) or $\hat{\beta}$, $\hat{k}$ (exponential) are uncorrelated as well. Unless using a large number of time-to-failure observations it was found (see Figure 2.1) that $\hat{k}$ is rather biased and variable. It is thus reassuring that the estimator for ρ (or β) is not affected by a faulty estimate for k.

The standard deviations of the ML estimators are obtained from the diagonal elements of matrix G:

$$\begin{aligned}
\sigma_{\hat{a}} &= \sqrt{G_{11}} = \frac{1}{\hat{c}\sqrt{n}}\sqrt{\frac{\overline{v^2}}{\overline{v^2}-\bar{v}^2} + \frac{6((1-\zeta)-\ln\ell)^2}{\pi^2}}, \\
\sigma_{\hat{b}} &= \sqrt{G_{22}} = \frac{1}{\hat{c}\sqrt{n}}\sqrt{\frac{1}{\overline{v^2}-\bar{v}^2}}, \\
\sigma_{\hat{c}} &= \sqrt{G_{33}} = \frac{\hat{c}}{\sqrt{n}}\sqrt{\frac{6}{\pi^2}}.
\end{aligned}$$

Apparently, for constant load experiments ($\hat{c} = \hat{k}$), large k (representative for a fiber with narrow time-to-failure distribution) translates into relatively accurate estimators for $\ln\hat{\gamma}$, $\hat{\rho}$ (power-law) or $\ln\hat{\alpha}$, $\hat{\beta}$ (exponential) whereas the estimator for k itself becomes more variable.

Appendix C

Transformations

Let L be a likelihood function parameterized by three parameters $\underline{a} = (a_1, a_2, a_3)$ with ML estimators $\hat{\underline{a}} = (\hat{a}_1, \hat{a}_2, \hat{a}_3)$. If L is reparameterized using a one to one function $\underline{b} = (b_1, b_2, b_3) = f(\underline{a})$, then ML estimator $\hat{\underline{b}}$ is calculated from $\hat{\underline{b}} = f(\hat{\underline{a}})$ due to the functional invariance of ML estimators.

Let A be the variance-covariance matrix with entries $a_{ij} = cov(a_i, a_j) = E\left[(a_i - \hat{a}_i)(a_j - \hat{a}_j)\right]$. In order to obtain the variance-covariance matrix B with respect to the ML estimator for $\underline{b}$, first $\underline{b}$ is linearized around $\hat{\underline{a}}$:

$$b_i = \hat{b}_i + \sum_{j=1}^{3} \frac{\partial b_i}{\partial a_j}(a_j - \hat{a}_j). \tag{C.1}$$

It follows that:

$$\begin{aligned} cov(b_i, b_j) &= E\left[(b_i - \hat{b}_i)(b_j - \hat{b}_j)\right] \\ &= E\left[\sum_{k=1}^{3}\sum_{l=1}^{3} \frac{\partial b_i}{\partial a_k}\frac{\partial b_j}{\partial a_l}(a_k - \hat{a}_k)(a_l - \hat{a}_l)\right] \\ &= \sum_{k=1}^{3}\sum_{l=1}^{3} \frac{\partial b_i}{\partial a_k}\frac{\partial b_j}{\partial a_l} cov(a_k, a_l). \end{aligned}$$

In matrix notation:

$$B = MAM^T, \tag{C.2}$$

with M an 3×3 matrix with entries $m_{ij} = \frac{\partial b_i}{\partial a_j}$.

Choose $(a_1, a_2, a_3) = (a, b, c)$ (the parameters describing the distribution of Z introduced in Appendix B) and $(b_1, b_2, b_3) = (\ln \gamma, \rho, k)$ or $(b_1, b_2, b_3) = (\ln \alpha, \beta, k)$ (the Coleman parameters for the power-law and exponential breakdown rule function respectively). The parameter sets are related via the transformation formulas given in Table B.1. It is found that the transformation

matrix M is the same for both breakdown function rules:

$$
\begin{aligned}
M &= \begin{pmatrix} 1 & 0 & 0 \\ 0 & 1 & 0 \\ 0 & 0 & 1 \end{pmatrix} \quad \text{constant load,} \\
&= \begin{pmatrix} -\frac{1}{\hat{b}} & -\frac{1}{\hat{b}} + \frac{\hat{a}}{\hat{b}^2} & 0 \\ 0 & \frac{1}{\hat{b}^2} & 0 \\ 0 & -\hat{c} & -\hat{b} \end{pmatrix} \quad \text{constant load rate.}
\end{aligned} \tag{C.3}
$$

Appendix D

Characteristics of the residual distributions

We start with the distribution function for the residual damage Ω_{res} (see equation (4.6)):

$$F_{\Omega_{\text{res}}}(x) = 1 - \exp\left(\left(\frac{\omega^*}{\omega_0}\right)^k - \left(\frac{x+\omega^*}{\omega_0}\right)^k\right), \quad \text{for } x > 0. \tag{D.1}$$

This distribution is identified as a translated, left-truncated Weibull distribution. Focus is now turned to the dimension-free residual damage $W_{res} = \frac{\Omega_{\text{res}}}{\overline{\Omega}}$ ($\overline{\Omega} = \omega_0\Gamma(1+1/k)$) with distribution function:

$$F_{W_{res}}(w) = 1 - \exp\left((\hat{\omega}^*)^k - (w\Gamma_k + \hat{\omega}^*)^k\right), \quad \text{for } w > 0, \tag{D.2}$$

with $\Gamma_x = \Gamma(1+1/x)$.

The relationships between residual damage and residual time-to-failure T_{res} and residual strength S_{res} (similar to equations (4.4) and (4.5)) read in dimension-free form:

$$\begin{aligned} U_{res} &= \frac{T_{res}}{\overline{T}} = W_{res}, \\ V_{res} &= \frac{S_{res}}{\overline{S}} = \frac{(W_{res}\Gamma_k)^{1/(\rho+1)}}{\Gamma_{k(\rho+1)}} \quad \text{power-law}, \\ V_{res} &= \frac{S_{res}}{\overline{S}} = \frac{1}{\beta\overline{S}}\ln\left(\eta W_{res}\Gamma_k + 1\right) \quad \text{exponential}, \end{aligned} \tag{D.3}$$

with $\eta = \frac{\beta\dot{\sigma}\omega_0}{\alpha}$ and:

$$\begin{aligned} \overline{T} &= t_0\Gamma_k = \frac{\omega_o}{\kappa_\sigma}\Gamma_k, \\ \overline{S} &= s_0\Gamma_{k(\rho+1)} = \left(\frac{\omega_0(\rho+1)\dot{\sigma}}{\gamma}\right)^{1/(\rho+1)}\Gamma_{k(\rho+1)} \quad \text{power-law}, \\ \overline{S} &= \frac{L(0;k,\eta)}{\beta} \quad \text{exponential}, \end{aligned} \tag{D.4}$$

with: $L(y;a,b) = \int_y^\infty \ln\left(b(z^{1/a} - y^{1/a}) + 1\right)\exp(y-z)\,dz$.

For any stochastic variable $X = f(W_{res})$ with f strictly increasing, the distribution function $F_X(x)$ follows from $F_{W_{res}}(w)$:

$$F_X(x) = P(X \leq x) = P(f(W_{res}) \leq x) = P(W_{res} \leq f^{-1}(x)) = F_{W_{res}}(f^{-1}(x)). \quad \text{(D.5)}$$

For $X = U_{res}, V_{res}$ and using (D.3) we find:

$$\begin{aligned} F_{U_{res}}(u) &= 1 - exp\left((\hat{\omega}^*)^k - (u\Gamma_k + \hat{\omega}^*)^k\right), \\ F_{V_{res}}(v) &= 1 - exp\left((\hat{\omega}^*)^k - \left(\left(v\Gamma_{k(\rho+1)}\right)^{\rho+1} + \hat{\omega}^*\right)^k\right) \quad \text{power-law,} \\ F_{V_{res}}(v) &= 1 - exp\left((\hat{\omega}^*)^k - \left(\frac{1}{\eta}\left(e^{vL(0;k;\eta)} - 1\right) + \hat{\omega}^*\right)^k\right) \quad \text{exponential.} \end{aligned} \quad \text{(D.6)}$$

For convenience, summarize equations (D.6) by:

$$F_X(x) = 1 - \exp\left((\hat{\omega}^*)^k - g(x)\right), \quad \text{(D.7)}$$

which corresponds to:

$$f_X(x) = \exp\left((\hat{\omega}^*)^k - g(x)\right) g'(x). \quad \text{(D.8)}$$

The mean $\overline{X} = E[X]$ is found from:

$$\begin{aligned} \overline{X} &= \int_0^\infty x f_X(x) dx = \int_{g(0)}^{g(\infty)} x \exp\left((\hat{\omega}^*)^k - g(x)\right) d\left(g(x)\right) \\ &= \int_{(\hat{\omega}^*)^k}^\infty g^{-1}(u) \exp\left((\hat{\omega}^*)^k - u\right) du. \end{aligned} \quad \text{(D.9)}$$

We derive $E[X]$ for $X = U_{res}, V_{res}$ from equations (D.6) and (D.9):

$$\begin{aligned} \overline{U}_{\text{res}} &= \overline{W}_{\text{res}} = I((\hat{\omega}^*)^k; k, 1), \\ \overline{V}_{\text{res}} &= I((\hat{\omega}^*)^k; k, \rho+1) \qquad \text{power-law,} \\ \overline{V}_{\text{res}} &= K((\hat{\omega}^*)^k; k, \eta) \qquad \text{exponential,} \end{aligned} \quad \text{(D.10)}$$

with:

$$\begin{aligned} I(y;a,b) &= \frac{J(y;a,b)}{J(0;a,b)}; \quad J(y;a,b) = \int_y^\infty \left(z^{1/a} - y^{1/a}\right)^{1/b} \exp\left(y - z\right) dz, \\ K(y;a,b) &= \frac{L(y;a,b)}{L(0;a,b)}; \quad L(y;a,b) = \int_y^\infty \ln\left(b(z^{1/a} - y^{1/a}) + 1\right) \exp\left(y - z\right) dz. \end{aligned}$$

Note that $J(y;a,1)$ can be evaluated analytically in terms of the incomplete gamma function:

$$J(y;a,1) = \exp(y)\,\Gamma_{\text{upper}}(1 + 1/a, y) - y^{1/a} \qquad \text{and} \quad J(0;a,1) = \Gamma_a,$$

with Γ_{upper} the upper incomplete gamma function defined by:

$$\Gamma_{\text{upper}}(p,x) = \int_x^\infty z^{p-1} \exp\left(-z\right) dz.$$

Apparently, $\overline{U}_{\text{res}} = \left(\exp((\hat{\omega}^*)^k)\,\Gamma_{\text{upper}}(1 + 1/k, (\hat{\omega}^*)^k) - \hat{\omega}^*\right)/\Gamma_k$ which is in accordance with equation (3.10) in Chapter 3 ($b = \Gamma_k^{-1}$, $c = k$, $u_1 = (\hat{\omega}^*)^k$, $t_1 = \Gamma_k^{-1}\hat{\omega}^*$).

Bibliography

[1] Alwis KGNC, Burgoyne CJ, Time temperature superposition to determine the stress-rupture of aramid fibres, Appl. Compos. Mater. 13:249-264, 2006

[2] Phoenix SL, Statistical theory for the strength of twisted fiber bundles with applications to yarns and cables, Text. Res. J. 49(7):407-423, 1979

[3] Phoenix SL, Tierney L-J, A statistical model for the time dependent failure of unidirectional composite materials under local elastic load-sharing among fibers, Eng. Fract. Mech. 18(1):193-215, 1983

[4] Baltussen JJM, Northolt MG, The viscoelastic extension of polymer fibers: creep behaviour, Polymer 42(8):3835-3846, 2001

[5] Tobolsky AV, Eyring H, Mechanical properties of polymeric materials, J. Chem. Phys. 11:125-134, 1943

[6] Henderson CB, Graham PH, Robinson CN, A comparison of reaction rate models for the fracture of solids, Int. J. Fract. Mech. 6(1):33-40, 1970

[7] Zhurkov SN, Kinetic concept of the strength of solids, Int. J. Fract. Mech. 1:311-323, 1965

[8] Pauchard V, Grosjean F, Campion-Boulharts H, Chateauminois A, Application of a stress-corrosion-cracking model to an analysis of the durability of glass/epoxy composites in wet environments, Compos. Sci. Technol. 62:493-498, 2002

[9] Coleman BD, Statistics and time dependence of mechanical breakdown in fibers, J. Appl. Phys. 29(6):968-983, 1958

[10] Kanters MJW, Kurokawa T, Govaerts LE, Competition between plasticity-controlled and crack-growth controlled failure in static and cyclic fatigue of thermoplastic polymer systems, Polym. Test. 50:101-110, 2016

[11] Marco SM, Starkey WL, A concept of fatigue damage, Trans ASME, 76:627-632, 1954

[12] Knoester H, Hulshof J, Meester RWJ, Modeling failure of high performance fibers: on the prediction of long-term time-to-failure, J. Mater. Sci. 50(19):6277-6290, 2015

[13] Alwis KGNC, Burgoyne CJ, Accelerated creep testing for aramid fibres using the stepped isothermal method, J. Mater. Sci. 43:4789-4800, 2008

[14] Burgoyne CJ, Alwis KGNC, Viscoelasticity of aramid fibres, J. Mater. Sci. 43:7091-7101, 2008

[15] Giannopoulos IP, Burgoyne CJ, Stepped isostress method for aramid fibers, Procs 8th Int. Conf on Fibre Reinforced Polymers for Reinforced Concrete Structures (FRPRCS9) Sydney, Australia, 2009

[16] Fallatah GM, Dodds N, Gibson AG, Long-term creep and stress rupture of aramid fibre, Plast. Rubber Compos. 36(9):403-412, 2007

[17] Chambers JJ, Burgoyne CJ, An experimental investigation of the stress-rupture behaviour of a parallel-lay aramid rope, J. Mater. Sci. 25:3723-3730, 1990

[18] Guimaraes GB, Burgoyne CJ, Parallel-lay aramid ropes for offshore structures. 7th International Symposium on Offshore Engineering, Rio de Janeiro, Brazil, 1989

[19] Gibson AG, Implementation of reinforced thermoplastic pipes (RTPs) in the oil and gas industry phase II. Creep and failure behaviour of aramid fibres. University of Newcastle, 2006

[20] Ulianov C, Robinson AM, Gibson AG, Fallatah GM, Reliability analysis of aramid fibre yarns, Plast. Rubber Compos. 39:157-164, 2010

[21] Zhurkov SN, Tomashevsky EE, An investigation of fracture process of polymers by electron spin resonance method. Conference Proceedings: Physical basis of yield and fracture Oxford, pp 200-208, 1966

[22] Pai GA, Batra SK, Hersh SP, Interpreting creep and fatigue failure of fibers via deformation kinetics, J. Polym. Sci. 47:127-141, 1991

[23] Zimmerman J, Failure mechanisms in polymeric fibers. In: Brostow W, Corneliussen RD (eds) Failure of plastics. Hanser Publishers, New York, pp 430-442, 1986

[24] Coleman BD, Time dependence of mechanical breakdown phenomena, J. Appl. Phys. 27(8):862-6, 1956

[25] Kelly A, McCartney LN, Failure by stress corrosion of bundles of fibers, Proc. R. Soc. Lond. A 374:475-489, 1981

[26] Cowking A, Attou A, Siddiqui AM, Sweet AS, An acoustic emission study of failure by stress corrosion in bundles of E-Glass fibres, J. Mater. Sci. 26:301-306, 1991

[27] Draper NR, Smith H, Applied regression analysis (Wiley series in probability and mathematical statistics). 2nd edn., 1981

[28] Reliawiki.org [Internet]. Experiment design and analysis reference: Chapter 3: simple linear regression analysis, Reliasoft. [updated 2013 Dec 13; cited 2014 March]. Available from: http://www.reliawiki.org/.

[29] Abramowitz M, Stegun IA, Handbook of Mathematical Functions With Formulas, Graphs, and Mathematical Tables. NBS Applied Mathematics Series 55, National Bureau of Standards, 1964

[30] Kendall MG, Stuart A, The advanced theory of statistics Vol. 2: Inference and relationships. Charles Griffin & Co. Ltd., London, 1961

[31] Lehmann EL, Casella G, Theory of point estimation 2nd edn. Springer-Verlag, New-York, 1998

[32] Jawitz W, Moments of truncated continuous univariate distributions, Adv. Water Resour. 27:269-281, 2004

[33] Philippidis TP, Passipoularidis VA, Residual strength after fatigue in composites: Theory vs. experiment, Int. J. Fatigue 29:2104-2116, 2007

[34] Siddiqui MM, Çaglar M, Residual lifetime distribution and its applications, Microelectron. Reliab. 34(2):211-227, 1994

[35] Palahi M, Pukkala T, Trasobares A, Modelling the diameter distribution of Pinus sylvestris, Pinus nigra and Pinus halepensis forest stands in Catalonia using the truncated Weibull function, Forestry 79(5):553-562, 2006

[36] Kantar YM, Usta I, Analysis of the upper-truncated Weibull distribution for wind speed, Energ. Convers. Manage. 96:81-88, 2015

[37] Pereira MG, Calado T, DaCamara CC, Leite SM, Parametric models of Portuguese fire size distribution, Geophys. Res. Abstr. 6:06008, 2004

[38] McEwen RP, Parresol BR, Moment expressions and summary statistics for the complete and truncated Weibull distribution, Commun. Stat.-Theor. M. 20(4): 1361-1372, 1991

[39] Wingo RD, The left-truncated Weibull distribution: theory and computation, Stat. Pap. 30:39-48, 1989

[40] McEwen RP, Parresol BR, Errata. Moment expressions and summary statistics for the complete and truncated Weibull distribution, Commun. Stat.-Theor. M. 22(8): 2399, 1993

[41] Murthy DNP, Xie M, Jiang R, Wiley Series in Probability and Statistics: *Weibull models.* Hoboken New Jersey: John Wiley & Sons, Inc., 2003

[42] Nadarajah S, Kotz S, Strength modeling using Weibull distributions, J. Mech. Sci. Technol. 22:1247-1254, 2008

[43] Zhang T, Xie M, On the upper truncated Weibull distribution and its reliability implications, Reliab. Eng. Syst. Safe. 96:194-200, 2011

[44] Lai C-D, Springer Briefs in Statistics: Generalized Weibull Distributions, Springer-Verlag Berlin Heidelberg, 2014

[45] Fu H, Noche B, Integration of truncated distributions in exponential family with simulation models of logistics and supply chain management, *Logistics Journal: proceedings*, 2012

[46] Knoester H, Hulshof J, Meester RWJ, A probabilistic approach on residual strength and damage buildup of high performance fibers, J. Mater. Sci. 52(4):1898-1910, 2017

[47] Coleman BD, Time dependence of mechanical breakdown in bundles and fibers. I. Constant total load, J. Appl. Phys. 28(9):1058-1067, 1957

[48] Coleman BD, On the strength of classical fibre and fibre bundles, J. Mech. Phys. Solids 7:60-70, 1958

[49] Phoenix SL, The asymptotic time to failure of a mechanical system of parallel members, Siam J. Appl. Math. 34(2):227-246, 1978

[50] Phoenix SL, Stochastic strength of fatigue of fiber bundles, Int. J. Fracture 14(3):327-344, 1978

[51] Chou PC, Croman R, Residual strength in fatigue based on the strength-life equal rank assumption, J. Compos. Mater. 12:177-194, 1978

[52] Barnard PM, Butler RJ, Curtis PT, The Strength-Life Equal Rank Assumption and its application to the fatigue life prediction of composite materials, Int. J. Fatigue 10(3):171-177, 1988

[53] Weibull W, A statistical distribution function of wide applicability, J. Appl. Mech-T. ASME 18(3):293-297, 1951

[54] Peirce FT, Tensile tests for cotton yarns v.—"The Weakest Link" theorems on the strength of long and of composite specimens, J. Text. I. 17:T355, 1926

[55] Paramonov Yu, Andersons J, A family of weakest link models for fiber strength distribution, Compos. Part A-Appl. S. 38:1227-1233, 2007

[56] Van der Zwaag S, The concept of filament strength and the Weibull modulus, J. Test. Eval. 17(5):292-298,1989

[57] Knoff WF, Combined weakest link and random defect model for describing strength variability in fibres, J. Mater. Sci. 28:921-931, 1993

[58] Sutherland LS, Shenoi RA, Lewis SM, Size and scale effects in composites: I. Literature review, Compos. Sci. Technol. 59(2):209-220, 1999

[59] Wagner HD, Phoenix SL, Schwartz P, A study of statistical variability in the strength of single aramid filaments, J. Compos. Mater. 28:312-327, 1984

[60] Shih TT, An evaluation of the probabilistic approach to brittle design, Eng. Fract. Mech. 13(2):257-271, 1980

[61] Yang JN, Residual strength degradation model and theory of periodic proof tests for graphite/epoxy laminates, J. Compos. Mater. 11:176-203, 1977

[62] Kenney MC, Mandell JF, McGarry FJ, Fatigue behaviour of synthetic fibres, yarns and ropes, J. Mater. Sci. 20:2045-2059, 1985

[63] Knoester H, Den Decker P, Van den Heuvel CJM, Tops NAN, Elkink F, Creep and failure time of aramid yarns subjected to constant loads, Macromol. Mater. Eng. 297(6):559-575, 2012

[64] Christensen RM, Residual strength determination in polymeric materials, J. Rheol. 25(5):529-536, 1981

[65] Ibnabdeljalil M, Phoenix SL, Creep-rupture of brittle matrix composites reinforced with time dependent fibers: Scalings and Monte Carlo simulations, J. Mech. Phys. Solids 43(6):897-931, 1995

[66] Kachanov LM, On the time to rupture under creep conditions, Izvestia Akademi Nauk SSSR, Otd. Tekhn. Nauk., 8:26-31 (Russian), 1958

[67] Palmgren A, Die Lebensdauer von Kugellagern, Zeitschrift VDI 68:339-341, 1924

[68] Miner MA, Cumulative damage in fatigue, J. Appl. Mech. 12:A159-A164, 1945

[69] Stigh U, Continuum damage mechanics and the Life-Fraction Rule, ASME J. Appl. Mech. 73(4):702-704, 2005

[70] Christensen RM, A physically based cumulative damage formalism, Int. J. Fatigue, 30:595-602, 2008

[71] Christensen RM, Probabilistic failure and probabilistic life prediction, chapter XIII www.failurecriteria.com

[72] Christensen RM, The Theory of Materials failure, Oxford University Press, 2013

[73] Shimokawa T, Tanaka S, A statistical consideration of Miner's rule, Int. J. Fatigue 2(4):165-170, 1980

[74] van Paepegem W, Degrieck J, Effects of load sequence and block loading on the fatigue response of fibre-reinforced composites, Mech. Adv. Mater. Struct. 9(1):19-35, 2002

[75] Fatemi A, Yang L, Cumulative fatigue damage and life prediction theories: a survey of the state of the art for homogeneous materials, Int. J. Fatigue, 20(1):9-34, 1998

[76] Allen SR, Roche EJ, Bennett B, Molaison R, Tensile deformation and failure of poly(p-phenyleneterephthalamide) fibres, Polymer 33(9):1849-1854, 1992

[77] Morton WE, Hearle JWS, Physical properties of textile fibers (4th edition), Woodhead publishing in textiles no. 68, Cambridge, England, 2008

Summary

.... for those who don't want to read the thesis but still want to know what it's all about ....
.... and for those who like fairytales ....

There once was a popular Twaron fiber type weighing 3.5 gram per 20 meter of length. With a diameter of less than 1 mm it can carry up to 40 kg or so. A thin Twaron rope, constructed from a few of these fibers, can easily lift a human being. Such a Twaron rope would have been a safe alternative for witch Gothel. She kidnapped this young girl, Rapunzel, and locked her up in the tower room. The only way to visit Rapunzel in her high level prison room was by climbing along the tower wall using the 20 meter long hair of Rapunzel, which hung out of the tower room window.

A smart witch would not replace Rapunzel's golden hair by Twaron rope just like that. First she would gather more information on this rope, more than strength only. After all, Rapunzel's hair is (slowly) growing and replaces itself, but the rope is used over and over again. So Gothel does want to know the time-to-failure of the rope. And what will happen to the rope if Gothel occasionally carries one of her black cats to the tower top? That would mean that the Twaron rope sometimes feels a higher load than usual. How does damage build up in the rope then?

This thesis is on the long-term mechanical properties of Twaron fiber. It is about simple models, describing how damage builds up in a fiber during its service life. From the models we derive a probability that the fiber will fail, provided the current level of damage and current load are known. The models are tuned with easy measurable fiber properties such as the virgin strength and the time-to-failure at constant load. Knowledge of damage build-up in Twaron fiber is important, not only for witch Gothel, but for anyone planning to use this fiber in load-bearing applications such as ropes, fiber reinforced composites, fiber braided hoses or fiber reinforced thermoplastic pipes.

Gothel now knows that climbing the tower wall using Rapunzel's hair is very unsafe. Twaron rope is a much safer alternative. But the best solution for Gothel is probably flying her broomstick to the top of the tower. Still, for anybody lacking such a broomstick, Twaron rope is the second best solution.

Fairytales are known for their implausible assertions. But in case of Rapunzel's hair strength, the story is quite realistic. Though very unpleasant for the owner of the hair, hair can very well be used as a kind of rope. According to L'óreal hair science, one single hair can carry about 100 gram. With a specific weight for hair of 1.3 gram/cm^3, the specific strength of Twaron is only about 15 times larger. However, we do not know anything about the time-to-failure of hair ....

Acknowledgements

For many people, more acquainted to the author than to the subject of this thesis, the acknowledgments are probably most fun reading. Do I know the colleagues, friends and family to whom Henk is expressing his gratitude? Perhaps he mentions me as well? If you want to know, quickly continue reading.

As from 1986 (oops, that long ago?) I have worked for Akzo Nobel (later Teijin Aramid) as mathematical and chemical engineer on a variety of subjects. In 2010 I was warmly welcomed by my current colleagues of the Fiber Physics department (QRS) of Teijin Aramid Research. I started working on time-to-failure of Twaron fibers, carrying on the work of Niek Tops, Jurriaan van den Heuvel and Piet den Decker. I am highly indebted not only to these three men but also to Frits Elkink. We have had stimulating discussions on the failure of Twaron yarns in all its appearances. Frits' dedication to this subject has motivated me a lot. Back in 2011, I was offered an opportunity to start a PhD project at the VU on this topic. My previous manager Jurriaan was enthusiastic right from the start. He arranged all internal approvals and legal matters, so I am grateful to him in more than one way. Naturally, I'm most grateful to my employer Teijin Aramid, especially Jan Roos, for the trust in me and allowing me to work on my PhD for so many years. Special thanks to Otto Grabandt for his patience and understanding that research takes time. Thanks Jason, for a final check.

And now for my colleagues at QRS. Thank you Corrine (or Corinne?), Elona and Michel for helping me out, always at the highest priority, by doing twisting and strength measurements on various fiber samples. Dear Aad, sadly you are not around anymore, but you must know that your message that *it makes no sense to measure 'one fiber samples' only* is heard. Not only by me but by all our colleagues. Thank you Hans V, Hans Q, Rike, Danny, Rik and Niek for our 'not-always-stimulating' lunch breaks and harsh discussions. I hope there are a lot of these ahead of us. Hans and Hans, your silly crypto-talks scared me of so much that my coffee/tea breaks fortunately did not take up too much time. Thanks Rike for your moral support and your quick literature deliveries. Thanks Annika for your optimism and thanks Sjaak and Danny for being annoying in the nicest possible way. Thank you Enno, you gave me all the freedom I needed to finalize this work. Thanks also to the ladies (and one man) of QRE for your pleasant company.

My parents would have been very proud on this achievement. Of course, at my age, it is not surprising that my mom and dad are not around anymore. Still, I want to express my deepest gratitude to them, for always having stimulated me and my brother Dick to never neglect our schoolwork. Special thanks to my granddad (mom's father), Henk Ekhardt. Everytime we visited our 'opa en oma' in Blerick I was looking forward to discussions with him on elementary physics and astronomy, and the stories about his heroes Einstein, Darwin and Maltus. They also became my heroes and they still are. I thank my brother Dick who was and still is so concerned that I work too hard. Thanks also to his wife Lhet and their son Lorenzo.

Thank you Petra for regularly lowering my stress levels. You tirelessly keep on organizing and arranging short and long trips and holidays. From early morning till the evening these ‘days off’ are filled with all kinds of activities. Physically tiring, but the mental refreshment very much helped take up daily work with new energy. Thanks also to my much beloved cats Poetin and Molly. You both cheered up my life so much during the years I worked on my PhD. I will always remember the two of you.

I end up with three people without whom this work would not have been possible. Very special thanks to Ronald Meester and Joost Hulshof. You constantly urged me to keep walking the main road and not to get lost in details. Stick to your goals and formulate your messages in a clear and straightforward manner. It wasn’t always easy. But after all, I now realize that your coaching was indispensable. Without it, I couldn’t have written this thesis. Finally, my very special thanks to Rein van der Hout, one of the finest mathematicians and nicest people I know. You initiated this PhD work and introduced me to the VU. It has been a privilege to know you for so many years. Not only did you teach me a lot of mathematics, but you always unconditionally encouraged me.